

FRESH AND HARDENED PROPERTIES OF
SELF-CONSOLIDATING CONCRETE INCORPORATING
METAKAOLIN

JUSTIN R. MAYO

Fresh and Hardened Properties of Self-Consolidating Concrete Incorporating Metakaolin

by

Justin R. Mayo

A Thesis submitted to the

School of Graduate Studies

in partial fulfillment of the requirements for the degree of

Masters of Engineering

Department of Engineering and Applied Sciences

Memorial University of Newfoundland

October 2013

St. John's, Newfoundland

Abstract

This thesis aims to study the fresh and hardened properties of self-consolidating concrete (SCC) produced with metakaolin. The first stage of the study was to identify the most favourable replacement of cement with metakaolin by varying the metakaolin content from 0 to 25% in SCC. Typical tests for SCC were conducted on the fresh and hardened properties for all mixtures. Based on these test results, the optimum metakaolin percentage was chosen and the effect of the mixture design on SCC was studied. Using the same tests as the first stage, the second stage varied the coarse-to-fine aggregate (C/F) ratio, coarse aggregate size, binder amount, and air content to optimize SCC containing metakaolin. The third stage of the program was to study the effect of metakaolin and mixture design on the shear capacity and cracking behaviour on full-scale SCC beams. The results indicated that 20% metakaolin replacement gave the optimal flowability, passing ability, segregation resistance, 28- and 90- compressive strengths, Flexural Strength (FS), Splitting Tensile Strength (STS) and Modulus of Elasticity (ME). However, the addition of metakaolin, increased the viscosity of the mixture and the high range water reducer (HRWR) demand. Varying the mixture design showed, using a lower C/F ratio of 0.7, increasing the coarse aggregate size to 20 mm, increasing the total binder content to 500 kg/m³, and using air entrainment up to 7%, all helped to improve the flowability, viscosity, and passing ability of SCC. However, when using a lower C/F ratio of 0.7, the HRWR demand increased for all mixtures, while all other design parameters reduced the HRWR demand. Examining the mechanical properties, it was seen that using either a lower C/F ratio of 0.7 or increasing the binder content to 500

kg/m³ improved the compressive strength as well as the strength development,, flexural strength, splitting tensile strength and the modulus of elasticity. While, increasing the coarse aggregate size to 20 mm or increasing the air entrainment to 7% resulted in a reduction in the compressive strengths and strength development, flexural strength, splitting tensile strength and the modulus of elasticity.. Using a larger C/F ratio of 1.2, was shown to decrease the normalized shear strength, while increasing the post diagonal cracking resistance in normal-strength SCC beams, although, in high-strength SCC beams, there was no significant variation. In addition, increasing the coarse aggregate size to 20 mm, increased the normalized shear strength and post diagonal cracking resistance in normal-strength SCC beams, and showed no affect in high-strength SCC beams.

ACKNOWLEDGEMENTS

I wish to express my great appreciation to Dr. Assem Hassan for his valuable and constructive suggestions during my Master's program and for this great opportunity.

I would also like to express my gratitude to Mr. Ahmed Abdallah Abouhussien for his assistance preparing all mixtures and his support during testing.

I would like to acknowledge the support provided by my family during my studies.

I would also like to extend my special thanks to the technicians of the laboratory of the Engineering department for their assistance in demonstrating and the running of various setups and test programs.

Table of Contents

Abstract	ii
Acknowledgements	iv
Table of Contents	v
List of Tables.....	xii
List of Figures	xiii
List of Symbols, Nomenclature, or Abbreviations.....	xvii
Introduction	1
1.1 Overview of Self-Consolidating Concrete	1
1.1.1 Fresh Properties of SCC	3
1.1.2 Mechanical Properties of SCC.....	5
1.1.3 Use of Supplementary Cementitious Materials	7
1.2 Shear Behaviour of Normal and SCC Beams	10
1.2.1 Analysis of Shear in Reinforced Concrete Beams.....	10
1.3 Significance of Research	12
1.4 Scope of Research	16
2. Literature Review.....	18
2.1 Concrete and SCC Containing Metakaolin	18
2.1.1 Fresh Properties	18

2.1.2 Mechanical Properties	20
2.2 Factors Influencing the Fresh and Mechanical Properties of SCC	23
2.2.1 Varying the Coarse Aggregate Volume and Size in SCC	23
2.2.2 Binder Content of SCC	25
2.2.3 Use of Air in SCC	26
2.3 Shear Strength in Normal and SCC Concrete Beams	28
2.4 Shear of High-Strength Beams	28
3. Experimental Program	30
3.1 Fresh and Mechanical Property Tests	30
3.1.1 Slump Flow Diameter and T_{50} Tests	30
3.1.2 J-Ring and T_{50J} Tests	31
3.1.3 L-Box Test	32
3.1.4 V-Funnel Test	33
3.1.5 Air Content Test	35
3.1.6 Compressive Strength and Strength Development Tests	36
3.1.7 Flexural Strength/Modulus of Rupture Test	37
3.1.8 Splitting Tensile Strength	38
3.1.9 Modulus of Elasticity	38
3.2 Shear Strength Test of SCC Beams	39

3.2.1 Crack Development.....	40
3.2.2 Post Diagonal Cracking.....	40
3.2.3 Crack Angle.....	41
3.2.4 Strain and Deflections.....	41
4. Mixture Design and Mixture Details	43
4.1 Materials.....	43
4.2 Mixtures for Stage 1 – Optimization of SCC Containing Metakaolin.....	45
4.3 Mixtures for Stage 2 – Improvement of SCC Containing Metakaolin.....	46
4.4 Mixture Design for Beams	50
5. Results.....	52
5.1 Fresh Properties.....	52
5.1.1 Viscosity and Flow Ability.....	52
5.1.1.1 Effect of Metakaolin	53
5.1.1.2 Effect of C/F Ratio	59
5.1.1.3 Effect of Coarse Aggregate Size.....	63
5.1.1.4 Effect of Binder Content.....	65
5.1.1.5 Effect of Air Content.....	68
5.1.2 Passing Ability and Segregation.....	71
5.1.2.1 Effect of Metakaolin	71

5.1.2.2 Effect of C/F Ratio	75
5.1.2.3 Effect of Coarse Aggregate Size	79
5.1.2.4 Effect of Binder Content	82
5.1.2.5 Effect of Air Content.....	85
5.1.3 HRWR Demand.....	89
5.1.3.1 Effect of Metakaolin	89
5.1.3.2 Effect of C/F Ratio	90
5.1.3.3 Effect of Coarse Aggregate Size	91
5.1.3.4 Effect of Binder Content	93
5.1.3.5 Effect of Air Content.....	94
5.2 Mechanical Properties	96
5.2.1 Strength Development	97
5.2.1.1 Effect of Metakaolin	97
5.2.1.2 Effect of C/F Ratio	102
5.2.1.3 Effect of Coarse Aggregate Size	103
5.2.1.4 Effect of Binder Content	105
5.2.1.5 Effect of Air Content.....	106
5.2.2 28- and 90-Day Compressive Strengths	108

5.2.2.1 Effect of Metakaolin	108
5.2.2.2 Effect of C/F Ratio	110
5.2.2.3 Effect of Coarse Aggregate Size	111
5.2.2.4 Effect of Binder Content	113
5.2.2.5 Effect of Air Content.....	115
5.2.3 Flexural Strength	116
5.2.3.1 Effect of Metakaolin	116
5.2.3.2 Effect of C/F Ratio	118
5.2.3.3 Effect of Coarse Aggregate Size	119
5.2.3.4 Effect of Binder Content	120
5.2.3.5 Effect of Air Content.....	121
5.2.4 Splitting Tensile Strength	122
5.2.4.1 Effect of Metakaolin	122
5.2.4.2 Effect of C/F Ratio	123
5.2.4.3 Effect of Coarse Aggregate Size	123
5.2.4.4 Effect of Binder Content	124
5.2.4.5 Effect of Air Content.....	124
5.2.5 Modulus of Elasticity.....	125

5.2.5.1 Effect of Metakaolin	125
5.2.5.2 Effect of C/F Ratio	126
5.2.5.3 Effect of Coarse Aggregate Size	126
5.2.5.4 Effect of Binder Content	126
5.2.5.5 Effect of Air Content	127
5.3 Optimal SCC Mixture	128
5.4 Shear of SCC Beams	130
5.4.1 Beam Loading Results	130
5.4.1.1 Fresh Properties of SCC Beams	130
5.4.1.2 Twenty Eight and 90-Day Compressive Strength Results	132
5.4.2 Shear Failure Capacity of SCC Beams	134
5.4.2.1 Failure Modes	134
5.4.2.2 Effect of C/F Ratio	134
5.4.2.3 Effect of Coarse Aggregate Size	136
5.4.2.4 Effect of High-Strength Concrete	137
5.4.3 Crack Development	139
5.4.3.1 Post Diagonal Cracking	139
5.4.3.3.1 Effect of C/F Ratio	140

5.4.3.3.2 Effect of Coarse Aggregate Size.....	140
5.4.3.3.3 Effect of High-Strength Concrete.....	141
5.4.3.3.4 Crack Failure Angles and Maximum Crack Width	141
5.4.4 Deflection versus Load	143
6. Conclusions	144
7. References	150
8.1 Appendix A -- Crack Development Figures for 10 SCC Beams.....	A1
8.2 Appendix B - LVDT Deflection Graphs for 10 SCC Beams	B1
8.3 Appendix C -- Strain vs. Loading Graphs for 10 SCC Beams.....	C1

List of Tables

Table 1 – Chemical and Physical Properties of all SCMs Used	43
Table 2 – Mixture Design for Stage 1	46
Table 3 – Mixture Design for Varying Mixture Parameters	48
Table 4 – Mixture Design for the 10 SCC Beams	51
Table 5 – Slump Flow, J-Ring Flow, J-Ring Height Difference, and Slump Flow – J-Ring Diameter for Stage 1	52
Table 6 – V-Funnel Times, Segregation Factor, H2/H1, and Air Content for Stage 1 Mixtures	53
Table 7 – Slump Flow, J-Ring Flow, J-Ring Height Difference, and Slump Flow – J-Ring Diameter for Varying Mixture Parameters	57
Table 8 – V-Funnel Times, Segregation Factor, H2/H1, and Air Content for Varying Mixture Parameters	58
Table 9 – Mechanical Properties for Stage 1 Mixtures.....	96
Table 10 - Strength Development for Stage 1 Mxitures	96
Table 11 – Mechanical Properties for Varying Mixture Parameters	99
Table 12 – Strength Development for Varying Mixture Parameters	101
Table 13 – Compressive Strengths, Failure Loads, and Load at First Diagonal Crack ...	130
Table 14 – Beam Cracking Results.....	142

List of Figures

Figure 1 – Description of SCC (Khayat 1999)	2
Figure 2 – Shear Mechanics in Concrete Beams (MacGregor 2000)	10
Figure 3 – a) Aggregate Interlock, b) Dowel Action, and c) Axial Steel Force (Walraven 1980)	11
Figure 4 – Compressive Strength Related to W/B Ratio and Air Entrainment (Minnesota Department of Transportation 2003).....	27
Figure 5 – Slump Flow Diameter Apparatus	31
Figure 6 – J-Ring Apparatus	32
Figure 7 – L-Box Test Apparatus	33
Figure 8 – V-Funnel Test Apparatus	35
Figure 9 – Reinforcement, Support, and Loading Details	40
Figure 10 – Strain Gauge Locations for all 8 Strain Gauges	42
Figure 11 – T_{50} , T_{50J} , and Initial V-Funnel Times for Stage 1 Mixtures	56
Figure 12 – T_{50} , T_{50J} , and Initial V-Funnel Times for Varying C/F Ratios	62
Figure 13 – T_{50} , T_{50J} , and Initial V-Funnel Times for Varying Coarse Aggregate Sizes ..	64
Figure 14 – T_{50} , T_{50J} , and Initial V-Funnel Times for Varying Binder Content	67
Figure 15 – T_{50} , T_{50J} , and Initial V-Funnel Times for Varying Air Percentages	70
Figure 16 – Passing Ability and Segregation Results for Stage 1 Mixtures (Units Denoted in Legend)	74
Figure 17 – Passing Ability and Segregation Results for Varying C/F Ratios (Units Denoted in Legend).....	78

Figure 18 – Passing Ability and Segregation Results for Varying Coarse Aggregate Sizes (Units Denoted in Legend).....	81
Figure 19 – Passing Ability and Segregation Results for Varying Binder Content (Units Denoted in Legend).....	84
Figure 20 – Passing Ability and Segregation Results for Varying Air Percentages (Units Denoted in Legend).....	88
Figure 21 – Effect of Metakaolin on HRWR Demand	90
Figure 22 – Effect of C/F Ratio on the HRWR Demand	91
Figure 23 – Effect of Coarse Aggregate Size on HRWR Demand	92
Figure 24 – Effect of Binder Content on HRWR Demand	94
Figure 25 – Effect of Air Content on HRWR Demand.....	95
Figure 26 – Strength Development for Stage 1 Mixtures	99
Figure 27 – Effect of C/F Ratio on Strength Development	103
Figure 28 - Effect of Coarse Aggregate Size on Strength Development	105
Figure 29 – Effect of Binder Content on Strength Development.....	106
Figure 30 – Effect of Air Content on Strength Development	108
Figure 31 – Effect of Metakaolin on 28- and 90-Day Compressive Strength	110
Figure 32 - Effect of C/F on 28- and 90-Day Compressive Strengths.....	111
Figure 33 – Effect of Coarse Aggregate Size on 28- and 90-Day Compressive Strengths	113
Figure 34 – Effect of Binder Content on 28- and 90-Day Compressive Strengths.....	114
Figure 35 – Effect of Air Content on 28- and 90-Day Compressive Strengths	116

Figure 36 – Effect of Metakaolin Partial Replacement on the Normalized FS, STS, and ME	117
Figure 37 – FS, STS, and ME for Mixtures Containing Metakaolin	118
Figure 38 – Effect of C/F Ratio on FS, STS, and ME	119
Figure 39 – Effect of Coarse Aggregate Size on FS, STS, and ME	120
Figure 40 – Effect of Binder Content on FS, STS, and ME.....	121
Figure 41 – Effect of Air Content on FS, STS, and ME	122
Figure 42 – T_{50} , Slump Flow Diameters, and HRWR Demand for the 10 SCC Beams..	132
Figure 43 – 28- and 90-Day Compressive Strengths for SCC Beams	133
Figure 44 – Shear Failure Capacity and Normalized Shear Failure Capacity for SCC Beams.....	136
Figure 45 – Post Diagonal Cracking Capacity Percentages.....	139
Figure A1 – Crack Development for a) 50%, b) 75%, and c) 100% of Max Load.....	A2
Figure A2 – Crack Development for a) 50%, b) 75%, and c) 100% of Max Load.....	A2
Figure A3 – Crack Development for a) 50%, b) 75%, and c) 100% of Max Load.....	A3
Figure A4 – Crack Development for a) 50%, b) 75%, and c) 100% of Max Load.....	A3
Figure A5 – Crack Development for a) 50%, b) 75%, and c) 100% of Max Load.....	A4
Figure A6 – Crack Development for a) 50%, b) 75%, and c) 100% of Max Load.....	A4
Figure A7 – Crack Development for a) 50%, b) 75%, and c) 100% of Max Load.....	A5
Figure A8 – Crack Development for a) 50%, b) 75%, and c) 100% of Max Load.....	A5
Figure A9 – Crack Development for a) 50%, b) 75%, and c) 100% of Max Load.....	A6

Figure A10 – Crack Development for a) 50%, b) 75%, and c) 100% of Max Load.....	A6
Figure B1 -- LVDT Deflection vs. Loading for Beam 1.....	B2
Figure B2 -- LVDT Deflection vs. Loading for Beam 2.....	B3
Figure B3 -- LVDT Deflection vs. Loading for Beam 3.....	B4
Figure B4 -- LVDT Deflection vs. Loading for Beam 4.....	B5
Figure B5 -- LVDT Deflection vs. Loading for Beam 5.....	B6
Figure B6 -- LVDT Deflection vs. Loading for Beam 6.....	B7
Figure B7 -- LVDT Deflection vs. Loading for Beam 7.....	B8
Figure B8 -- LVDT Deflection vs. Loading for Beam 8.....	B9
Figure B9 -- LVDT Deflection vs. Loading for Beam 9.....	B10
Figure B10 -- LVDT Deflection vs. Loading for Beam 10.....	B11
Figure C1 -- Strain vs. Loading for Beam 1.....	C2
Figure C2 -- Strain vs. Loading for Beam 2.....	C3
Figure C3 -- Strain vs. Loading for Beam 3.....	C4
Figure C4 -- Strain vs. Loading for Beam 4.....	C5
Figure C5 -- Strain vs. Loading for Beam 5.....	C6
Figure C6 -- Strain vs. Loading for Beam 6.....	C7
Figure C7 -- Strain vs. Loading for Beam 7.....	C8
Figure C8 -- Strain vs. Loading for Beam 8.....	C9
Figure C9 -- Strain vs. Loading for Beam 9.....	C10
Figure C10 -- Strain vs. Loading for Beam 10.....	C11

List of Symbols, Nomenclature, or Abbreviations

0% C – Control mixture using 450 binder, C/F of 0.9, 10 mm stone size, and 0% air

0% MK – 20% partial cement replacement with MK, 450 binder, C/F of 0.9, 10 mm stone size, and 0% air

0% SF – 8% partial cement replacement with SF, 450 binder, C/F of 0.9, 10 mm stone size, and 0% air

0% SG – 30% partial cement replacement with SG, 450 binder, C/F of 0.9, 10 mm stone size, and 0% air

0.7 C – Control mixture using 450 binder, C/F of 0.7, and 10 mm stone size

0.7 MK – 20% partial cement replacement with MK, 450 binder, C/F of 0.7, and 10 mm stone size

0.7 SF – 8% partial cement replacement with SF, 450 binder, C/F of 0.7, and 10 mm stone size

0.7 SG – 30% partial cement replacement with SG, 450 binder, C/F of 0.7, and 10 mm stone size

0.9 C – Control mixture using 450 binder, C/F of 0.9, and 10 mm stone size

0.9 MK – 20% partial cement replacement with MK, 450 binder, C/F of 0.9, and 10 mm stone size

0.9 SF – 8% partial cement replacement with SF, 450 binder, C/F of 0.9, and 10 mm stone size

0.9 SG – 30% partial cement replacement with SG, 450 binder, C/F of 0.9, and 10 mm stone size

1.2 C – Control mixture using 450 binder, C/F of 1.2, and 10 mm stone size

1.2 MK – 20% partial cement replacement with MK, 450 binder, C/F of 1.2, and 10 mm stone size

1.2 SF – 8% partial cement replacement with SF, 450 binder, C/F of 1.2, and 10 mm stone size

1.2 SG – 30% partial cement replacement with SG, 450 binder, C/F of 1.2, and 10 mm stone size

10 C – Control mixture using 450 binder, C/F of 0.9, and 10 mm stone size

10 MK – 20% partial cement replacement with MK, 450 binder, C/F of 0.9, and 10 mm stone size

10 SF – 8% partial cement replacement with SF, 450 binder, C/F of 0.9, and 10 mm stone size

10 SG – 30% partial cement replacement with SG, 450 binder, C/F of 0.9, and 10 mm stone size

20 C – Control mixture using 450 binder, C/F of 0.9, and 20 mm stone size

20 MK – 20% partial cement replacement with MK, 450 binder, C/F of 0.9, and 20 mm stone size

20 SF – 8% partial cement replacement with SF, 450 binder, C/F of 0.9, and 20 mm stone size

20 SG – 30% partial cement replacement with SG, 450 binder, C/F of 0.9, and 20 mm stone size

450 C – Control mixture using 450 binder, C/F of 0.9, and 10 mm stone size

450 MK – 20% partial cement replacement with MK, 450 binder, C/F of 0.9, and 10 mm stone size

450 SF – 8% partial cement replacement with SF, 450 binder, C/F of 0.9, and 10 mm stone size

450 SG – 30% partial cement replacement with SG, 450 binder, C/F of 0.9, and 10 mm stone size

5% C – Control mixture using 450 binder, C/F of 0.9, 10 mm stone size, and 5% air

5% MK – 20% partial cement replacement with MK, 450 binder, C/F of 0.9, 10 mm stone size, and 5% air

5% SF – 8% partial cement replacement with SF, 450 binder, C/F of 0.9, 10 mm stone size, and 5% air

5% SG – 30% partial cement replacement with SG, 450 binder, C/F of 0.9, 10 mm stone size, and 5% air

500 C – Control mixture using 500 binder, C/F of 0.9, and 10 mm stone size

500 MK – 20% partial cement replacement with MK, 500 binder, C/F of 0.9, and 10 mm stone size

500 SF – 8% partial cement replacement with SF, 500 binder, C/F of 0.9, and 10 mm stone size

500 SG – 30% partial cement replacement with SG, 500 binder, C/F of 0.9, and 10 mm stone size

7% C – Control mixture using 450 binder, C/F of 0.9, 10 mm stone size, and 7% air

7% MK – 20% partial cement replacement with MK, 450 binder, C/F of 0.9, 10 mm stone size, and 7% air

7% SF – 8% partial cement replacement with SF, 450 binder, C/F of 0.9, 10 mm stone size, and 7% air

7% SG – 30% partial cement replacement with SG, 450 binder, C/F of 0.9, 10 mm stone size, and 7% air

a – shear span from support to load application

a/d – shear span of concrete beam

AEA – Air Entraining Agent

C_1 – Compressive force in the un-cracked concrete zone

C/F – Coarse-to-Fine Aggregate Ratio

CA – Coarse Aggregate

d – Depth of beam to the reinforcement

E_c – Modulus of elasticity of concrete

FA – Fine Aggregate

f'_c – 28 Day Compressive Strength

f_r – Modulus of Rupture

FS – Flexural Strength

GU cement – General use cement

H1 – The height of the concrete at the beginning of the L-Box apparatus, after it has stopped flowing. Calculated by 600 mm – measured height

H2 – The height of concrete at the end of the L-Box apparatus after it has stopped flowing. Calculated by $150 \text{ mm} - \text{measured height}$

HRWR – High Range Water Reducer

ITZ – Interfacial Transition Zone

L/4 – LVDT location at $\frac{1}{4}$ of the span length, L

3L/4 – LVDT location at $\frac{3}{4}$ of the span length, L

LVDT – Linear Variable Differential Transformer

ME – Modulus of Elasticity

MK – Metakaolin

MK0 – 0% partial cement replacement with MK, 450 binder, C/F of 0.9, and 10 mm stone size

MK10 – 10% partial cement replacement with MK, 450 binder, C/F of 0.9, and 10 mm stone size

MK15 – 15% partial cement replacement with MK, 450 binder, C/F of 0.9, and 10 mm stone size

MK20 – 20% partial cement replacement with MK, 450 binder, C/F of 0.9, and 10 mm stone size

MK25 – 25% partial cement replacement with MK, 450 binder, C/F of 0.9, and 10 mm stone size

MK5 – 5% partial cement replacement with MK, 450 binder, C/F of 0.9, and 10 mm stone size

MSA – Maximum aggregate size

SCC – Self-Consolidating Concrete

SCM – Supplementary Cementitious Material

S_f – Segregation factor

SF – Silica Fume

SF8 – 8% partial cement replacement with SF using 450 binder, C/F of 0.9, and 10 mm stone size

SG – Slag Cement

SG30 – 30% partial cement replacement with SG, 450 binder, C/F of 0.9, and 10 mm stone size

STS – Splitting Tensile Strength

T_1 – Tension force in the reinforcement

t_0 – Initial V-funnel time

t_5 - V-funnel time after 5 minutes

T_{50} – The time for SCC to reach a 500 mm slump diameter

T_{50j} – The time for SCC to reach a 500 mm slump diameter during the J-Ring Test

VEA – Viscosity-enchaining admixture

VMA - Viscosity modifying admixture

V_{ay} – Shear resistance due to aggregate interlock

V_c - Shear transfer through the concrete

V_{cz} – Shear resistance of the uncracked concrete in the compression zone

V_d – Shear resistance due to dowel action

V_r – Maximum shear resistance of a concrete beam

V_s – Shear transferred by the transverse reinforcement

W/B – Water-Binder ratio

W/C – Water-Cement ratio

Introduction

1.1 Overview of Self-Consolidating Concrete

Self-consolidating concrete (SCC) is a highly flowable concrete that flows into place without requiring mechanical vibrations to fill forms. It is also characterized by having a low-yield stress while having a moderate viscosity, which ensures adequate particle suspension (and avoids segregation) during filling of the formwork. According to many sources, a mixture with a high flowability is not sufficient to classify it as acceptable SCC. The current adopted definition of acceptable SCC is as follows: i) high flowability to ensure it can flow around the reinforcement and fill the formwork, ii) an adequate passing ability to flow through congested reinforcement or tight spaces, and iii) good stability to ensure the mixture remains homogenous and the aggregate does not separate from the cement paste (Self-Consolidating High Performance Concrete, n.d.).

From Figure 1, it can be seen that SCC can be proportioned by varying the mixture parameters to meet the criteria of excellent deformability, good stability, and low risk of blockage required to meet a variety of demands. Figure 1 outlines the properties that make SCC attractive to many users and demonstrates that good flowability does not necessarily mean SCC. However, these properties can come with some added disadvantages, as seen in Figure 1, and come at the cost of the viscosity and low-yield values.

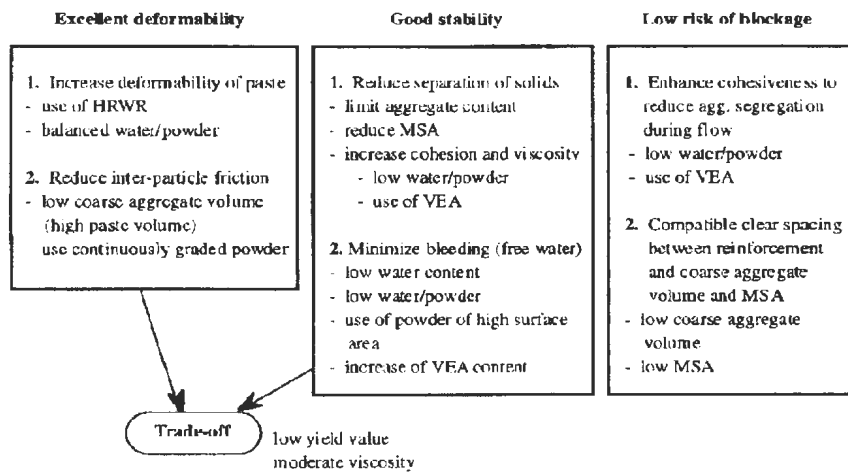


Figure 1 – Description of SCC (Khayat 1999)

Since its first use in Japan in the late 1980s, SCC has become a more viable replacement to normal concrete due to its high flowability and ease of placement, which result in reduced placement costs. In North America, SCC gained popularity due to several key factors: i) its reduced cost for placing, which can speed up construction (by reducing labour costs) and truck turnaround, ii) improved working environment and safety caused by the elimination of mechanical vibrations (trip hazards due to cords, fall hazards from placing concrete in high places, etc.), and iii) improved aesthetics due to its high flow, which creates smooth formed surfaces (Grace Construction, n.d.). When SCC was first introduced to the North American market, it relied on relatively higher binder contents and larger quantities of chemical admixtures (i.e. superplasticizers) to achieve the desired flowability and stability (Self-Consolidating High Performance Concrete, n.d.). Due to these factors, which play a major role in the cost of SCC, its early use in North America was limited.

The production of SCC is normally achieved by a) increasing the quantity of fines in the mixture, which can be achieved by incorporating mineral admixtures such as fly ash, ground granulated blast furnace slag, volcanic ash, cement kiln dust, etc., b) adding viscosity modifying admixtures (VMA) (Khayat et al. 2001), and/or c) decreasing the coarse aggregate content in the mixture (Khayat et al. 1997; Lachemi et al. 2005).

1.1.1 Fresh Properties of SCC

Normal concrete mixtures use a procedure called the slump test to measure the workability of the mixture. This test, the only test typically conducted for normal concrete, measures the vertical slumping distance of the mixture. Properties such as viscosity, passing ability, and segregation are not measured when using normal concrete. The viscosity of a mixture is its ability to gradually resist deformation by shear or tensile stress. Viscosity is due to friction caused by the surrounding particles of the mixture (Symon 1971). A mixture (or fluid) that has zero or little resistance to shear stress is said to have zero viscosity. Therefore, in concrete a decrease in the viscosity of the mixture means a decrease in the resistance to the shear stress (self-weight) and allows for faster flow rates, indicating better flowability. A decrease in the viscosity can, however, lead to a greater chance for segregation, due to the mixture losing its ability to suspend (or resist) the weight of the aggregates. The passing ability of the mixture refers to its ability to pass through reinforcement with little or no blocking behind the reinforcement. When placing SCC, the aggregates need to be able to pass through the reinforcement; this is done through the suspension of the aggregate in the paste matrix that carries the aggregate. As

mentioned with respect to the viscosity, the passing ability can be affected by the viscosity of the mixture or the ability of the mixture to hold particles in suspension.

Segregation in SCC is referred to as the separation of the particles from the paste matrix. When the viscosity of the mixture is decreased to a large extent, the mixture loses its ability to keep the aggregates in suspension. The aggregates then separate and sink to the bottom. This is undesirable and can cause loss of strength and poor passing ability.

Since SCC flows, the normal slump test cannot measure the slump of the mixture as the concrete spreads horizontally. This horizontal spread is measured and is referred to as the slump flow diameter (Section 3.1.1). For SCC there are also other tests that have been developed to measure how well the SCC mixture performs. As already mentioned, the slump flow test is conducted to measure the flowability (or filling ability) of the mixture. This test can also be used to judge the viscosity of the mixture by recording the time it takes the concrete to reach a 500 mm diameter; this is called the T_{50} time. A final observation from this test can be done, by visual inspection only, to judge the segregation or the stability of the mixture. In addition to using the T_{50} time to measure the viscosity of the mixture, another apparatus, called the V-Funnel, is used (Section 3.1.4). It consists of a V-shaped device with an opening at the bottom, which is filled with concrete. The time it takes for the V-Funnel to empty is used as a measure of the viscosity of the mixture. To measure how well the mixture can pass through reinforcement, a test referred to as the J-Ring test (Section 3.1.2) has been developed. The test consists of a ring of reinforcing bars that fit around the base of the slump cone. The test is performed in the same manner as the slump flow test. The flow with and without the J-Ring is measured and used to

judge the passing ability of the mixture. As with the slump flow test, the time it takes the concrete to reach a 500 mm diameter is recorded, referred to as the T_{50J} , and can be used to measure the passing ability of the mixture. When using the J-Ring test, the segregation of the mixture can also be measured using a blocking index. Another device called the L-Box (Section 3.1.3) can also be used in conjunction with the J-Ring apparatus to measure the passing ability of the mixture. The L-Box is an L-shaped device with three or four reinforcing bars with a gate. The device is filled with concrete and the gate is opened. The height of the concrete, after it has stopped flowing, is measured at the end (H2) and beginning (H1) of the device, and the H2/H1 ratio is taken to measure the passing ability. The closer the ratio of H2/H1 is to one, the more desirable and better passing ability the mixture has.

1.1.2 Mechanical Properties of SCC

For both normal concrete and SCC, the mechanical properties are measured to determine the compressive strength, flexural strength, tensile strength, and elasticity of the mixture. These parameters are important in designing all structural elements: for example, for determining loads and reinforcement requirements.

The compressive strength (Section 3.1.6) of the mixture, when used in calculating loads and resistances, is typically measured at 28 days. However, the development of the compressive strength of the mixture is important during construction for the removal of the formwork, as well as when loads of the structure can be placed or continued. The compressive strength is measured by means of a compressive testing machine, which

applies a load at a constant rate. When the cylinder fails, the compressive strength is recorded.

Flexural strength of concrete (Section 3.1.7) is used to calculate the modulus of rupture of a concrete specimen. It is the ability of the hardened mixture to resist deformation under an applied load. It is a measure of an unreinforced concrete beam or slab to resist failure in bending. Since concrete is weaker in tension compared to its compressive strength, a rectangular specimen is placed in a three- or four-point bending configuration and a load is applied until fracture to measure its capacity. As this test measures the unreinforced capability of concrete, the measurement is rarely used in structural design and is considered more appropriate for concrete pavements and unreinforced slab designs (National Ready Mixed Concrete Association 2000).

The indirect tensile test, also known as the splitting tensile strength (Section 3.1.8), is an indirect measure of the tensile forces in concrete. As with the flexural tests, the indirect tensile test is a measure of the tensile forces in concrete and its ability to resist these forces (Building Research Institute (P) Ltd., n.d.). However, unlike the flexural test, which simulates more bending forces, the indirect tensile stress represents more of a pulling apart (tension) of the concrete. It is normally performed on cylinders placed lengthwise with a compressive load applied to them. Modulus of Elasticity (Section 3.1.9) describes the ability of an object to deform elastically when a force is applied. Typically, the Modulus of Elasticity is defined as the slope of the linear region (elastic region) of a stress-strain curve.

Young's modulus describes the tensile or compressive elasticity of an object to deform along an axis when resisting forces are applied, and is defined as the ratio of tensile stress to tensile strain. In concrete, the Modulus of Elasticity is a function of the aggregate and the paste matrix, and therefore can be affected by the use of stronger aggregates or supplementary cementitious materials (SCMs). The Modulus of Elasticity of concrete is relatively constant at low stress levels, but it starts to decrease at higher stresses due to the formation of micro cracks.

The mechanical properties of concrete can be affected by the mixture design. Using SCMs, varying the coarse aggregate size and/or volume, as well as changing the air content can impact the hardened properties (the effect of SCMs is discussed in section 1.1.3 and further discussion can be found in Chapter 2). However, one major concept that can influence the mechanical properties is known as the Interfacial Transition Zone (ITZ), further discussed in Chapter 2. The ITZ is a zone that forms around the aggregate and can cause weak chains to form in the concrete. The bigger the size and thickness of the ITZ, the weaker the mechanical properties would be. This zone is highly dependent on the size and volume of the coarse aggregate used.

1.1.3 Use of Supplementary Cementitious Materials

SCMs have been used in concrete for decades and their use is a common practice to reduce costs and improve the fresh and mechanical properties of concrete. The most widely used SCMs in concrete are fly ash, slag, and silica fume and are normally used as partial cement replacements.

Mineral admixtures have been used in SCC to improve the quality of both the fresh and mechanical properties, such as compressive strength, slump flow, and passing ability (Ding et al. 2003; Balaguru 2001). These same admixtures have been used as partial replacements with cement to reduce the overall cost while maintaining (with either a small or no change at all) essential fresh and mechanical properties of SCC (Uysal et al. 2011).

Silica fume has been used in concrete since the mid 1900s. Silica fume is a by-product of the silicon and ferrosilicon alloy production and consists primarily of SiO_2 . On average, silica fume particles are approximately 100 times smaller compared to cement particles with a surface area of 15,000 to 30,000 m^2/kg (Kosmatka et al. n.d.). Because silica fume consists of extremely fine particles and has a high silica content, silica fume is a very effective pozzolanic material and is usually added as a partial replacement to cement. It has been observed to assist in increasing the mechanical properties. This is due to the addition of very fine powder material and from the reaction between the silicates and free calcium hydroxide in the paste matrix (Detwiler et al. 1989). Due to its high surface area, the addition of silica fume can cause a loss in the workability because of the water absorbed by the silica fume. However, this property makes silica fume favourable in reducing coarse aggregate segregation. Since silica fume is a very fine material, it is widely used in SCC applications that require an increase in the amount of fine materials. As mentioned, the addition of silica fume absorbs water due to its large surface area, and this means that more admixtures are required to account for this loss in workability.

Ground granulated slag is also a by-product resulting from the process of smelting ore. Unlike silica fume, slag is an SCM that, when combined with water, can form some cementitious materials, whereas silica fume will not. The use of slag in concrete can slow down the setting time as well, since the strength gain is usually up to seven days, but it gains strength over a longer period of time compared to ordinary plain cement. Slag usually increases the workability of the mixture due to the increase in the paste volume caused by the lower relative density (Hinczak 1990). This increase in the workability makes it attractive in the production of SCC, since less admixtures are required to achieve the high flowability of SCC. Additionally, the high replacement percentages that can be used by slag allow for greater replacement of cement, thus reducing the cost. Slag is also beneficial on the mechanical properties, where it can improve the strength of the concrete as well as the flexural strength (Transportation Research Board, National Research Council 1990).

In recent years, a new type of SCM, known as metakaolin, has been used in the production of normal concrete, with limited applications with SCC. Metakaolin is a kaolin clay that is burned at temperatures ranging from 600° to 900° Celsius in a process that turns the kaolinite into calcinate, which can then be used as a cement replacement. Unlike other SCMs (especially silica fume), metakaolin is carefully produced in a controlled manner to remove impurities and obtain particular particle sizes. It therefore has a much higher degree of pozzolanic reactivity (Brooks 2001; Ding 2002). Metakaolin can also be used in concrete to increase the compressive strength and strength gain, as well as the flexural strength. Use of metakaolin reduces the permeability, thus increasing

the density of the concrete and improving the durability (Metakaolin Application and Benefits, n.d.). In SCC mixtures, the use of metakaolin has also been shown to improve the passing ability of the mixture and increase the viscosity (Hassan et al. 2012).

1.2 Shear Behaviour of Normal and SCC Beams

1.2.1 Analysis of Shear in Reinforced Concrete Beams

The ability of concrete beams or slabs to resist shear forces is dependent on many factors, such as the mixture design and reinforcement details. In terms of the mixture design, the types of SCMs that increase the mechanical properties (silica fume and metakaolin, for example) can be used to increase the compressive strength, thus increasing the concrete shear resistance. Also, the volume and size of the coarse aggregate is important for the aggregate interlock to resist the shear forces as well as their impact on the ITZ, which affects the hardened properties of concrete.

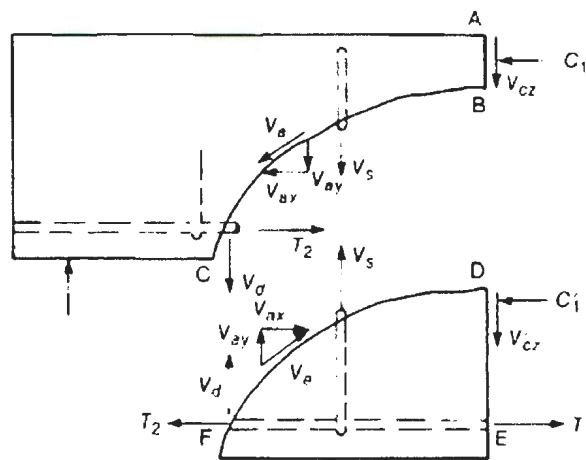


Figure 2 – Shear Mechanics in Concrete Beams (MacGregor 2000)

Figure 2 shows the shear mechanics in concrete beams. The maximum shear resistance of a concrete beam (V_r) is equal to the shear transfer by the concrete (V_c) plus the shear transferred by the transverse reinforcement (V_s). The shear transferred by the concrete is the sum of the resistance of the uncracked concrete in the compression zone (V_{cz}), the dowel force resulting from the longitudinal reinforcement (V_d) and the vertical component of the aggregate interlock (V_{ay}). Each of these individual components and their respective effect on the shear resistance can be seen in Figure 3. In concrete beams, the two main components that affect the shear capacity of the beam are the aggregate interlock, which normally accounts for 35 to 50% of V_c , and the uncracked concrete in the compression zone, which accounts for 20 to 40% of V_c . Normally, the dowel action is not very significant if transverse reinforcement is not present in the beam (MacGregor et al. 2000). Therefore, in SCC, which normally uses more fine materials, the shear capacity can be greatly affected by the reduction in the aggregate interlock contribution to the shear capacity compared to normal concrete mixtures.

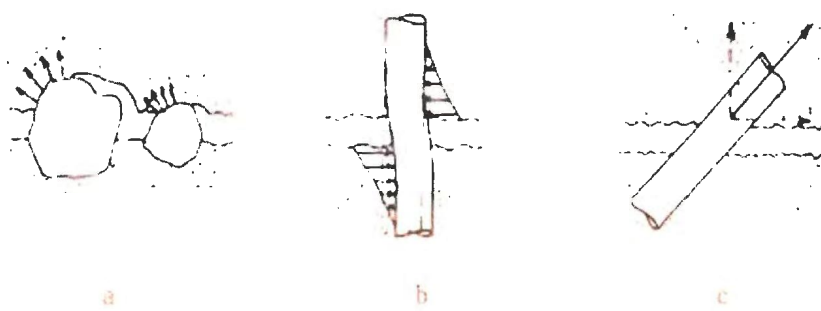


Figure 3 – a) Aggregate Interlock, b) Dowel Action, and c) Axial Steel Force (Walraven 1980)

In high-strength concrete, the paste matrix is usually stronger than the aggregate; therefore, the cracks that develop go through the aggregate and cause a smooth surface along the fracture, which then causes a reduction in the total shear transfer through the aggregate interlock.

1.3 Significance of Research

As mentioned earlier, the cost of concrete relies heavily on the cement dosage used in the mixture. Therefore, when designing concrete mixtures for affordability, it is necessary to limit the cement dosage (while maintaining acceptable fresh and hardened properties) to keep costs at a minimum. Producing SCC relies on increasing the amount of fine materials in order to make the mixture flow. This is usually done using higher cement amounts. Due to the expected higher cement content in SCC mixtures, many construction projects that plan on using SCC see an increase in costs through the amount of cement used. The cost of SCC is also heavily dependent on the amount of chemical admixtures required to produce such high flow rates and to adjust the viscosity of the mixture. High dosages of high range water reducer (HRWR) admixtures are normally required to achieve flow and can greatly increase the cost of the mixture when combined with the high amount of cement required. Normal concrete, compared to SCC, requires mechanical vibrations to be placed, which can subsequently lead to increased labour costs and concerns with regard to finishing and environmental impact.

Therefore, there is a growing need to develop cost-effective SCC mixtures containing relatively low cement content, while also maintaining the proper flowability of the mixture with high strengths and good mechanical properties. Proportioning SCC with

SCMs allows for the replacement of cement with equivalent or even finer materials (such as metakaolin, fly ash, silica fume, and/or slag) and can reduce the amount of cement in the mixture while maintaining high total cementitious materials. Metakaolin has been successfully used in normal concrete since the 1990s and has proved to be quite effective in improving the overall mechanical and durability of normal concrete. Metakaolin, similar to silica fume, reacts with the calcium hydroxide formed during Portland cement hydration (creating additional cementitious products), which modifies the concrete structure and enhances its overall mechanical and durability performance. Metakaolin has a particle size that is much finer than cement but not as fine as silica fume, and it therefore offers better workability. Metakaolin has a number of other benefits as well: it has a creamier texture, generates less bleed water, provides better particle suspension, and has better finish-ability than concrete containing silica fume. However, using metakaolin as a cement replacement in the production of SCC is a relatively new approach in concrete technology.

The effect of metakaolin in the development of SCC mixtures is relatively new. It needs to be further investigated in order to study the impact it will have on SCC and to determine the optimum replacement percentage that will ensure maximum benefits in terms of fresh and mechanical properties. The mixture design is especially important when using SCC, since SCC requires an increase in the amount of fine materials in order to achieve good flowability with a lower possibility of segregation. Therefore, most SCC mixtures use a much lower C/F ratio compared to normal concrete, which means an increase in the fine aggregate, but also a decrease in the coarse aggregate. However, the

coarse aggregate plays an important role in the structural properties, especially the shear capacity of concrete structures (through aggregate interlock). Therefore, decreasing the C/F ratio can also decrease the structural performance of the SCC mixture, although it is beneficial to its fresh properties (such as the flowability and passing ability).

The size of the coarse aggregate should also be taken into consideration when designing SCC. Using smaller coarse aggregates allows for higher mixture strengths due to the increase in the improvement of the ITZ around the coarse aggregate. Using a smaller coarse aggregate can increase the passing ability of the mixture and allows the mixture to fill congested reinforced structures. The aggregate size also plays an important role in the shear capacity of concrete structures by means of aggregate interlock, which assists with the post diagonal cracking resistance. In addition, the mixture design can be varied to increase or decrease the total binder content of the mixture. The air content of the mixtures can also be varied to try and improve the fresh properties of the mixture. Adding air entrainment, however, causes the formation of tiny air bubbles, which can reduce friction and enhance flowability and can cause losses in the mechanical properties of the mixture. The impact on the mechanical properties may deter designers from using air entrainment.

Therefore, it is necessary to optimize the mixture design of SCC in order to reduce the amount of cement in the mixture, as well as to limit the amount of chemical admixtures required to achieve the desired flowability. The mixture design needs to be varied to achieve the maximum benefits for the fresh properties and to achieve good flowability, passing, viscosity, and to limit the segregation of the mixture.

The mechanical properties of SCC also need to be optimized by varying the mixture design to achieve the highest compressive strengths, flexural strength, and to enhance other mechanical properties in order to reduce the cost associated with using SCC. Shear strength of SCC mixtures is an important factor for engineers to consider when designing structural elements, such as SCC beams, since the shear strength is likely to be affected by varying the mixture design (change in the size or volume of the coarse aggregate). It is also important to study the shear strength when optimizing the mixture proportions of SCC.

To summarize, the main objective of this research is to develop optimum SCC mixtures incorporating metakaolin – using different percentages of metakaolin to achieve excellent flowability and passing ability without the mixture segregating – and varying the design of the mixture to reduce costs and improve the fresh properties of plain SCC. The mechanical properties of the developed SCC mixtures will be optimized by varying the mixture design to obtain the highest mechanical properties, while replacing the higher amount of cement in the mixture to increase the mixture's affordability. To correlate the structural performance to the fresh and mechanical performances of the developed mixtures, the research will also include optimizing the structure's performance (mainly the shear resistance of full-scaled concrete beams) of the developed SCC mixtures. This investigation will also compare the fresh, mechanical, and structural performance of the developed SCC mixtures with the performance of some common SCMs.

1.4 Scope of Research

This thesis aims to study the fresh and mechanical properties of SCC produced with metakaolin. The first stage of the study identified the optimum metakaolin replacement with cement by varying the metakaolin content from 0 to 25% in SCC mixtures. To study the impact of metakaolin on the fresh properties of SCC containing metakaolin, the slump flow, J-Ring, V-Funnel, and L-Box values were performed to measure the flowability, passing ability, and segregation factor for each SCC mixture. To study the hardened properties of the tested mixtures, the 28- and 90-day compressive strengths, strength development, flexural strength, splitting tensile, and Modulus of Elasticity tests were used to determine the effect of metakaolin.

Based on the results obtained from the first stage, the optimum metakaolin percentage was chosen and the effect of the mixture design on the fresh and mechanical properties of SCC mixtures were studied in the second stage. The C/F ratio, coarse aggregate size, binder amount, and air content were varied in this stage to optimize SCC containing metakaolin.

The third stage studied the effect of metakaolin and mixture design on the shear capacity of full-scale SCC beams. The results from the first stage were used to determine the optimum metakaolin replacement to use in the SCC beams. The C/F ratio, coarse aggregate size, and concrete strength were varied to study the effect of the mixture design on the shear strength of the tested SCC beams. Similar to the first stage, the slump flow test and the 28- and 90-day compressive strengths were conducted to ensure proper SCC had been obtained and that normal- and high-strength concrete beams had been achieved.

In this stage, strain gauges were placed on the reinforcing steel at the supports and mid-span of the beam; two strain gauges were placed on the surface of the concrete at the midpoint to study the strain of the concrete and reinforcement during the test. LVDTs were placed at $\frac{1}{4}$, $\frac{1}{2}$, and $\frac{3}{4}$ of the span length to study the deflection of all SCC beams. They were also used to determine the first diagonal crack in addition to the strain gauges. The loading, done using a manual hydraulic jack in three stages, was applied to 50%, 75%, and 100% of the theoretical calculated failure load, and at the end of each stage the crack widths were measured by means of a crack-measuring device. The overall behaviour of the beams, including the development of cracks, crack patterns, crack widths, crack heights, and failure modes, were observed and sketched for all beams.

2. Literature Review

2.1 Concrete and SCC Containing Metakaolin

2.1.1 Fresh Properties

Metakaolin has been used as a cement replacement for both normal concrete and with little applications in SCC. The use of metakaolin in concrete has been shown to reduce the workability and increase the viscosity of the mixture with an increasing replacement percentage. The effect of metakaolin on the fresh properties has been studied by many researchers and has also been compared to other typical SCMs, such as silica fume. Most have showed the effect that increasing the partial cement replacement with metakaolin has on the viscosity, yield stress, water demand, and HRWR demand. Keeping the metakaolin replacement percentage constant and adjusting the amount of water in the mixture was shown to increase the HRWR, as this reduces the water-to-binder ratio (W/B). Using a W/B ratio of 0.4 with an 8% metakaolin replacement has been shown to double the amount of HRWR compared to the control mixture (Justice et al. 2007). Khatib (2007) studied the effect of varying the metakaolin replacement percentage from 0 to 20% while using a low W/B ratio and showed that increasing the metakaolin replacement percentage led to a loss in the slump and ultimately the workability of the mixture. Also, Qian et al. (2001) showed the impact that increasing the metakaolin replacement percentage from 0 to 15% had on the slump flow when using a fixed amount of superplasticizer and a fixed W/B ratio. They showed that increasing metakaolin results in a reduction in the slump flow compared to normal concrete, and to

achieve a comparable slump flow required the addition of more superplasticizer (Qian et al. 2001). Using SCC requires a higher workability compared to normal concrete. Thus to achieve this high flow, a higher W/B ratio can be used but at a cost to the mechanical properties, as discussed later. In addition to increasing the W/B ratio, an HRWR admixture can be used to reduce the particle friction and enhance the flowability. However, using a low binder W/B ratio that has been used in normal concrete applications with metakaolin would require a large HRWR demand due to the loss of the slump flow. Therefore, it is essential to increase the W/B to offset this HRWR demand, but the effect on the mechanical properties must be taken into consideration as well. For use in SCC, Hassan et al (2010) studied the effects of metakaolin on the fresh properties of SCC. They found that increasing the metakaolin content increased the plastic viscosity of the mixture, which is beneficial for SCC as it slows down particle sedimentation and helps enhance the dispersion of solids in the plastic state (Hassan et al. 2010).

When compared to the use of other SCMs, such as slag and fly ash, metakaolin has been shown to have a higher HRWR demand. Guneyisi et al. (2011) conducted a permeation study between various SCMs and combinations of SCMs. Their study showed that using any percentage of metakaolin in SCC requires a greater amount of HRWR to produce a comparable slump than the other SCC mixtures investigated (Guneyisi et al. 2011).

Vejmelkova et al. (2011) showed that using a high replacement level of metakaolin (40%) required a larger amount of superplasticizer to achieve SCC compared to using SCC containing slag. Similar to Hassan et al. (2010), Vejmekova also showed

that SCC containing metakaolin has a large yield stress and lower viscosity (Vejmelkova et al. 2011). The loss of workability due to the addition of metakaolin can be offset due to the increase in the mechanical properties.

2.1.2 Mechanical Properties

There have been many investigations into the effects that using metakaolin has on the mechanical properties of SCC, including the compressive strengths, Modulus of Elasticity, flexural strength, and splitting tensile strength. The use of lower C/F ratios in SCC impacts some of the mechanical properties; however, much research has been done on the effects of metakaolin in normal concrete but few studies done with SCC. The main issue is that SCC normally requires the use of a higher W/B to assist in obtaining high flowability. Therefore, using a lower W/B ratio to achieve higher strengths is not common with SCC, due to the increase in the HRWR demand. Khatib (2008) studied the effect of replacing some of the cement in concrete with metakaolin in normal concrete. Khatib (2008) changed the metakaolin replacement percentage from 0 to 20%, while fixing the W/B ratio, and showed that increasing the partial replacement increased the compressive strength for all test days. As mentioned, Khatib (2008) limited the W/B ratio to 0.3, which is not common for use in SCC applications, and found that an optimum metakaolin replacement percentage was achieved at 15%, while others, such as Wild et al. (1996), have shown that when using a higher W/B ratio, a 20% replacement level provided better mechanical properties with use in normal concrete. As with Khatib (2008), some researchers have shown the optimum metakaolin replacement level when using normal concrete (and a low W/B ratio) to be around 15%. Qian et al. (2001) studied

various metakaolin replacements up to 15% while using a W/B ratio of 0.38 in normal concrete. It was shown that the compressive strengths greatly increased compared to the control mixture; the tensile properties of concrete were also shown to increase. However, around this W/B ratio the optimum metakaolin replacement level has been observed to be higher at 20%. Using a higher W/B ratio of 0.45, and adjusting the metakaolin replacement percentage from 0 to 30%, showed an optimum replacement level of 20%, which yielded the highest long-term compressive strengths (Wild et al. 1996). Other research, such as that done by Justice et al. (2007), has shown the impact of metakaolin on the mechanical properties of concrete at various W/B ratios. Justice et al. (2007) showed that using a metakaolin replacement of 8% greatly improved the compressive strength of concrete, and showed improvements in the Modulus of Elasticity and flexural strength of 5-19% and 20-40%, respectively. This study was conducted for normal concrete at W/B ratios of 0.4, 0.5, and 0.6, and, regardless of the W/B, the mechanical properties were improved. However, the mechanical properties decreased with an increasing W/B ratio. Since mechanical properties such as the flexural strength, splitting tensile strength, and Modulus of Elasticity are dependent on the compressive strength, this highlights the importance of maintaining a low W/B to maximize the mechanical properties – more importantly the compressive strength – but for use with SCC a higher W/B is recommended for the workability requirements.

Metakaolin, compared to other SCMs, has been shown to obtain higher compressive strengths and similar and/or higher flexural strength, splitting tensile strength, and Modulus of Elasticity depending on the replacement levels used. Using a

similar metakaolin replacement to the typical silica fume replacement of 8% resulted in an average compressive strength that is higher at all test days, regardless of the W/B ratio used. In addition, the similar metakaolin replacement percentage to that of silica fume resulted in higher splitting tensile strength and flexural strength, but showed a reduction in the Modulus of Elasticity for W/B ratios of 0.4, 0.5, and 0.6 in normal concrete (Justice et al. 2005). Similar studies done by Razak et al. (2000), when using 10% metakaolin and silica fume replacements, showed that the compressive strengths obtained were higher when using metakaolin than those obtained when using silica fume at a W/B ratio of 0.3. Hassan et al. (2012) showed that using higher metakaolin replacement percentages of 20 and 25% resulted in higher 28-day compressive strengths compared to typical silica fume replacement percentages up to 11%. As with silica fume, slag has been used in normal concrete and SCC to enhance the mechanical properties while replacing large quantities of cement. Slag has been shown to achieve similar or slightly higher compressive strengths than normal concrete. Compared to using metakaolin, slag has been shown to produce 28- and 90-day compressive strengths lower, regardless of the metakaolin replacement percentage, when using SCC (Guneyisi et al. 2011). Also, when using higher replacement levels or metakaolin of 40% compared to high slag partial replacements of 60% in SCC, metakaolin still displays a higher compressive strength at any age of testing (Vejmelkova et al. 2011). Higher replacement percentages allow the use of less cement while still achieving high strength and improved mechanical properties and thus reducing the cost. Using SCMs that greatly improve the mechanical properties, even at smaller

replacement levels, can also allow for the use of less cement. For SCC, this can offset the cost of large amounts of HRWR necessary to produce the required flowability.

2.2 Factors Influencing the Fresh and Mechanical Properties of SCC

2.2.1 Varying the Coarse Aggregate Volume and Size in SCC

When designing normal concrete and/or SCC mixtures, it is important that the proportions of the mixture be carefully selected to meet the fresh and mechanical property requirements. A large part of this proportioning involves the aggregates, in particular the size and volume of the coarse aggregate. Basic proportioning, as stated in the literature, looks at various factors when designing a concrete mixture, such as flowability consistency and strength, to list some of the more widely used factors when designing concrete (ACI 211.1-91, 2002). From the ACI standard practice for mix proportioning, it can be seen that workability, consistency, and strength are dependent on the size and proportioning of the coarse aggregate. The ACI standard shows that when designing a mixture, increasing the nominal maximum size of the coarse aggregate tends to require less water to achieve the required slumps. In addition, the standard states that to achieve higher compressive strengths, less mixing water should be used in the proportioning (ACI 211.1-91, 2002).

When designing SCC, the coarse aggregate size and volume play a key role in the fresh properties of the mixture, especially for the passing ability, as indicated by tests such as the L-Box. SCC uses large amounts of HRWR to achieve the high flowability of the mixture, but ensuring proper mixture proportioning can ensure improved passing

ability, or the ability of the mixture to flow through any confined spaces and properly fill the formwork. Jawahar et al. (2012) studied the effect of varying the blend of the coarse aggregate volume by using 10 and 20 mm coarse aggregate sizes. In addition, they investigated the effect of changing the total volume that the coarse aggregate makes up in SCC (increasing/decreasing the C/F ratio). Looking first at the effect of coarse aggregate size on SCC, it can be seen that when decreasing the amount of 20 mm coarse aggregate and increasing the volume of the 10 mm coarse aggregate, there was an improvement in the fresh properties indicated by the T_{50} , V-Funnel times, and the L-Box ratio. In addition to changing the coarse aggregate sizes, as the total coarse aggregate volume was decreased, the T_{50} , V-Funnel times, and L-Box ratio were enhanced (indicating better fresh properties) when the amount of water and superplasticizer were kept constant (Jawahar et al. 2012). Su et al. (2002) also showed the effect on SCC of decreasing the volume of the coarse aggregate and increasing the fine aggregate. The C/F ratio was changed from 2.3 to 0.8, which increased slump flow as well as the amount of superplasticizer, but there was little difference in the compressive strength and the Modulus of Elasticity was not significantly affected.

As reported by Mehta et al. (1993), the flexural, tensile, and Modulus of Elasticity are more dependent on the ITZ around the coarse aggregate compared to the effect of increasing the compressive strength. Jennings et al. (2008) reported that an increase in the volume of the coarse aggregate caused an increase in the porosity around the aggregate and is non-uniform compared to the surrounding paste. This area between the aggregate and the surrounding paste, referred to as the ITZ, resulted in a weak chain and produced a

loss in the mechanical properties of the concrete. Also, Larbi (1993) stated that the transition zone has low-density cement grains and contributed to a reduction in the overall strength and porosity of the concrete. As the volume of the coarse aggregate was increased, the total volume of ITZ increased, which reduced the quality of the concrete and the strength development.

It was reported by Loannides et al. (2006) in a study carried out for the Ohio Department of Transportation that larger coarse aggregates can lead to a reduction in the mechanical properties, such as compressive strength. This can be attributed to the smaller surface-to-volume ratios of the larger coarse aggregates compared to smaller coarse aggregates. The decrease in the surface area resulted in a weakened bond between the coarse aggregate and the paste matrix on which the mechanical properties rely.

2.2.2 Binder Content of SCC

The total binder, or the total cementitious materials, has a direct correlation to the fresh and mechanical properties of any concrete mixture. One investigation performed by Marar et al. (2011) varied the cement from 300 to 650 kg/m³ (total binder) and found that increasing the cement content was shown to increase the slump of the concrete mixture. In addition to the increase seen in the slump of the mixture, the 28-day compressive strength increased as the total binder (cement content) was increased. An increase in the compressive strength of 144%, as the cement content was increased from 300 to 650 kg/m³, was observed (Marar et al. 2011). In addition to this, an increase in the binder amount/content when using SCC can reduce the amount of HRWR and VMA required to produce the high slump flows desired. While optimizing the performance of air-entrained

SCC, Khayat (1996) varied the total binder content for some mixtures while fixing the W/B ratio. Mixtures used a combination of SCMs such as fly ash and slag, but the results were the same. Increasing the binder content, regardless of the type of SCMs used, showed that less HRWR was required to produce the same slump flow for the mixtures, or less HRWR was used and a larger slump flow diameter was obtained.

2.2.3 Use of Air in SCC

Air entraining admixtures (AEA) have been used in concrete to improve the fresh properties and durability characteristics of the mixture. Using an AEA causes the formation of tiny air bubbles that form bubble bridges. These have been shown to increase the yield stress, while the fluid action of the bubbles results in a decrease in the mixture's viscosity, and mixtures using HRWR show an increase in the yield stress and viscosity (Struble et al. 2004). These tiny air bubbles act the same way as ball bearings, and have been shown to improve the flowability of concrete (Mindess et al. 2003). In addition to the improvement seen in the flowability and passing ability, air entrainment can decrease bleeding in concrete due to the reduction in the movement of water (Shetty 2001) and can reduce the segregation resistance of the concrete by affecting the plastic viscosity of the mixture (Khayat 2000). As well, standard practices, such as Standard Practice for Selecting Proportions for Normal, Heavyweight and Mass Concrete, state that the use of an AEA causes a lubrication effect due to the formation of air bubbles, and thus mixtures incorporating entrained air can be proportioned with up to 10% less water than non-air-entrained concrete (ACI 211.1-91 2002).

AEAs, however, can have a negative impact on the concrete mixture. The use of entrained air has been shown to reduce the mechanical properties of concrete. A loss of compressive strength after 7 and 28 days was reported by Yogendran et al. (1987) who showed that increasing the air content of the mixture resulted in a 25% and 22% decrease in the 7- and 28-day compressive strengths, respectively. Various manuals for designing concrete state that air entrainment is beneficial for workability and durability but can cause a loss in the mechanical properties, and, therefore, to maintain the integrity of the mechanical properties, air entrainment should be taken into consideration (this could be done by lowering the W/B ratio or by increasing the binder content) (ACI 211.1-91, 2002; Minnesota Department of Transportation 2003). From Figure 4, it can be seen that using air entrainment, regardless of the W/B ratio, reduced the compressive strength and its associated mechanical properties related to the strength of the concrete (flexural strength, indirect tensile strength, etc.).

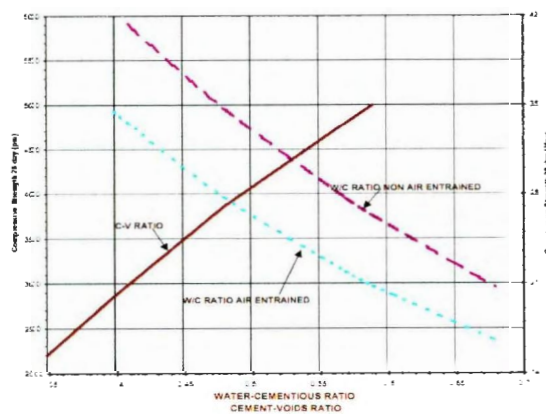


Figure 4 – Compressive Strength Related to W/B Ratio and Air Entrainment (Minnesota Department of Transportation 2003)

2.3 Shear Strength in Normal and SCC Concrete Beams

The shear strength of SCC mixtures is an important factor for engineers to consider in the design of structural elements such as SCC beams. Many factors in the mixture design have an impact on the shear resistance of concrete beams and their cracking behaviours. Previous research has shown that an increase in the coarse aggregate content or size in concrete causes a loss in the mechanical properties due to the increasing volume of bonds in the ITZ (Akcaoglu et al. 2002). As with SCC beams, the aggregate plays an important part in the shear resistance and assists with post diagonal cracking due to aggregate interlock, which is a major role in the shear capacity of concrete beams (Taylor 1970). Another study carried out by Lachemi et al. (2005) used different sizes and contents of coarse aggregate to compare the shear resistance of SCC and NC beams. Lachemi et al. (2005) concluded that the increase in size and content of the coarse aggregate improved the post-cracking shear transfer mechanisms and increased the ultimate shear strength of SCC beams.

2.4 Shear of High-Strength Beams

The strength of the concrete mixture should also be taken into consideration when designing SCC beams. The mechanical properties of any concrete mixture are often related to the compressive strength of the mixture. Thus increasing the compressive strength can improve such mechanical properties as the splitting tensile strength or flexural strength. When using high-strength concrete, the paste matrix becomes as strong or stronger than the aggregates. Hence, the diagonal crack failure can penetrate the coarse aggregates rather than finding a way around them, which causes a smoother failure path,

and therefore properties such as aggregate interlock could be reduced. There is limited research, however, on the effect that concrete strength plays on the aggregate interlock. A study performed by Kim et al. (2010) showed that when using higher-strength SCC beams the aggregate tended to have more fractures and, therefore, did not contribute significantly to the aggregate lock. These fractures caused a smooth surface and the forces that resist the shear forces were reduced. However, when using lower-strength beams the aggregates tended to fracture less, resulting in a greater aggregate interlock effect (Kim et al. 2010).

3. Experimental Program

3.1 Fresh and Mechanical Property Tests

3.1.1 Slump Flow Diameter and T_{50} Tests

The slump flow diameter test is a measure of the flow time and flowability of the mixture. The test involves filling a slump cone with SCC, as shown in Figure 5, and lifting the cone in an upward motion for a 3–5-second interval. As the cone is lifted, the concrete flows in a diameter on the slump plate; when the SCC mixture has stopped (with no noticeable flowing of the mixture), three diameters are recorded to obtain an average slump flow diameter.

The T_{50} time is a measurement of the flowability of the SCC mixture. To obtain the T_{50} time, a circle with a diameter of 500mm is drawn on the slump plate. The time it takes for the SCC mixture to reach this 500 mm diameter is recorded, and this is denoted as the T_{50} time (time to reach a 500 mm slump flow diameter). The slump flow diameters and T_{50} times are dependent on the flowability the user wants. To obtain a larger slump flow diameter or a faster T_{50} time, more HRWR can be added or SCMs, such as slag, can be used to improve these values.

According to the European Guidelines for Self-Consolidating Concrete (European Project Group 2005), the required slump flow diameter is dependent on job requirements but should be no less than 520 mm.



Figure 5 – Slump Flow Diameter Apparatus

3.1.2 J-Ring and T_{50J} Tests

The J-Ring is an apparatus that simulates SCC flowing through reinforcement and measures the passing ability of the SCC mixture. The test is the same as the slump flow diameter test, but instead a ring, as seen in Figure 6, is placed on the slump plate and the slump cone is placed inside the ring. The time to a 500 mm diameter is also recorded and this represents the T_{50J} time, or the time for the SCC mixture to flow through the “reinforcement” and reach a 500 mm diameter.



Figure 6 – J-Ring Apparatus

As with the slump flow diameter and T_{50J} times, these parameters are affected by the viscosity and segregation of the SCC mixture. Using SCMs can affect the viscosity and segregation of the mixture, and thus greatly impact the passing ability, as measured by the J-Ring test.

3.1.3 L-Box Test

A typical L-Box apparatus can be seen in Figure 7. The L-Box device is used to test the passing ability of SCC by simulating SCC that has been poured into a form and flows down around the “reinforcement.” Unlike the J-Ring test (which measures the horizontal flow and passing ability), the SCC in the L-Box has a greater height difference and represents a more vertical flowability of the SCC down through the formwork. To determine the L-Box ratio, $H2/H1$, the height of the SCC mixture is taken at two locations. Once the SCC has stopped flowing, the first height, $H1$, is measured at the start location of the L-Box, while the second height, $H2$, is measured at the end of the L-Box

apparatus. H1 and H2 are used to determine the ratio of $H2/H1$, which represents how well the SCC mixture passed through the openings. A higher $H2/H1$ ratio (e.g. 0.9) means the SCC mixture is very efficient in passing through the openings. A lower ratio represents the opposite, where most of the unacceptable SCC mixture built up behind the openings and did not pass through the openings.



Figure 7 – L-Box Test Apparatus

The European Guidelines state that SCC mixtures should obtain an $H2/H1$ ratio greater than 0.75 to ensure an adequate passing ability (European Project Group 2005).

3.1.4 V-Funnel Test

A typical V-Funnel test apparatus can be seen in Figure 8. The V-Funnel tests can be used to measure the viscosity of any SCC mixture, as well as the segregation factor. The viscosity is measured using the initial V-Funnel time. This time represents the time for the SCC mixture to flow through a restricted opening. As the SCC mixture becomes more viscous, the time for the SCC to flow through this opening increases. A good SCC

mixture should have a low initial V-Funnel time of less than 10 seconds (European Project Group 2005), whereas an SCC mixture with a higher viscosity has a slower flow time and is therefore not desirable for filling formwork. However, an increase in the viscosity can be beneficial to the thixotropy of the mix, which can assist in the segregation of the mixture by ensuring proper suspension of the aggregate during the flow.

To measure the segregation factor using the V-Funnel, the V-Funnel time after 5 minutes is required. To obtain this value, the V-Funnel is filled with the SCC mixture and allowed to settle for 5 minutes. After waiting 5 minutes the gate is opened and the SCC mixture is allowed to flow; the time to empty the V-Funnel is then recorded. The V-Funnel time after 5 minutes is affected by the viscosity and segregation of the mixture. A less viscous mixture results in a matrix that cannot hold the coarse aggregate in suspension, and thus they settle and block the gate. Increasing the volume of coarse aggregate can also compound with this issue and increase the segregation factor. The segregation factor is calculated using Equation 1, where t_0 is the initial V-Funnel time and t_5 is the V-Funnel after 5 minutes.

$$\text{Segregation Factor, } S_f = \frac{t_5 - t_0}{t_0} \quad (\text{Equation 1})$$



Figure 8 – V-Funnel Test Apparatus

3.1.5 Air Content Test

Air content is a measure of the percentage of either entrapped or entrained air in any concrete mixture. All concrete mixtures have a small amount of air within the mixture due to mixing and placing of the concrete. This air percentage is referred to as entrapped air and normally ranges anywhere from 0 to 2%. These air pockets are usually large in size and are randomly distributed and not interconnected, and they can be very harmful to any concrete mixture when the air content is high. However, another type of air known as entrained air is added using a chemical compound. This chemical introduces small, connected air bubbles into the mixture and is usually better for the concrete durability compared to entrapped air. Both entrapped and entrained air reduces the overall

mechanical properties of the concrete mixture, but can improve the fresh properties of the mixture such as viscosity.

3.1.6 Compressive Strength and Strength Development Tests

The 28-day strength test is the most important compressive test result, as most mixtures are designed to reach their compressive strength at this day. Further development of the strength after 28 days should also be conducted to see the improvement in strength after 28 days, since some concretes will still show a moderate strength gain after 28 days depending on factors such as the type of SCM used (fly ash, for example). From the compressive strength tests at different ages, the strength development can be determined and compared across various mixtures to show how fast or slow concrete mixtures gain strength. This is important in the precast industries, for example. The strength development is a measure of the development of the 1-, 3-, and 7-day compressive strengths (and sometimes the 14-day strength) respective to the mixture's 28-day strength. The 1-, 3-, and 7-day compressive strengths are all normalized by dividing this value by the 28-day compressive strength for that mixture and yield a percentage of the strength that has been developed. The strength development can be affected by the type of SCMs used, water/binder ratio (W/B), curing method, air content, as well as coarse aggregate size and volume.

To test the compressive strengths and strength developments, three cylinders with a diameter of 100 mm and length of 200 mm were tested after 1, 3, 7, 14, 28, and 90 days, and their respective strengths were recorded.

3.1.7 Flexural Strength/Modulus of Rupture Test

The flexural strength is used to determine the modulus of rupture to measure the concrete's ability to resist tensile forces when subjected to bending forces. In plain concrete structures, such as concrete pavements or slabs on grade, little to no reinforcement is used and only the concrete resists the tension forces. Along with other mechanical properties, the flexural strength is usually related to a percentage of the compressive strength, as seen in Equation 2. The flexural strength of concrete is affected by the use of SCMs, the W/B ratio, as well as the volume and size of the coarse aggregate.

Looking closer at the area around the coarse aggregate (ITZ), this zone has been shown to greatly affect the mechanical properties of concrete by causing weak bonds to form around the surface of the aggregate. Water particles can build up around the surface of the coarse aggregate and cause a larger crystalline structure to form, increasing the pore size with respect to the surrounding paste matrix. These less dense areas that form around all of the coarse aggregate create a weak chain through the concrete structure. Increasing the aggregate size or increasing the volume of the coarse aggregate amplifies this weakness and results in a decrease of the mechanical properties, in this case the flexural strength (also a reduction in the modulus of rupture) (Larbi 1993; Metha et al. 1993).

$$FS = 0.62 \text{ to } 0.87 \sqrt{f'_c} \quad (\text{Equation 2})$$

A three-point bending apparatus is used to apply a load at the centre of the prism and is loaded until failure, as prescribed in ASTM C293. The modulus of rupture is then calculated using Equation 3.

$$\text{Modulus of Rupture, } f_r = 3PL/bd^2 \quad (\text{Equation 3})$$

3.1.8 Splitting Tensile Strength

The splitting tensile strength is a measure of the tensile forces applied to concrete; it is used to determine the loads at which the concrete structure may crack and is related to a type of tension failure.

As previously mentioned, the splitting tensile strength for concrete is affected by the volume and size of the coarse aggregate. This is related to the ITZ discussed in Section 3.1.7, where the coarse aggregate causes weak bonds around its surface, which can lead to a weak chain throughout the sample. This can also cause the aggregate to not properly bond to the surrounding paste matrix and thereby offers little resistance to tensile forces. The splitting tensile strength is also related to the compressive strength of the concrete; a typical value is usually 10% of the 28-day compressive strength. A compression-testing machine was used to apply a load to the cylinder on its side until failure, as described in ASTM C496.

3.1.9 Modulus of Elasticity

The Modulus of Elasticity for concrete is dependent on the Modulus of Elasticity of the aggregates and the paste matrix. It is a measure of the elastic region of the concrete and how stress affects the strain of the concrete. Similar to the other mechanical

properties, the various mixture parameters – such as the type and amount of SCMs used, the volume and size of coarse aggregate, the W/B ratio, and the curing techniques – all affect the Modulus of Elasticity. A typical value for the modulus of normal-weight concrete can be seen in Equation 4.

$$E_c = 4731\sqrt{f'_c}, MPa \quad \text{(Equation 4)}$$

To measure the Modulus of Elasticity, a 25 mm strain gauge was glued to the cylinders prior to testing, and the load and strain were recorded. The load rate of the cylinders was kept constant, as per ASTM C469. Stress versus strain plots were plotted to determine the Modulus of Elasticity.

3.2 Shear Strength Test of SCC Beams

SCC beams were designed with no shear reinforcement so that the shear strength of SCC could be studied, and to examine the impact certain factors have on the shear resistance of concrete beams. All SCC beams were 1500 mm in length and 250 mm by 250 mm in width and depth, respectively. A total of 10 SCC beams were tested and for all SCC beams two #10M rebar were placed on the compression side and two #25M rebar were placed on the tension sides. As well, stirrups were only added at the location of the supports directly under the loading apparatus, so that no shear was resisted by the stirrups. The depth of all ten beams was constant at 187.5 mm, while the shear span was 495mm for all ten SCC beams. The shear span ratio (a/d) was held constant and was 2.5 for all ten SCC beams. A side profile showing the rebar, stirrup, supports, and loading details can be seen in Figure 9.

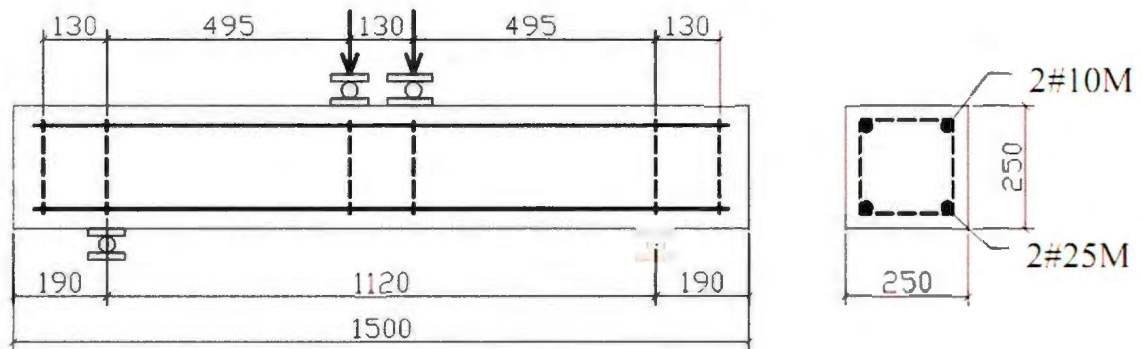


Figure 9 – Reinforcement, Support, and Loading Details

3.2.1 Crack Development

3.2.2 Post Diagonal Cracking

The post diagonal cracking represents the percentage of load capacity that the beam withstands after the first diagonal crack occurs. The post diagonal cracking resistance of concrete is affected by the strength of the concrete (i.e., high-strength versus normal-strength concrete), use of SCMs, as well as the coarse aggregate size and volume. It is measured by examining the load when the first diagonal crack occurs and finding the percentage the beam withstood until failure (max load) after the first diagonal crack occurred. The load at the first diagonal crack was visually observed during the time of testing, and the strain gauge data as well as the LVDT were examined. The load of the first post diagonal crack was denoted when the strain gauges and LVDT (at either end, depending on where the crack develops) suddenly jumped, noting the diagonal crack. This was done to confirm the visual observation during testing (Hassan et al. 2008; Hassan et al. 2010). This method of crack detection was also observed and performed by Li et al. (2001)

3.2.3 Crack Angle

The crack angle is referred to as the angle that the failure crack creates and is measured from the face of the beam. In normal-strength concrete, the crack failure angle is typically 30° , while for high-strength concrete this angle is shallower. A higher angle observed in the normal-strength concrete resulted in a reduction in the shear capacity of the beam compared to high-strength concrete. This is due to the decrease in the shear resistance area from the larger angle causing a shorter cracking path. The crack angle was visually observed during testing and sketched to scale.

3.2.4 Strain and Deflections

To measure the strain of the steel reinforcement and the concrete, a total of 8 strain gauges were placed in strategic locations, as seen in Figure 10. Strain gauges 1 and 4 were placed just outside the supports, while strain gauges 2 and 3 were placed on the inside of the supports and were used to aid detecting the load at the first diagonal crack. Finally, strain gauges 5 and 6 were placed at the centre of each of the two reinforcements (also centre of the beam), and two strain gauges were placed on the concrete at the same location as strain gauges 5 and 6. In addition to the strain gauges, three LVDTs were placed at $\frac{1}{4}$, $\frac{1}{2}$, and $\frac{3}{4}$ of the length to measure the deflection of the beams at these locations.

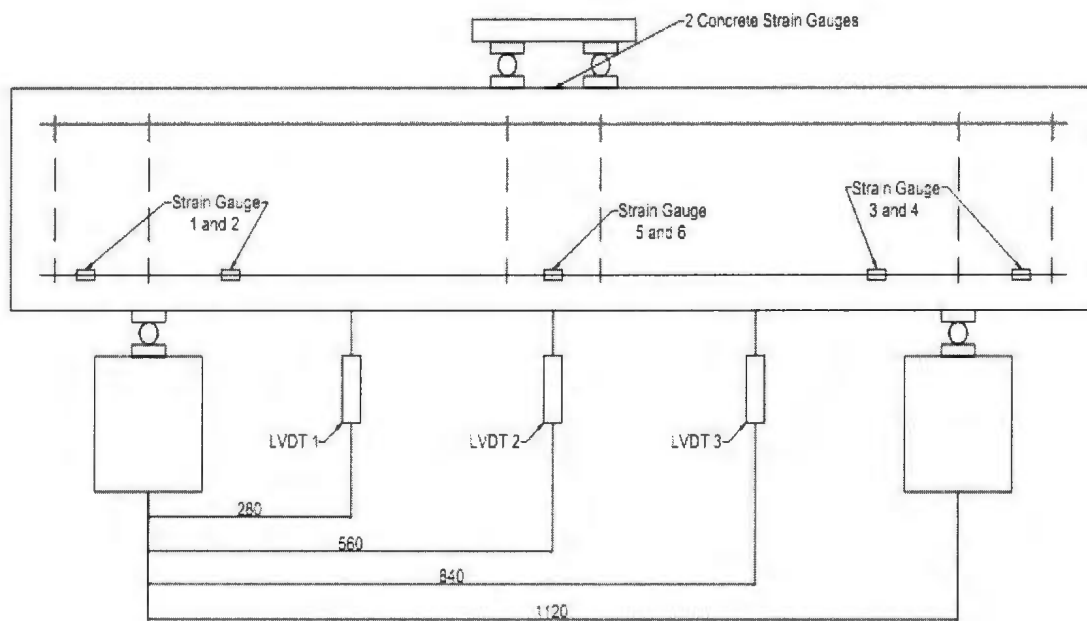


Figure 10 – Strain Gauge Locations for all 8 Strain Gauges

4. Mixture Design and Mixture Details

4.1 Materials

The metakaolin used in this research was delivered from the Eastern United States by Advanced Cement Technologies, conforming to ASTM C-618 Class N. The chemical and physical properties of cement, metakaolin, slag, and silica fume are shown in Table 1. Slag, silica fume, and type GU cement used in this investigation were conforming to ASTM Type I. Natural crushed stone with a 10 mm maximum size and natural sand were used for the coarse and fine aggregates, respectively. Each aggregate type had a specific gravity of 2.6 and absorption of 1%. HRWR conforming to Type F (ASTM C494) was used to adjust the flowability of the mixture. The specific gravity, volatile weight, and pH of the HRWR were 1.2, 62%, and 9.5, respectively.

An AEA similar to ASTM C260 was used to increase the air content of the required SCC mixtures. The specific gravity and pH of AEA were 1.01 and 10.7 to 12.3, respectively.

Table 1 – Chemical and Physical Properties of all SCMs Used

Chemical Properties (%)				
Chemical Properties (%)	Cement	MK	SG	SF
SiO ₂	19.64	51-53	40.3	>85
Al ₂ O ₃	5.48	42-44	8.4	-

Fe ₂ O ₃	2.38	<2.2	0.5	-
FeO	-	-	-	<5
TiO ₂	-	<3.0	-	-
C	-	-	-	<10
Cr ₂ O ₃	-	-	-	-
MnO	-	-	-	-
P ₂ O ₅	-	<0.2	-	-
SrO	-	-	-	-
BaO	-	-	-	-
SO ₄	-	<0.5	-	-
CaO	62.44	<0.2	38.71	<5.0
MgO	2.48	<0.1	11.06	<5.0
Na ₂ O	-	<0.05	-	-
C ₃ S	52.34	-	-	-
C ₂ S	16.83	-	-	-
C ₃ A	10.50	-	-	-
C ₄ AF	7.24	-	-	-
K ₂ O	-	<0.40	0.37	-
L.O.I	2.05	<0.50	0.65	-
Physical Properties				
Specific gravity	3.15	2.56	2.89	2.2

Grain Size, μm	45	45	-	-
Blaine Fineness (m^2/kg)	410	410	-	-
Color	Grey	Pink	Grayish white	Black

4.2 Mixtures for Stage 1 – Optimization of SCC Containing Metakaolin

The first stage was to investigate the effect of metakaolin on the fresh and mechanical properties of SCC to determine the optimum partial replacement level of cement with metakaolin. The mixture proportion for these 8 mixtures can be seen in Table 2. For this stage, 8 SCC mixtures that varied the metakaolin partial cement replacement level from 0 to 25% were investigated, while the remaining two mixtures contained selected replacement levels of silica fume and slag and were used for comparison. 8% and 30% cement replacement levels were chosen for silica fume and slag, respectively, based on optimal values obtained from previous work carried out with these SCMs (Hassan et al. 2010; Hassan et al. 2008). For these 8 mixtures, the C/F ratio was kept at 0.9 and the W/B ratio was held constant at 0.4. For all mixtures, enough HRWR was added to obtain a slump flow diameter of 650 ± 50 mm. Note, the amount of HRWR was guessed until the desired slump flow of 650 ± 50 mm and normally 3 to 4 mixtures were done to reach the required slump flow. The idea is to maintain the slump flow at 650 ± 50 mm and test the other properties. This is because the slump flow is the most critical property in terms of SCC placement. When this diameter was reached, the

slump flow, J-Ring, V-funnel, and L-Box tests were conducted, and then the required number of cylinders and prisms were formed.

The mixtures were designated according to the type of SCM replacement (silica fume, slag, and metakaolin) and percentage of cement replacement (0, 5, 10, etc.). For example, a mixture with a 10% metakaolin replacement would be designated as MK10.

Table 2 – Mixture Design for Stage 1

Concrete Type	Cement (kg/m ³)	SCM Type	SCM (kg/m ³)	CA (kg/m ³)	FA (kg/m ³)	Water (l/m ³)	HRWR (l/m ³)
Control	450	-	-	833.95	926.62	180	1.69
MK5	427.5	MK	22.5	831.93	924.36	180	2.38
MK10	405	MK	45.0	829.90	922.11	180	4.46
MK15	382.5	MK	67.5	827.87	919.86	180	5.29
MK20	360	MK	90.0	825.85	917.61	180	4.92
MK25	337.5	MK	112.5	823.82	915.35	180	5.38
SF8	414	SF	36.0	831.61	924.01	180	2.92
SG30	315	SG	135.0	831.02	923.36	180	1.38

*Note: The C/F ratio was fixed at 0.9 for stage 1.

4.3 Mixtures for Stage 2 – Improvement of SCC Containing Metakaolin

The optimum replacement percentage of metakaolin was chosen from stage 1 to improve the fresh and mechanical properties of SCC by varying the C/F ratio, coarse aggregate size, binder content, and percentage of air in the mixtures. In addition, SCC mixtures

using silica fume and slag replacements were conducted to be used as a comparison. For this stage, 24 SCC mixtures were produced with varying mixture parameters. Four mixtures used a C/F ratio of 0.7 and another four used a C/F ratio of 1.2. These mixtures are denoted by the SCM type used (metakaolin, silica fume, and slag) and the C/F ratio used for the mixture (0.7 or 1.2). For example, a mixture using slag and a C/F ratio of 1.2 would be designated as 1.2SG. A 20 mm natural coarse aggregate was used to produce another 4 mixtures using a constant C/F ratio of 0.9. These mixtures were designated based on the SCM used and the coarse aggregate size. Therefore, using slag and a 20 mm coarse aggregate would be denoted as 20SG. The 20 mm coarse aggregate had similar properties to the 10 mm coarse aggregate. Another four mixtures were used by increasing the binder content from 450 to 500 kg/m³ with a C/F ratio fixed at 0.9. As with the other mixtures, they were designated by the SCM type and binder amount; therefore, using metakaolin and 500 kg/m³ was labelled as 500MK. The last eight SCC mixtures varied the air content by 5 and 7%, and an AEA was added to produce the required air content of either 5 or 7%. These mixtures were denoted by SCM type and air content; 7%MK would represent an SCC mixture using metakaolin with 7% air content. As with stage 1, enough HRWR was added to produce a slump flow diameter of 650 ± 50 mm. When this diameter was reached, the slump flow, J-Ring, V-Funnel, and L-Box tests were conducted, and then the required number of cylinders and prisms were cast.

Table 3 – Mixture Design for Varying Mixture Parameters

Concrete Type	Binder Amount (kg/m ³)	Cement (kg/m ³)	SCM Type	SCM (kg/m ³)	C/F Ratio	Stone Size (mm)	CA (kg/m ³)	FA (kg/m ³)	Water (l/m ³)	HRWR (l/m ³)	AEA (ml/m ³)
0.7C	450	450	-	-	0.7	10	724.94	1035.63	180	2.88	0
0.7MK	450	360	MK	90.0	0.7	10	717.89	1025.56	180	5.72	0
0.7SF	450	414	SF	36.0	0.7	10	719.66	1028.08	180	3.31	0
0.7SG	450	315	SG	135.0	0.7	10	720.81	1029.73	180	1.85	0
1.2C	450	450	-	-	1.2	10	960.31	800.26	180	2.27	0
1.2MK	450	360	MK	90.0	1.2	10	950.97	792.48	180	4.62	0
1.2SF	450	414	SF	36.0	1.2	10	953.31	794.43	180	3.02	0
1.2SG	450	315	SG	135.0	1.2	10	954.84	795.70	180	1.24	0
5%C	450	450	-	-	0.9	10	833.95	926.62	180	2.31	26.15
5%MK	450	360	MK	90.0	0.9	10	825.85	917.61	180	4.60	35.38

5%SF	450	414	SF	36.0	0.9	10	827.88	919.86	180	3.20	21.54
5%SG	450	315	SG	135.0	0.9	10	829.21	921.34	180	1.41	15.38
7%C	450	450	-	-	0.9	10	833.95	926.62	180	2.15	40.00
7%MK	450	360	MK	90.0	0.9	10	825.85	917.61	180	4.82	53.85
7%SF	450	414	SF	36.0	0.9	10	827.88	919.86	180	3.22	40.00
7%SG	450	315	SG	135.0	0.9	10	829.21	921.34	180	1.43	23.08
20C	450	450	-	-	0.9	20	833.95	926.62	180	1.78	0
20MK	450	360	MK	90.0	0.9	20	825.85	917.61	180	4.62	0
20SF	450	414	SF	36.0	0.9	20	827.88	919.86	180	2.54	0
20SG	450	315	SG	135.0	0.9	20	829.21	921.34	180	1.23	0
500C	500	500	-	-	0.9	10	789.77	877.53	200	2.31	0
500MK	500	400	MK	100	0.9	10	780.76	867.52	200	4.92	0
500SF	500	460	SF	40	0.9	10	783.02	870.02	200	3.08	0
500SG	500	350	SG	150	0.9	10	784.50	871.66	200	1.69	0

4.4 Mixture Design for Beams

The optimum metakaolin replacement percentage from stage 1 was chosen to be used in SCC beams. It was found that 20% partial metakaolin replacement resulted in the best fresh and mechanical properties. Ten SCC beams with varying C/F ratios, coarse aggregate size, and strengths were prepared, and their respective mixture designs can be seen in Table 4. For all beams, the binder content was held constant at 500 kg/m^3 so that high-strength SCC could be produced for certain beams. In addition, the W/B ratio was held constant at 0.4. Six beams (beams 1 through 6) used a fly ash replacement of 60% so that these beams would produce a typical-strength SCC beam. The remaining four beams (beams 7 through 10) used 20% metakaolin as a partial cement replacement to obtain high-strength SCC. Beams 1 through 3 (denoted as B1, B2, and B3) used a 10 mm coarse aggregate, with a C/F ratio varying from 0.7 to 1.2, while beams 4 through 6 (known as B4, B5, and B6) used a 20 mm coarse aggregate, with a C/F ratio varying from 0.7 to 1.2. The high-strength SCC beams used C/F ratios of 0.7 for beams 7 and 9 (B7 and B9) and a C/F ratio of 1.2 for beams 8 and 10 (B8 and B10). Beams 7 and 8 used a 10 mm coarse aggregate, and beams 9 and 10 (B9 and B10) used a 20 mm coarse aggregate.

Table 4 – Mixture Design for the 10 SCC Beams

Concrete Type	Binder Amount (kg/m ³)	Cement (kg/m ³)	SCM Type	SCM (kg/m ³)	C/F Ratio	Stone Size (mm)	CA (kg/m ³)	FA (kg/m ³)	Water (l/m ³)	HRWR (l/m ³)
B1	500	200.00	FA	300	0.7	10	652.98	932.83	200	2.50
B2	500	200.00	FA	300	0.9	10	751.17	834.64	200	1.95
B3	500	200.00	FA	300	1.2	10	864.99	720.82	200	1.75
B4	500	200.00	FA	300	0.7	20	652.98	932.83	200	2.08
B5	500	200.00	FA	300	0.9	20	751.17	834.64	200	1.67
B6	500	200.00	FA	300	1.2	20	864.99	720.82	200	1.39
B7	500	400.00	MK	100	0.7	10	678.70	969.58	200	5.42
B8	500	400.00	MK	100	1.2	10	899.06	749.22	200	3.96
B9	500	400.00	MK	100	0.7	20	678.70	969.58	200	4.67
B10	500	400.00	MK	100	1.2	20	899.06	749.22	200	3.41

5. Results

5.1 Fresh Properties

5.1.1 Viscosity and Flow Ability

The results from the slump flow, J-Ring flow, slump flow – J-Ring flow and the J-Ring height differences are presented in Table 5. Table 6 shows the results for the V-funnel tests, the L-Box tests, segregation resistance and the air content for each mixture.

Table 5 – Slump Flow, J-Ring Flow, J-Ring Height Difference, and Slump Flow – J-Ring Diameter for Stage 1

Concrete Type	Slump Flow		J-Ring Flow		Slump flow – J-Ring Height	
	Diameter, mm	T ₅₀ , s	Diameter, mm	T _{50J} , s	J-Ring Diameter, mm	Difference, mm
Control	632	2.34	545	2.99	87	50
MK5	632	3.17	565	3.35	67	45
MK10	677	3.41	632	3.78	45	40.5
MK15	655	3.71	620	4.10	35	37.5
MK20	665	4.46	633	4.74	32	30
MK25	665	5.20	623	5.48	42	32.5
SF8	665	3.03	617	3.98	48	40
SG30	635	2.31	587	2.50	48	42.5

Table 6 – V-Funnel Times, Segregation Factor, H2/H1, and Air Content for Stage 1 Mixtures

Concrete Type	V-Funnel Times		Segregation Factor	L-Box H2/H1	Air Content, %
	Initial, s	After 5 minutes, s			
Control	16.76	42.91	1.560	0.18	1.35
MK5	25.33	56.00	1.211	0.23	1.20
MK10	28.83	49.21	0.707	0.30	1.45
MK15	29.67	45.60	0.537	0.34	1.55
MK20	31.44	42.72	0.359	0.43	0.95
MK25	33.16	71.69	1.162	0.39	0.70
SF8	13.72	34.23	1.495	0.38	0.80
SG30	14.74	32.70	1.218	0.42	1.75

5.1.1.1 Effect of Metakaolin

As previously mentioned, the viscosity of the concrete mixture has a direct impact on the T_{50} and V-Funnel times. As the viscosity of the mixture increases, the T_{50} and V-Funnel times increased. The ability of the mixture to flow around the reinforcement was measured by the T_{50J} time. Mixtures with low flowability should show a longer time to reach a 500 mm diameter (T_{50J} time). The results for the T_{50} , T_{50J} , and initial V-Funnel times are shown in Tables 5 and 6, as well as in Figure 11. The figure indicates that increasing the partial metakaolin replacement level increased the viscosity of the mixtures. The T_{50} times for mixtures using metakaolin as a partial cement replacement

increased with an increasing percentage of replacement from 0 to 25%. The T_{50} time for the control mixture was 2.34 seconds; it increased to 5.2 seconds when the partial metakaolin replacement level was increased to 25%. This is the expected result of replacing cement with metakaolin, which shows that by increasing the percentage of metakaolin, the viscosity of the SCC mixtures also increased (Cry et al. 2010). Compared to the other SCMs tested, metakaolin as a partial cement replacement had a higher viscosity for all replacement levels compared to 8% silica fume and 30% slag as partial cement replacements.

The T_{50J} times for all mixtures containing metakaolin were higher compared to the control mixture, indicating an increase in the viscosity and lower flowability. As the partial metakaolin replacement was increased from 0% up to 25%, the T_{50J} time increased by 83% while the T_{50J} time rose by 122% compared to the control mixture. This indicates a decrease in the flowability, which is expected as the percentage of metakaolin is increased in SCC (Hassan et al. 2010).

The viscosity of the mixture is also indicated by the V-Funnel test. The times for the V-Funnel test, as seen in Figure 11, were scaled down by dividing them by 10. From this test it was observed that increasing the percentage of metakaolin replacement increased the initial V-Funnel times, indicating an increasing viscosity. Madandoust et al. (2012) showed similar results: as the percentage of metakaolin increased, the V-Funnel flow times increased as well. The initial V-Funnel time increased by 98% as the partial metakaolin replacement percentage was increased from 0 to 25%. Also, all metakaolin mixtures showed higher V-Funnel times when compared to both 8% silica fume and 30%

slag partial replacements. The mixture incorporating 25% metakaolin as a partial cement replacement increased the initial V-Funnel time by 142% compared to silica fume and by 125% compared to slag. It should also be noted that when 5% metakaolin was used, the initial V-Funnel time was the uppermost limit, as stated in the European guidelines for SCC, while using a larger partial metakaolin replacement resulted in unacceptable V-Funnel times (European Project Group 2005).

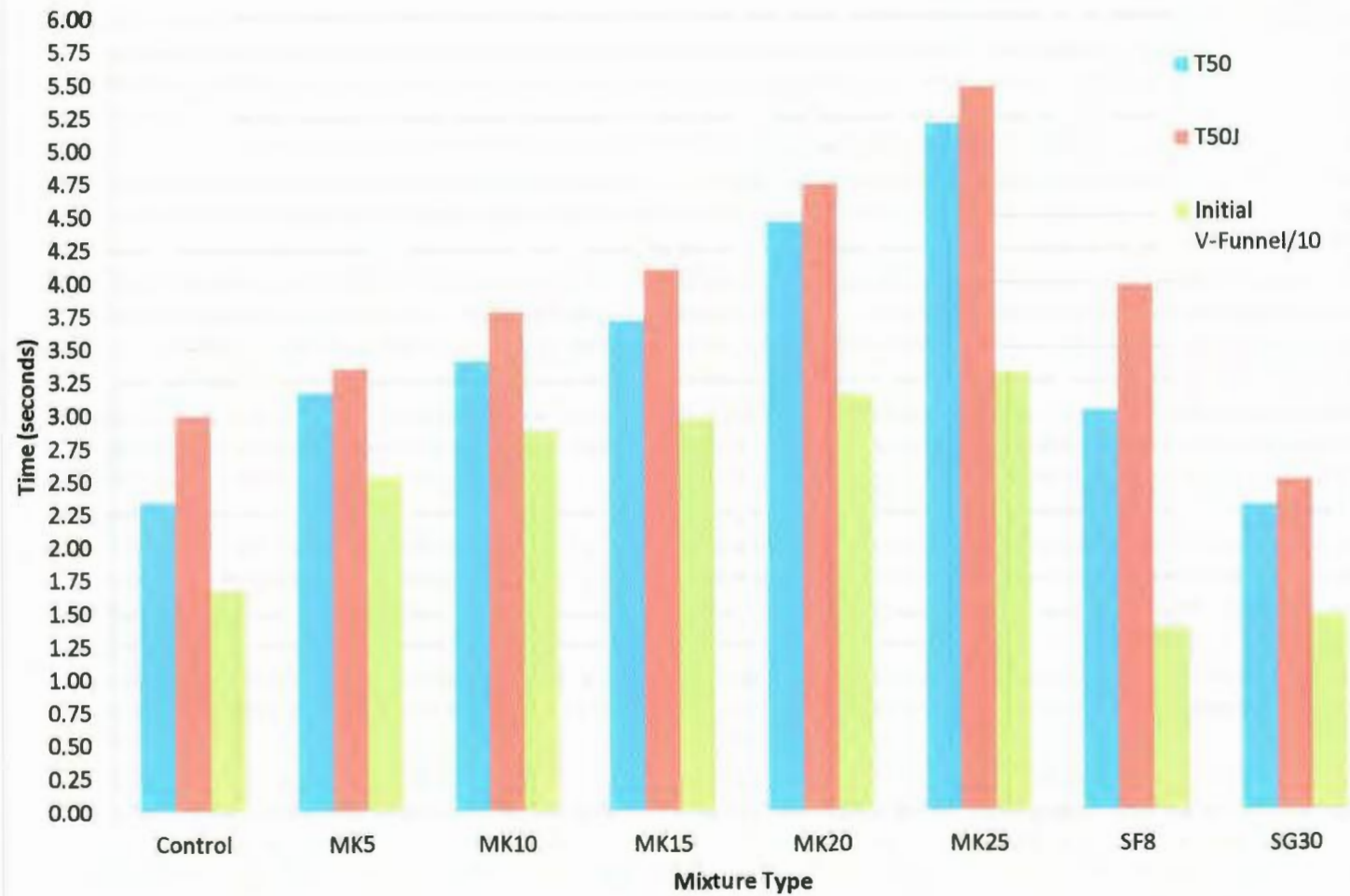


Figure 11 – T_{50} , T_{50J} , and Initial V-Funnel Times for Stage 1 Mixtures

Table 7 – Slump Flow, J-Ring Flow, J-Ring Height Difference, and Slump Flow – J-Ring Diameter for Varying Mixture Parameters

Concrete Type	Slump Flow		J-Ring Flow		Slump flow – J-Ring	J-Ring Height
	Diameter, mm	T ₅₀ , s	Diameter, mm	T _{50J} , s	Diameter, mm	Difference, mm
0.7C	638	1.86	575	2.56	63	36
0.7MK	673	3.19	667	4.6	7	25
0.7SF	638	1.97	610	3.86	28	25.5
0.7SG	625	1.45	610	2.36	15	33.5
1.2C	615	2.03	560	3.17	55	44
1.2MK	635	3.66	440	-	195	56
1.2SF	615	2.29	575	4.00	40	44
1.2SG	655	1.9	647	1.96	8	32.5
5%C	643	2.21	587	2.64	56	39
5%MK	653	3.1	650	4.64	3	23.5
5%SF	668	1.47	638	2.64	29	32
5%SG	675	0.97	627	3.01	48	27.5
7%C	643	1.62	605	2.54	38	27.5
7%MK	648	2.83	623	4.55	24	28.5
7%SF	668	1.39	637	2.50	31	29
7%SG	630	1.22	595	2.10	35	29.5

20C	648	2.09	568	2.99	80	50.5
20MK	655	2.44	625	4.84	30	32.5
20SF	650	1.65	615	2.67	35	30.5
20SG	633	1.38	612	1.84	21	31.5
500C	615	1.32	567	2.17	48	43
500MK	675	2.13	672	3.81	3	3
500SF	680	1.36	645	2.0	35	35
500SG	615	0.93	610	1.67	5	5

Table 8 – V-Funnel Times, Segregation Factor, H2/H1, and Air Content for Varying Mixture Parameters

Concrete Type	V-Funnel Times		Segregation Factor	L-Box H2/H1	Air Content, %
	Initial, s	After 5 minutes, s			
0.7C	7.44	10.23	0.375	0.40	1.60
0.7MK	2.11	24.83	0.175	0.25	1.70
0.7SF	7.03	9.99	0.421	0.26	1.50
0.7SG	4.41	6.57	0.483	0.34	1.40
1.2C	11.06	28.94	1.617	0.30	1.80
1.2MK	33.13	60.26	0.819	0.12	1.30
1.2SF	11.63	22.89	0.968	0.16	1.60
1.2SG	10.30	20.08	0.950	0.36	2.00

5%C	14.92	18.67	0.251	0.42	4.90
5%MK	12.16	14.22	0.169	0.84	4.90
5%SF	7.21	12.82	0.778	0.50	4.50
5%SG	6.60	6.63	0.00454	0.80	4.70
7%C	4.83	4.93	0.0207	0.76	6.70
7%MK	9.48	16.32	0.200	0.67	6.00
7%SF	6.09	6.86	0.126	0.74	7.50
7%SG	5.14	5.51	0.0720	0.76	7.40
20C	9.17	10.06	0.0971	0.66	0.60
20MK	10.25	15.54	0.5160	0.65	1.50
20SF	9.55	9.61	0.00628	0.63	1.35
20SG	6.85	7.72	0.1270	0.72	1.20
500C	5.61	5.65	0.00713	0.53	1.40
500MK	6.85	8.59	0.2540	0.77	1.20
500SF	6.58	7.73	0.1748	0.73	2.00
500SG	4.80	4.91	0.0229	0.68	0.85

5.1.1.2 Effect of C/F Ratio

The results for the T_{50} , T_{50J} , and initial V-Funnel times are shown in Figure 12 and Tables 7 and 8. From the figure and tables it can be seen that increasing the C/F ratio for the mixtures using metakaolin as a partial cement replacement tended to decrease the

flowability of the mixtures (indicated by the T_{50J}), while the viscosity of the mixtures (indicated by the T_{50}) increased when the C/F ratio was changed from 0.7 to 0.9 and decreased when the C/F ratio was further increased to 1.2. The T_{50} time for the metakaolin mixtures increased from 3.19 to 4.46 seconds, indicating an increase in the viscosity, and then decreased to 3.66 seconds, resulting in a reduction in the viscosity, as the C/F ratio was increased from 0.7 to 0.9 and then to 1.2, respectively. Also, the T_{50J} times increased from 4.6 to 4.74 seconds as the C/F ratio changed from 0.7 to 0.9, marking a decrease in the flowability. As the ratio was further increased to 1.2, the mixture did not even reach a 500 mm diameter, as seen in Figure 12. The control mixtures showed the same pattern, in which the flowability of the mixture decreased as C/F ratio was increased from 0.7 to 1.2, and the viscosity increased as the C/F ratio was increased from 0.7 to 0.9, then decreased when further increasing the ratio to 1.2. However, this result was slightly unexpected as the C/F ratio was further increased, since Sonebi et al. (2007) found that the V-Funnel time constantly increased as the coarse aggregate volume was increased. In this study a fixed amount of HRWR was added to the mixtures, which could lead to a slight difference since the slump flow was not controlled, as seen with the results in Figure 12.

The same trend that emerged with the mixtures incorporating metakaolin can be seen with 8% silica fume and 30% slag as partial cement replacements, where the viscosity increased as the C/F ratio was changed from 0.7 to 0.9 and then decreased as the ratio was further raised to 1.2. In general, the decrease of the mixtures' flowability when the C/F ratio increased to 1.2 is believed to be caused by the increased particle collisions

due to the higher volume of coarse aggregate used. With the increasing volume of coarse aggregate in the mixture, the ability of the paste to carry and move the coarse aggregate becomes more difficult. The flowability of 8% silica fume as a partial replacement showed a decrease of around 3.6% as the C/F ratio was increased up to 1.2. In addition, 30% slag as a partial cement replacement showed little change in the flowability of the mixture as the C/F ratio was increased from 0.7 to 1.2.

The results of the V-Funnel tests showed a similar variation as those of the T_{50} times, but were different than those of the T_{50J} tests. Although the T_{50J} and V-Funnel tests can both indicate the mixture's viscosity, the V-Funnel test did not show the same trend as the T_{50J} results. The V-Funnel times for all mixtures (except those containing metakaolin) increased as the C/F ratio was increased to 0.9 and then decreased as the C/F ratio was further increased to 1.2. Contrary to this, the T_{50J} times continuously increased as the C/F ratio was increased from 0.7 to 1.2. The reason for this could be related to the collision of the coarse aggregate at the J-Ring bars during the flow, whereas the V-Funnel and slump flow tests result in a more free flow of the SCC mixture. As the C/F ratio is increased in the mixture, there is more coarse aggregate that can collide with the J-Ring bars and delay the flow time. Su et al. (2002) showed similar results; as the volume of the coarse aggregate was reduced, the ability of the mixture to pass through reinforcement increased, as indicated by the filling height. Whereas increasing the coarse aggregate volume decreased the filling height (similar to the J-Ring test in which the concrete flows through openings representing reinforcement).

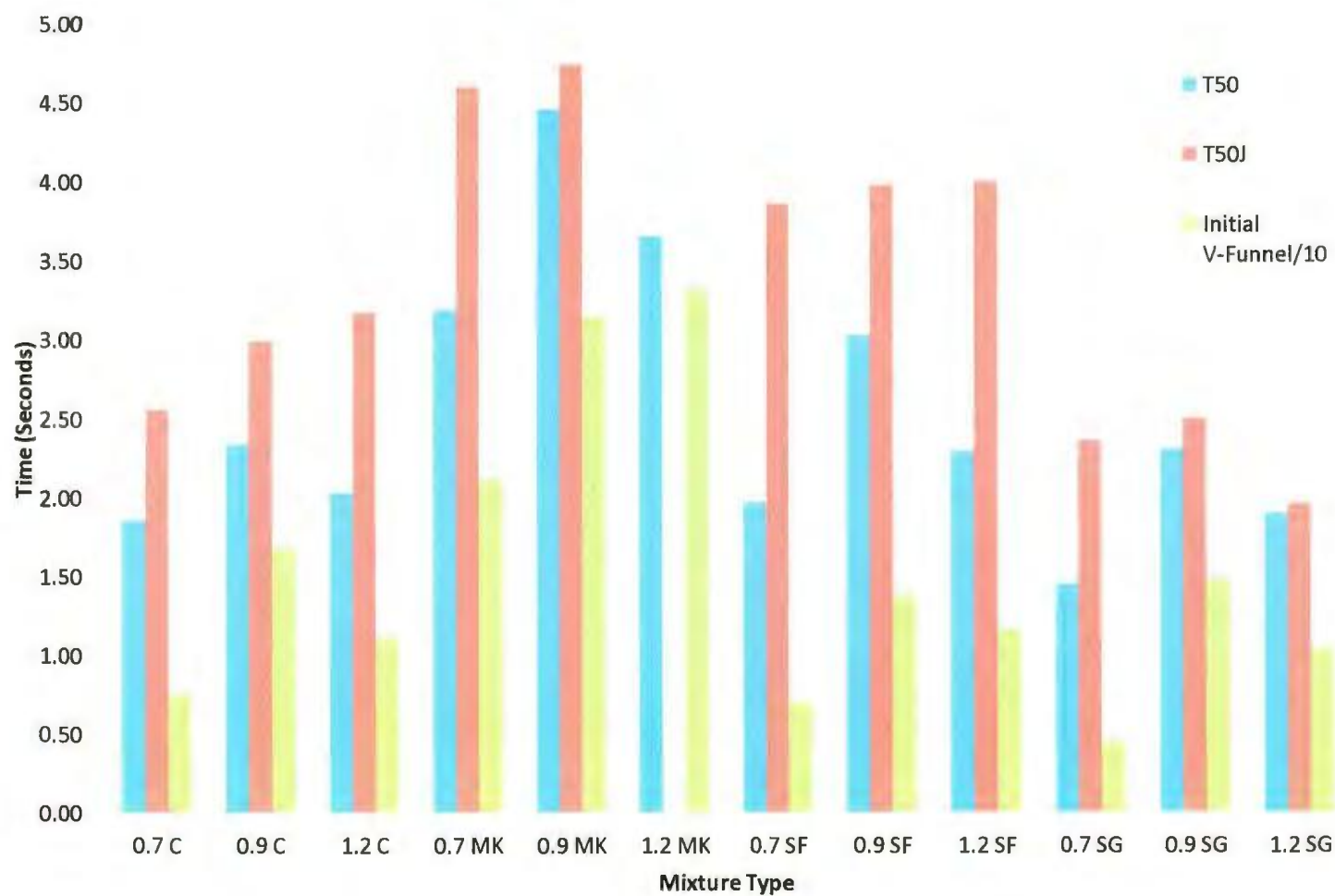


Figure 12 – T_{50} , T_{50J} , and Initial V-Funnel Times for Varying C/F Ratios

5.1.1.3 Effect of Coarse Aggregate Size

Tables 7 and 8, in addition to Figure 13, show the results for the T_{50} , T_{50J} , and initial V-Funnel times for varying coarse aggregate sizes. Figure 13 shows that increasing the stone size for all mixtures, except for metakaolin, from 10 mm to 20 mm decreased the viscosity, while the flowability for all mixtures also increased. For the mixture containing metakaolin as a partial cement replacement, the T_{50} and V-Funnel times both decreased with increasing stone size. The T_{50} time decreased by 1.8 fold, while the V-Funnel time decreased by 3.1 fold. The control mixture saw a decrease in the T_{50} time by 11% and the V-Funnel time decreased by 45%. Mixtures containing 8% silica fume and 30% slag partial replacements showed a decrease of 45% and 40% in their T_{50} times, respectively. Both showed a decrease in their V-Funnel times of 30% and 53.5%, respectively, as the coarse aggregate size was increased to 20 mm. Hu et al. (2011) obtained similar results when increasing the coarse aggregate size and showed that the viscosity decreased (the mixture becomes more flowable) by increasing the coarse aggregate size.

The T_{50J} for the control mixture decreased with an increasing coarse aggregate size; using a partial cement replacement with metakaolin mixtures showed little change in the flowability with the increasing coarse aggregate size. Partial replacements with 8% silica fume and 30% slag also showed a decrease in their T_{50J} times with increasing coarse aggregate size, which showed an increase in the flowability.

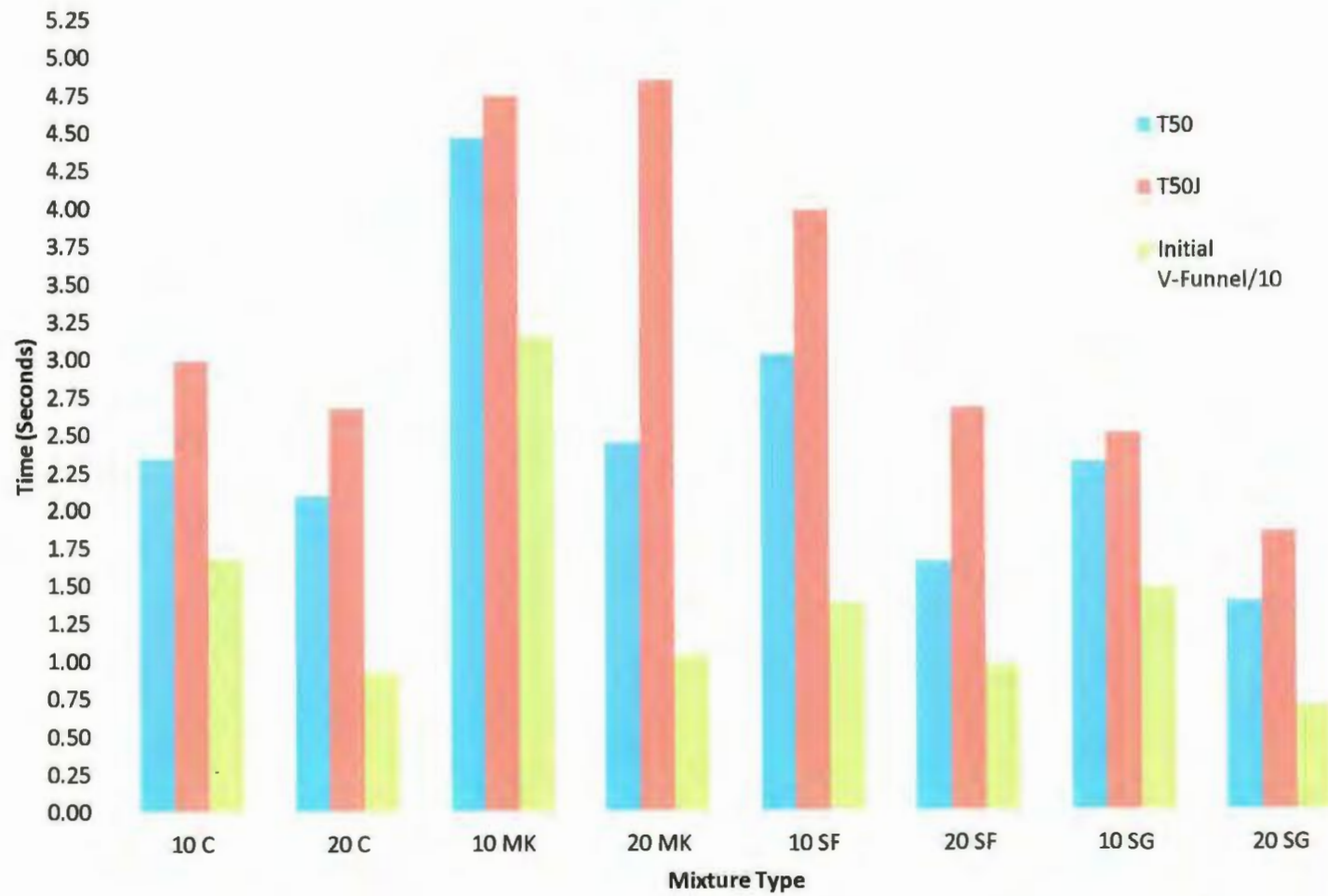


Figure 13 – T₅₀, T_{50J}, and Initial V-Funnel Times for Varying Coarse Aggregate Sizes

5.1.1.4 Effect of Binder Content

The T_{50} , T_{50J} , and initial V-- funnel results are shown in Figure 14, as well as Tables 7 and 8. The figure shows that as the binder content for all four mixtures was increased from 450 to 500 kg/m³, the viscosity of the mixtures decreased, and the flowability of the mixtures increased. All T_{50} times were reduced for all mixtures, which indicates that the viscosity decreased as the amount of binder was increased. Similar studies have shown that increasing the total binder content (increasing the paste volume) reduced the viscosity and can increase the flow of the mixture. A study by Koehler et al. (2005) showed that an increase in the paste volume (increasing the total binding material) decreased the viscosity of the mixture. For the mixture using metakaolin as a partial cement replacement, the T_{50} time decreased by 2.33 seconds when the binder content was increased to 500 kg/m³. Also, the control mixture saw a decrease of 1.02 seconds in the T_{50} time. Both partial replacements with 8% silica fume and 30% slag saw decreases of 1.67 and 1.38 seconds, respectively. The T_{50J} times for both the control and the mixture containing 20% metakaolin as a partial cement replacement decreased with increasing binder. The T_{50J} time decreased by 27.4% for the control mixture and decreased by 19.6% for the 20% partial metakaolin replacement mixture. For both 8% silica fume and 30% slag partial replacements, the T_{50J} times were reduced by 49.7% and 33.2%, respectively. In addition to these two tests, the initial V-Funnel time also showed that the viscosity decreased with an increasing binder content. The V-Funnel time for the mixture using 20% metakaolin as a partial cement replacement greatly decreased by 78.2% as the cement content increased from 450 to 500 kg/m³. The control mixture also saw a large a

decrease in the V-Funnel time of 68.2% when a higher binder content was used. Gencil et al. (2011) also saw decreases in the V-Funnel times in fibre-reinforced concrete as the total binding material was increased from 470 to 570 kg/m³ and was observed regardless of the percentage of fibres used.

The mixtures using 8% silica fume and 30% slag as partial cement replacements showed V-Funnel times that decreased with increasing binder content. The V-Funnel time decreased by 52% for 8% silica fume partial replacement and by 67.4% for 30% slag partial replacement when using a 500 kg/m³ binder content. Nanthagopalan et al. (2009) found similar results when increasing the total powder content for SCC mixtures. A small decrease in the T_{50} and V-Funnel times was reported, indicating a decrease in the viscosity with increasing binder content.

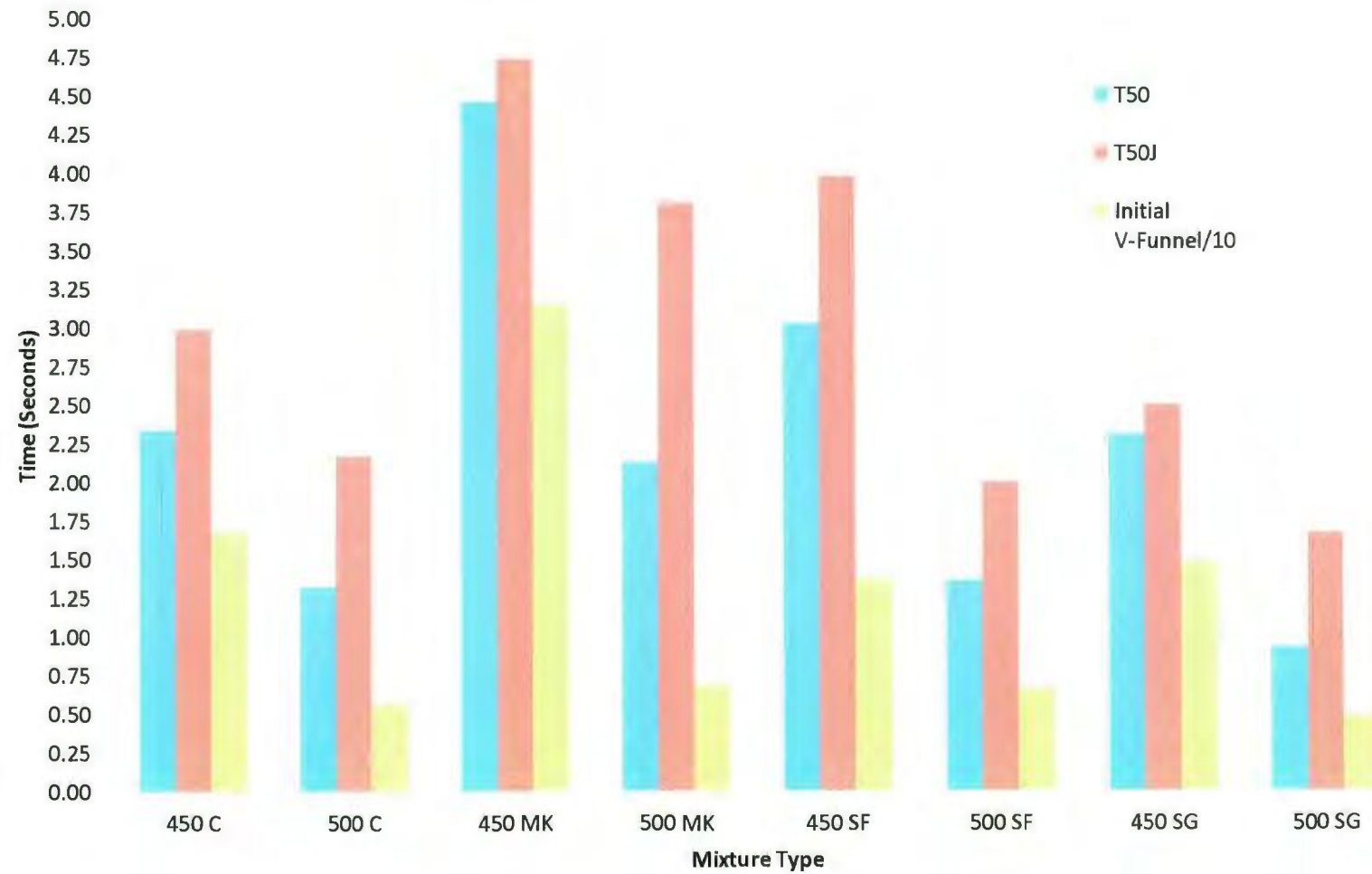


Figure 14 – T_{50} , T_{50J} , and Initial V-Funnel Times for Varying Binder Content

5.1.1.5 Effect of Air Content

The T_{50} , T_{50J} , and initial V-Funnel results for varying air contents are shown in Tables 7 and 8 and Figure 15. Figure 15 shows that increasing the air content of all the mixtures from 0 to 7% decreased the viscosity and increased the flowability. A paper published by Struble (2004) showed that concrete using no HRWR saw a reduction in the viscosity of the mixture with the use of an AEA due to the formation of bubble bridges that reduced interparticle friction. The T_{50} time for the mixtures containing metakaolin decreased by 1.36 seconds (30%) when the air content was increased from 0 to 5%, and it further decreased by 0.27 seconds (8.7%) as the air percentage was raised to 7%. Furthermore, the T_{50J} times for all air mixtures using 20% metakaolin as a partial cement replacement decreased by 4% and partial replacements with 8% silica fume saw a large decrease in both the T_{50} time and T_{50J} when the air content was increased from 0 to 5%. Further increasing the air content to 7% slightly decreased both the T_{50} and T_{50J} times for 8% silica fume partial replacement. There was a 51.5% and a 33.7% drop in the T_{50} and T_{50J} times, respectively, when the air content was increased from 0 to 7% for the 8% silica fume mixture. As the air content was increased, the 30% slag as a partial cement replacement showed a generally decreasing trend in both the T_{50} and T_{50J} times. When the air content was increased from 0 to 7%, the 30% partial slag replacement showed a 47.2% and 16% decrease in the T_{50} and T_{50J} times, respectively. The initial V-Funnel times for all mixtures also decreased as the air content was increased. Thus, increasing the air content from 0 to 7% decreased the V-Funnel times for the control, 20% metakaolin, 8% silica fume, and 30% slag partial replacement mixtures by 71%, 70%, 56%, and 65%,

respectively. Khayat (2000) also showed a decrease in the viscosity of SCC as the air content was increased, and Lee et al. (1977) found results showing that increasing the air content in concrete led to an increase in the slump of the mixtures.

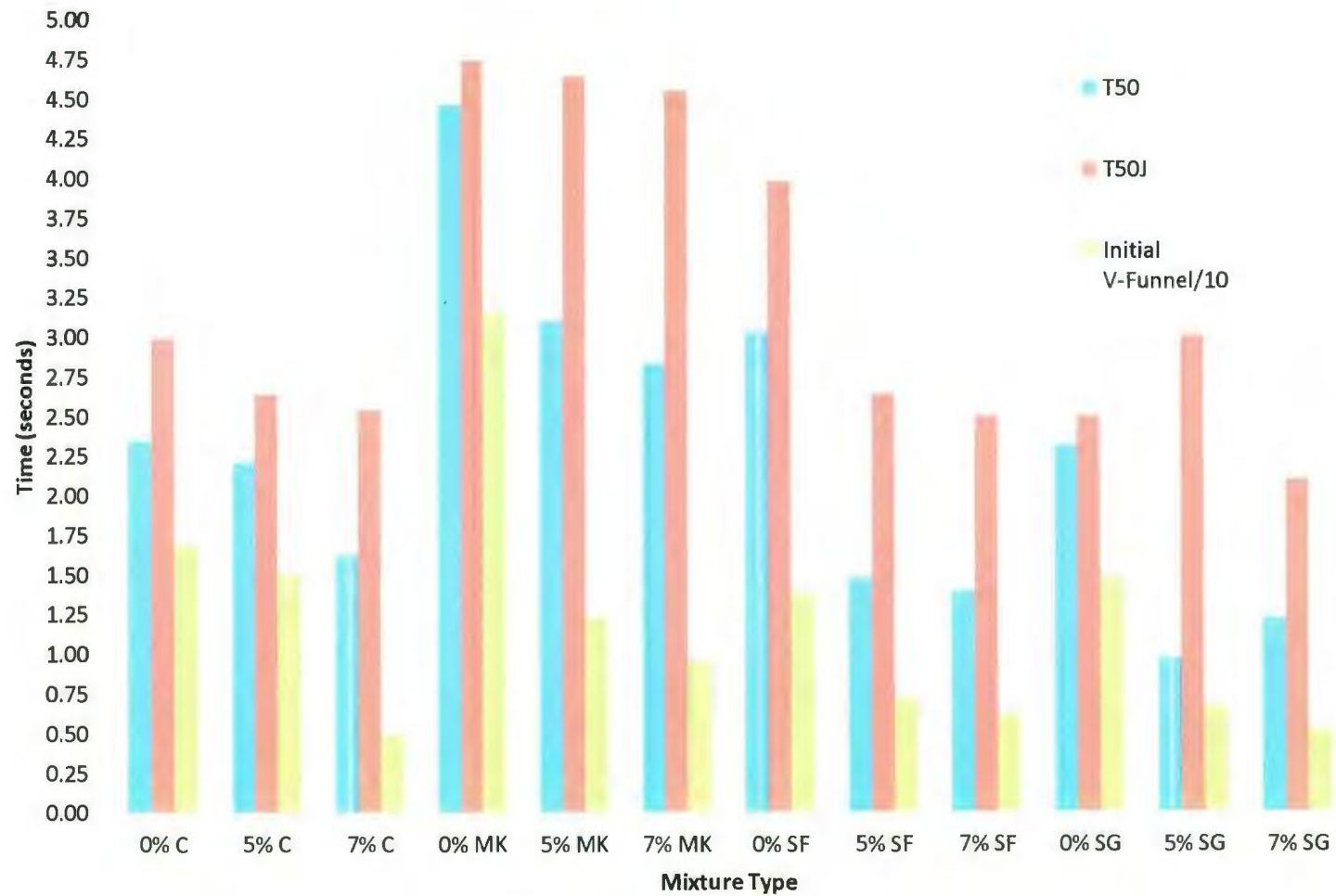


Figure 15 – T_{50} , T_{50J} , and Initial V-Funnel Times for Varying Air Percentages

5.1.2 Passing Ability and Segregation

5.1.2.1 Effect of Metakaolin

The effect of segregation and the passing ability of the mixtures were studied using the L-Box, J-Ring, and V-Funnel tests, as previously described. The results for the slump flow – J-Ring diameter, J-Ring height difference, L-Box H2/H1 ratio, and segregation factor are shown in Figure 16 as well as Tables 5 and 6. The passing ability of the mixtures containing metakaolin as a partial cement replacement increased with an increasing percentage of metakaolin compared to the control mixture. The slump flow – J-Ring diameter was greatly reduced when the partial metakaolin replacement percentage was increased to 20%. Using a 20% partial replacement of cement with metakaolin resulted in a reduction in the slump flow – J-Ring diameter of 2.72 fold. As well, the J-Ring height difference showed a decreasing trend as the partial replacement level of metakaolin was increased. The height difference for the mixture using 20% metakaolin partial replacement decreased by 60% compared to the control mixture. This shows an improved passing ability when high levels of metakaolin are used as a partial cement replacement. A similar result showing that increasing the metakaolin content increases the passing ability of the mixture matches the results of Hassan et al. (2012). In comparison to both 8% silica fume and 30% slag as partial cement replacements, it seems that using a partial metakaolin replacement of 10% or greater improved the passing ability, as indicated by the slump flow – J-Ring diameters and J-Ring height differences. Compared to using a 20% partial replacement, using a 25% partial replacement of metakaolin decreased the passing ability of the mixture. The slump flow – J-Ring diameter increased

by 68% and the J-Ring height difference increased by 8.3% with an increase of the partial metakaolin replacement percentage from 20 to 25%. The result showing that using SCMs increased the passing ability of SCC mixtures matches that of Khayat et al. (2002). As previously described, the segregation was measured by using the S_f ratio and is affected by the thixotrophy and segregation. The thixotrophy of the mixture depends mainly on the type of SCM and the amount of HRWR used. As seen in Figure 16, the segregation factor shows a decreasing trend as the partial percentage of metakaolin replacement was increased up to 25% compared to the control mixture. The segregation factor decreased by 77% as the partial metakaolin replacement was increased to 20%.

Compared to the control mixture, the L-Box H2/H1 ratio increased with an increasing percentage of metakaolin as a partial cement replacement. The H2/H1 ratio increased from 0.182, when no metakaolin replacement was used, to 0.42 when a 20% partial metakaolin replacement was used. All the mixtures tested showed unacceptable H2/H1 ratios. Even though all mixtures had an acceptable value for the T_{50} and V-Funnel times, the passing ability for both mixtures did not meet the acceptable range of values as indicated by European guidelines for the L-Box (The European Guidelines for Self-Compacting Concrete 2005). Using 20% metakaolin as a partial cement replacement had a similar H2/H1 ratio compared to using a 30% slag partial replacement, which obtained an H2/H1 ratio of 0.417. And 20% partial metakaolin replacement had a higher H2/H1 ratio when compared to 8% silica fume partial replacement, which was 0.385.

Increasing the partial metakaolin replacement to 25% showed to increase the J-Ring height differences, slump flow – J-Ring diameter, and H2/H1 and segregation factor

ratios slightly compared to using a 20% metakaolin partial replacement. The results still indicate a reduction in the segregation and an increase in the passing ability compared to the control mixture, but a decrease in the passing ability compared to the mixture using a partial replacement of 20% metakaolin. This decrease seen in the test results could have contributed to the high thickening of the mixture containing 25% metakaolin as a partial replacement, which resulted from the high dosage of metakaolin or the excessive amount of HRWR added. A thickening of the paste obstructs the whole paste from being able to flow through the bars of the J-Ring and L-Box. However, an increase in the viscosity of the mixture, as seen when increasing the metakaolin content, reduces the chance for separation of the coarse aggregate from the paste matrix and allows for the mixture to carry the coarse aggregate, which reduces the segregation risk of the mixture (Zhu et al. 2003).

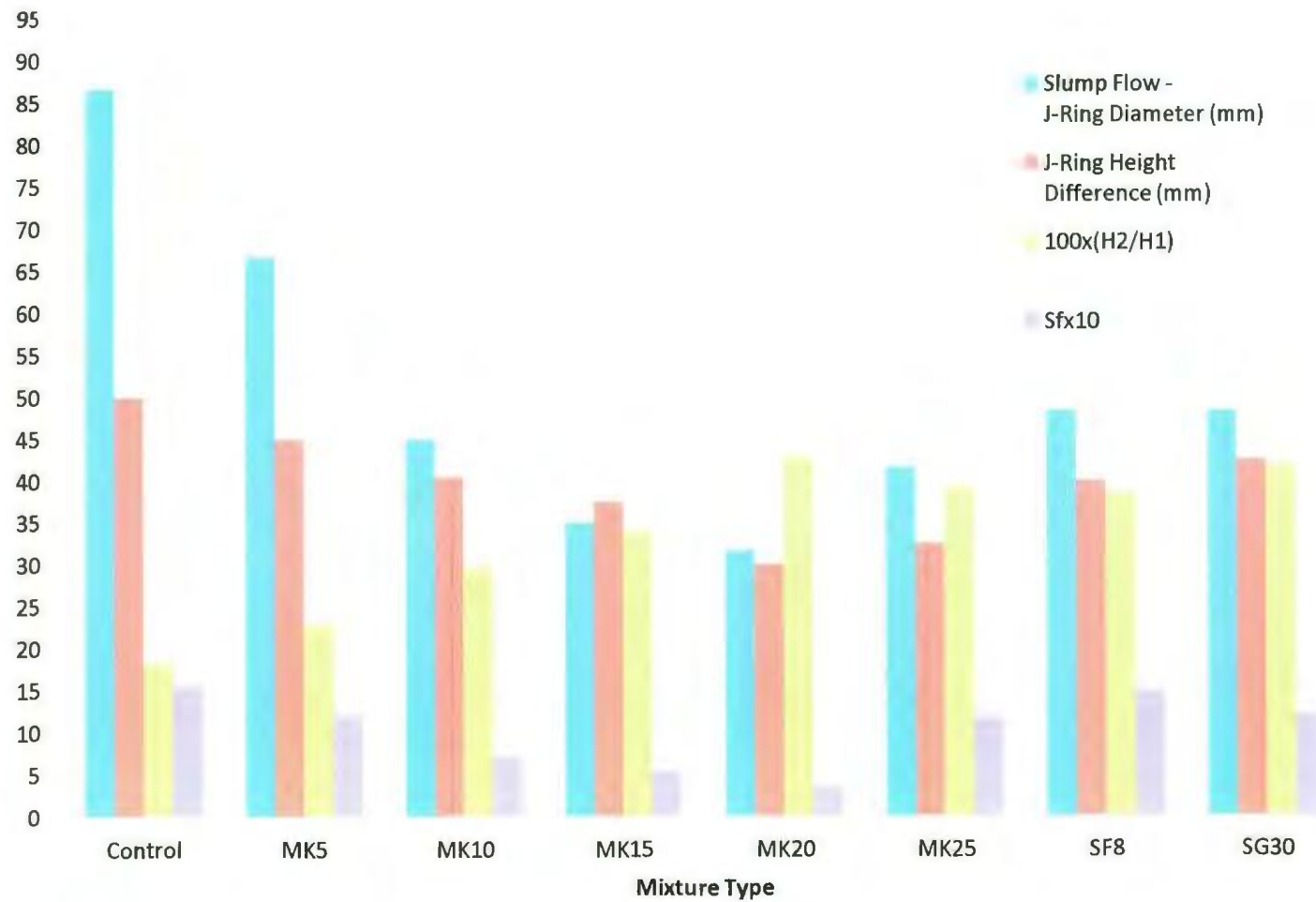


Figure 16 – Passing Ability and Segregation Results for Stage 1 Mixtures (Units Denoted in Legend)

5.1.2.2 Effect of C/F Ratio

Figure 17 and Tables 7 and 8 display the results for the slump flow – J-Ring diameter, J-Ring height differences, H2/H1 ratio, and the segregation factor for the effect of the C/F ratio on SCC. Figure 17 shows a decreasing trend in the passing ability of metakaolin mixtures as the C/F ratio was increased from 0.7 to 1.2. The slump flow – J-Ring diameter greatly increased by 27 fold as the C/F ratio was increased from 0.7 to 1.2. In addition, the J-Ring height difference increased by 124% and the H2/H1 ratio decreased by 84%. The decrease in the L-Box H2/H1 ratio was expected as the C/F ratio was increased. Sonebi et al. (2007) found similar results in plain SCC: there was a significant drop in the H2/H1 ratio as the C/F ratio was increased. This may have contributed to the increased risk of blockage due to the collision of the coarse aggregate behind the reinforcing bars of the L-Box. For the mixture using metakaolin, the segregation factor also increased when there was an increase in the C/F ratio. The segregation factor increased by a factor of 4.68 as the C/F ratio was increased from 0.7 to 1.2. The control also showed a reduction in the passing ability, indicated by the J-Ring test, as the C/F ratio was increased from 0.7 to 0.9. Further increasing the ratio to 1.2 showed an enhancement in the passing ability. This could be due to the increase in the flowability and reduction in viscosity, as discussed earlier. For the control mixture, the slump flow – J-Ring diameter increased 24 mm as the C/F ratio was increased from 0.7 to 0.9 and then decreased by 32 mm as the ratio was further increased to 1.2. However, the segregation factor for the control mixture increased when increasing the C/F ratio from 0.7 to 1.2 by 4.3 times. In SCC, the segregation resistance of the mixture, as observed by

El-Chabib et al. (2006), was shown to decrease slightly as the volume of the coarse aggregate was increased.

The 8% silica fume partial replacement showed a similar trend as the control mixture, in terms of a decreasing passing ability, indicated by the J-Ring tests, when the C/F ratio was increased from 0.7 to 0.9, and then increased as the C/F ratio was further increased to 1.2. For the 8% partial silica fume replacement, the J-Ring height difference increased by 72% and the H2/H1 ratio decreased by 79% with an increasing C/F ratio. The segregation factor for the 8% partial silica fume replacement increased as the C/F ratio was increased from 0.7 to 0.9, but it decreased as the ratio was further increased to 1.2. Again, this could be due to the decreasing viscosity and increase in the flowability, as discussed earlier. Using 30% partial slag replacement with a varying C/F ratio decreased the passing ability of the mixture, indicated by the J-Ring test, up to a C/F ratio of 0.9, and showed little change in the passing ability as the C/F ratio was further increased to 1.2. The J-Ring height difference increased by 9 mm as the C/F ratio was increased to 0.9, and then decreased 10 mm as the ratio was further increased to 1.2. Also, when using 30% slag as a partial cement replacement, the H2/H1 ratio decreased by 49% when the C/F ratio was increased to 0.9 from 0.7. Increasing the C/F further to 1.2 showed a slightly lower H2/H1 ratio to that obtained when a C/F ratio of 0.9 was used. The segregation of the mixture containing slag increased by a factor of 2.5 and then decreased by a factor of 1.3 as the C/F ratio was increased from 0.7 to 0.9 and then to 1.2, respectively. The segregation factor for all mixtures showed different trends of variations. As previously mentioned, the segregation factor is dependent on the thixotropy and the

segregation of the mixture. The thixtropy of the mixture is affected by the type of SCM and the amount of HRWR used, while the segregation is dependent on the volume of the coarse aggregate content and the viscosity of the mixture.

It should be noted that the results of the L-Box and J-Ring tests are commonly used to judge the passing ability. In this investigation, the results of the J-Ring test for all mixtures, except metakaolin, showed a reduction in the passing ability as the C/F ratio was increased from 0.7 to 0.9, and that further increasing the C/F ratio to 1.2 resulted in an enhancement in the passing ability. The L-Box results, however, showed a continuous reduction in the passing ability with an increasing C/F ratio. The L-Box gate retains a large volume of concrete at a higher elevation compared to the slump cone used in the J-Ring test. The L-Box test also has a smaller opening in which the concrete must pass compared to the ring used for the J-Ring test. This high elevation of the concrete and reduced size of the opening in the L-Box caused a higher discharge of concrete to pass through a relatively smaller space, which provided a better chance for the coarse aggregate to collide and accumulate behind the L-Box gate, thus reducing the H2/H1 ratio. Therefore, the L-Box test showed a continuous reduction in the passing ability as the C/F ratio was increased. Aggarwal et al. (2011) produced a mixture design for SCC that obtained the desired results for the L-Box test as the coarse aggregate content was decreased. This situation was not as clear with the metakaolin mixtures. The reason for this could be related to the high viscosity of the metakaolin paste, which provided a better suspension of the coarse aggregate and allowed a better flowability.

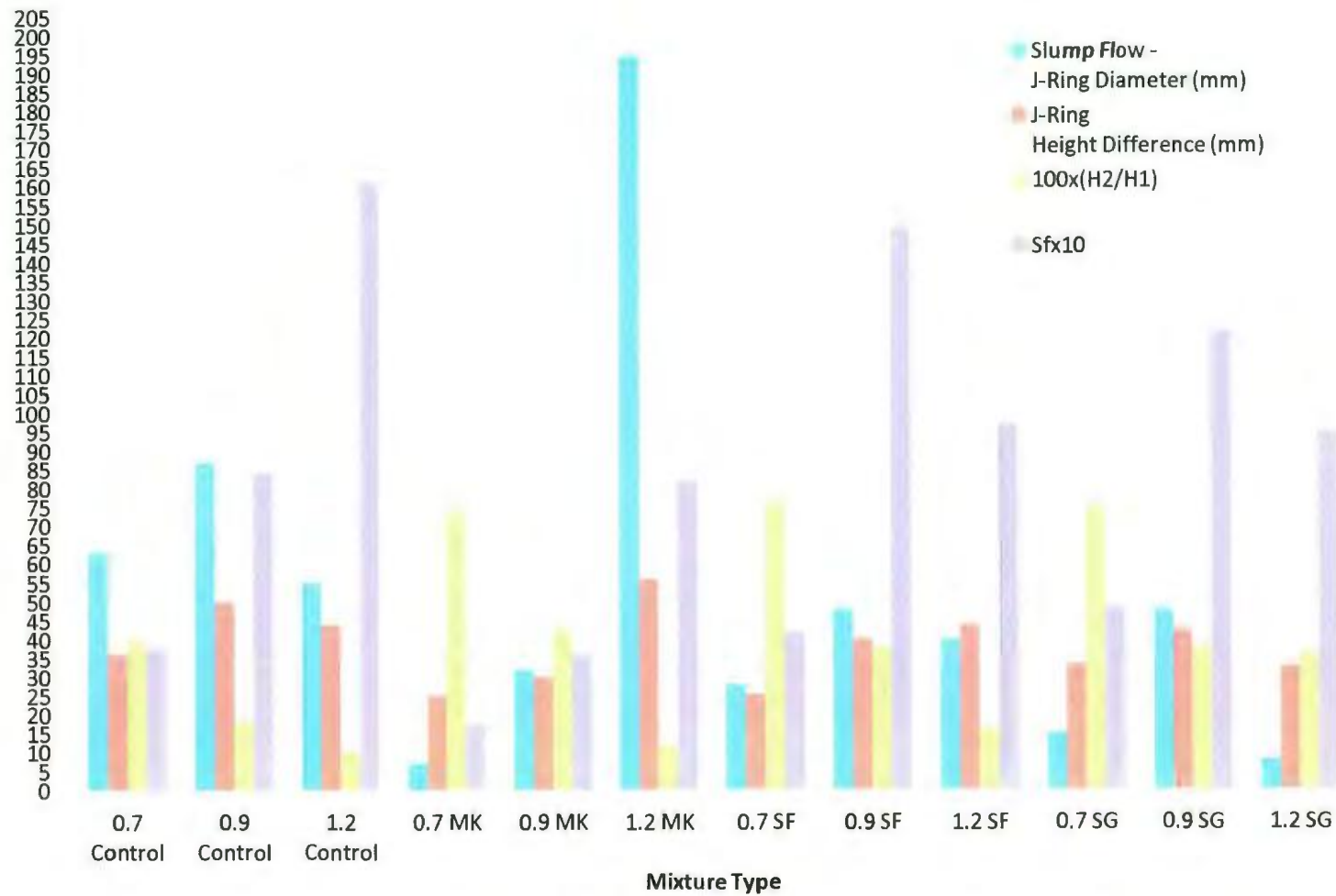


Figure 17 – Passing Ability and Segregation Results for Varying C/F Ratios (Units Denoted in Legend)

5.1.2.3 Effect of Coarse Aggregate Size

As seen in Figure 18 and Tables 7 and 8, the passing ability of all mixtures increased when the coarse aggregate size was increased. For both the control and 20% partial metakaolin replacement mixtures, the slump flow – J-Ring diameters decreased by 8% and 6%, respectively, when the coarse aggregate size was increased to 20 mm. The L-Box ratio for both mixtures also showed an increase of 3.7 fold for the control mixture and 1.5 fold for the 20% metakaolin partial replacement mixture. An increase in the L-box ratio, as well as a reduction in the slump flow – J-Ring diameters, indicates an improvement in the passing ability of SCC. This indicates that the coarse aggregate is flowing more easily through the openings of the L-Box and J-Ring apparatus', thus improving the passing ability.. The J-Ring height differences for both the control and metakaolin mixtures showed little to no difference in the results, as the coarse aggregate size was increased from a 10 mm to 20 mm stone. The segregation factor for the control mixture decreased with the increasing stone size, while the segregation factor increased for the metakaolin mixture. As noted before, the segregation factor is influenced by both the thixtropy and the segregation of the mixtures.

The other SCMs, 8% silica fume and 30% slag partial replacements also showed an increasing passing ability with an increasing coarse aggregate size. Both mixtures had a reduction in their respective slump flow – J-Ring diameters, J-Ring height differences, and an increase in the H2/H1 ratios of 27%, 24%, and 66% for the 8% silica fume partial replacement, respectively, and 56%, 26%, and 71% for the 30% slag partial replacement, respectively. Also, for both mixtures using partial replacements of 8% silica fume and

30% slag, the segregation factors were greatly reduced. The 8% silica fume and 30% slag partial replacements showed a decrease of 238 and 9.6 fold as the coarse aggregate size was increased from 10 mm to 20 mm. Ozkul et al. (2006) found similar results when increasing the coarse aggregate size from 12 to 20 mm. It was observed that the free flow of the mixture when using a similar binder of 450 kg/m³ increased when the coarse aggregate size increased; the confined flow rose as well, indicating an improvement in the passing ability of the mixtures. Similar results for improvement in the passing ability were seen when using higher binder contents and increasing the maximum aggregate size.

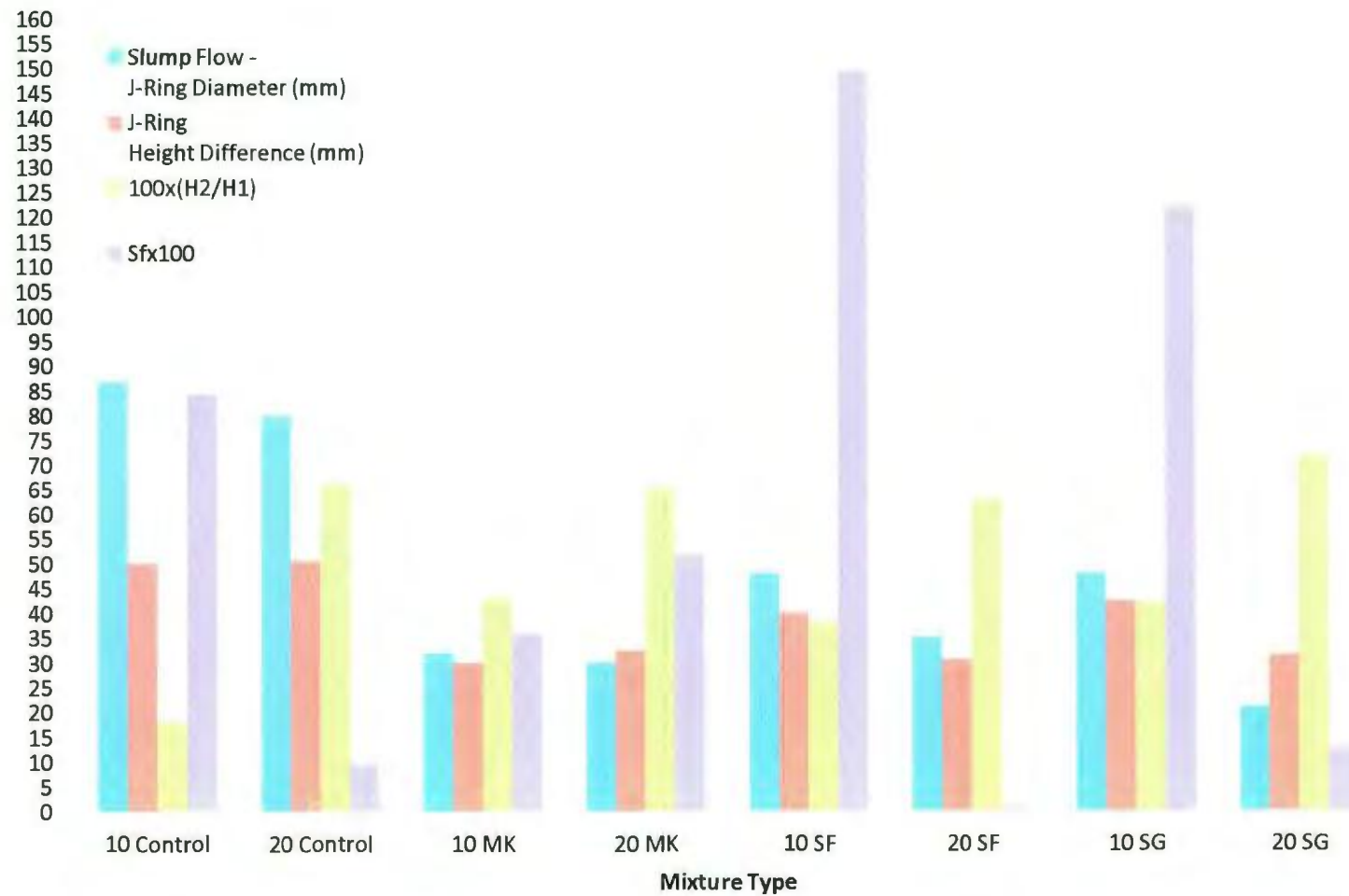


Figure 18 – Passing Ability and Segregation Results for Varying Coarse Aggregate Sizes (Units Denoted in Legend)

5.1.2.4 Effect of Binder Content

Tables 7 and 8, as well as Figure 19, show the results of the passing ability and segregation factor for varying binder contents. It can be seen from Figure 19 that increasing the binder content of the mixtures from 450 to 500 kg/m³ improved the segregation and passing ability of the mixtures. The mixtures containing 20% metakaolin as a partial cement replacement showed a reduction of 90% in the slump flow – J-ring diameter as the binder was increased to 500 kg/m³. In addition, the J-Ring height difference decreased by 5 mm with an increased binder content. The H2/H1 ratio from the L-Box increased by 79%, from 0.43 to 0.77, when the binder was changed from 450 to 500 kg/m³. This value for the L-Box is within an acceptable range of values for SCC, as stated in the European guidelines (The European Guidelines for Self-Compacting Concrete 2005). This indicated an improved passing ability of the mixtures using a binder content of 500 kg/m³ compared to those using 450 kg/m³. Assaad et al. (2005) also reported an improvement in the H2/H1 ratio when the total cementing material was increased in SCC. The control mixture also had an increased passing ability as the binder content was increased. All tests showed improved values for the slump flow – J-Ring diameter, J-Ring height differences, and L-Box ratio. The slump flow – J-Ring diameter decreased by 45%, the J-Ring height difference fell by 14%, and the H2/H1 rose by 194% for the control as the binder content was increased from 450 to 500 kg/m³. These results were similar to those studied by Koehler et al. (2005), in which an increase in the paste volume or an equivalent increase in the binder content resulted in improved J-Ring heights. Nanthagopalan et al. (2009) also showed that increasing the total binding

material in SCC resulted in a decrease in the slump flow – J-Ring diameters, thereby improving the passing ability of the mixture.

Both the 8% silica fume and 30% slag partial replacement mixtures showed a large improvement in the passing ability and segregation factor when the binder content was increased to 500 kg/m³. Partial replacement with 8% silica fume showed a decrease in the slump flow – J-Ring diameter and a J-Ring height difference of 27% and 39%, respectively. The H2/H1 ratio also increased by 92% when the binder content was increased to 500 kg/m³. The mixture using 30% slag as a partial cement replacement had a decrease in the slump flow – J-Ring diameter and a J-Ring height difference of 90% and 38%, respectively, while the H2/H1 ratio increased by 62% when the binder content was increased from 450 to 500 kg/m³. Increasing the binder content for both mixtures to 500 kg/m³ showed a large decrease in the segregation factor. There was an 88.3% and 98.1% drop in the segregation factor for 8% silica fume and 30% slag partial replacements, respectively, with increasing binder content. Su et al. (2001) reported an improvement in the segregation resistance when the binder volume was increased. In addition to an improvement in the segregation resistance, Su et al. (2001) also noticed an increase in the passing ability, as indicated by the L-Box test. Ozkul et al. (2006) found similar results and came to the conclusion that an increase in the amount of powder material (binder) indicated an improved passing ability.

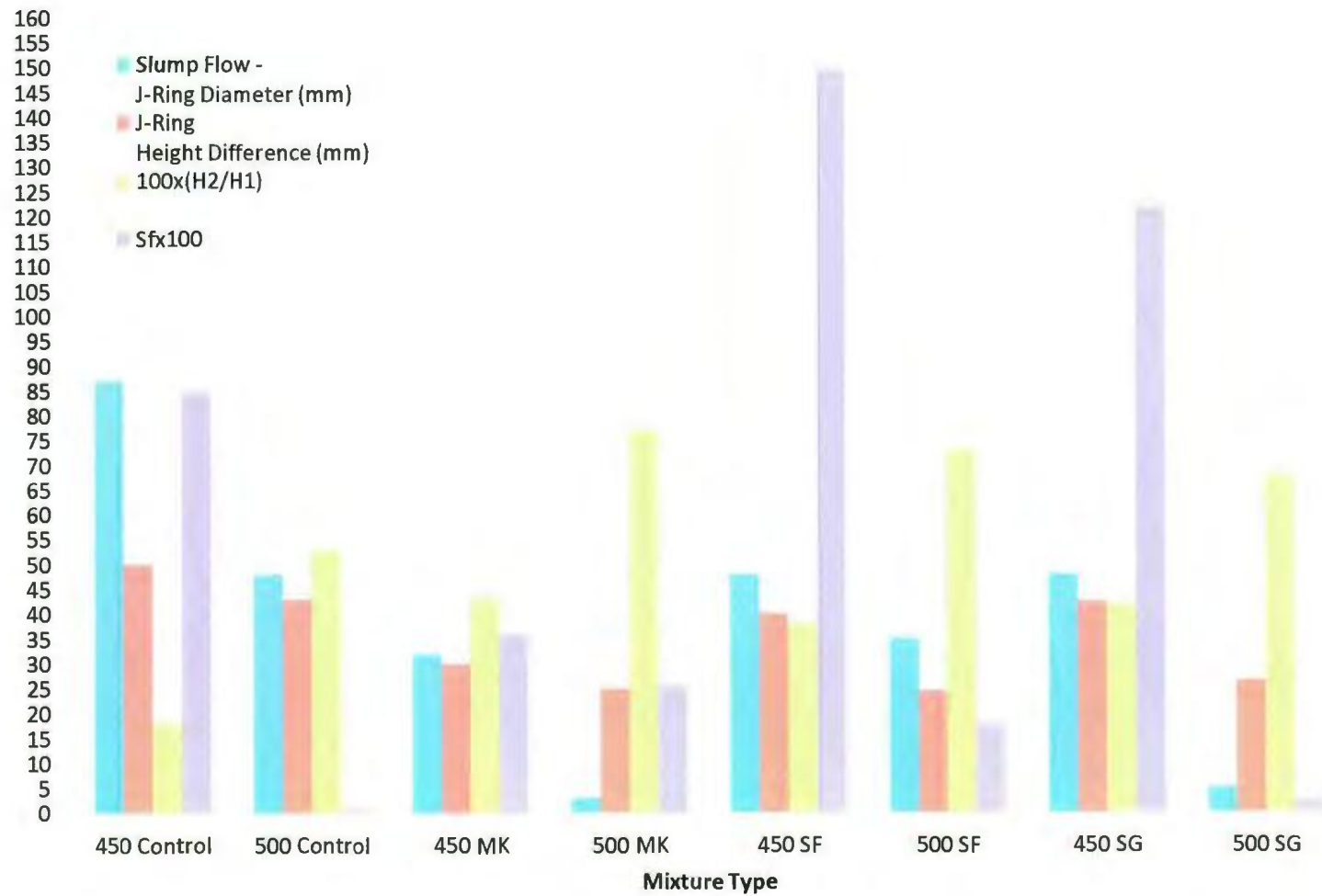


Figure 19 – Passing Ability and Segregation Results for Varying Binder Content (Units Denoted in Legend)

5.1.2.5 Effect of Air Content

Figure 20 and Tables 7 and Table 8 show that as the percentage of air is increased from 0 to 7%, the segregation factor appears to decrease and the passing ability, indicated by the slump flow – J-Ring diameter, showed an increasing trend. This improvement in the passing ability was expected and shown by Safiuddi (2008), who showed, through the use of an AEA, an improved passing ability when increasing the air content. The mixture containing 20% metakaolin as a partial cement replacement showed an improvement in the passing ability as the air content was increased to 5%. The slump flow – J-Ring diameter decreased by 91% (from 32 to 3 mm), and the J-Ring height difference decreased by 22% (from 30 to 23.5 mm) as the air content increased from 0 to 5%. The L-Box ratio also increased with increasing air content, the same as the other tests. As the air content was increased to 5%, the H2/H1 ratio increased 95% to 0.84. This value for the L-Box ratio is well within the acceptable range of > 0.75 (European Project Group 2005). Further increasing the air content to 7% yielded no additional benefits to the passing ability of the mixture using 20% metakaolin partial replacement, as indicated by the slump flow – J-Ring diameter. The same trend was observed for the segregation factor as it decreased from 0 to 5% air content and resulted in no further benefit when the air content was increased to 7%.

For the control mixture, the passing ability greatly improved when the air content was increased from 0 to 7%. Increasing the air content to 5% reduced the slump flow – J-Ring diameter by 31 mm, decreased the J-Ring height difference by 11 mm, and increased the L-Box H2/H1 ratio by 129%. Further increasing the air content to 7%

reduced the slump flow – J-Ring diameter by 18 mm, reduced the J-Ring height difference by 12.5 mm, and increased the L-Box ratio by 84%. In addition, the segregation factor for the control mixture decreased by 70% when the air content was increased to 5%, and was further reduced by 92% when the air content was increased to 7%.

Both the 8% silica fume and 30% slag partial replacement mixtures showed an increase in the passing ability when the air content was increased from 0 to 7%. Using 8% silica fume as a partial cement replacement showed a 40% decrease in the slump flow – J-Ring diameter and a 20% decrease in the J-Ring height difference when the air content was increased to 5%. The H2/H1 ratio for the 8% silica fume partial replacement mixture increased by 30% when 5% air content was used. Further increasing the air content to 7% resulted in a slight decrease in the J-Ring height difference of 3 mm, and no further benefit was seen in the slump flow – J-Ring diameter for the 8% silica fume mixture. The L-Box ratio for the 8% silica fume partial replacement mixture increased by 47% when the air content was increased to 7%. It had an acceptable value of 0.73, which is close to a normal value for SCC (The European Guidelines for Self-Compacting Concrete 2005). The mixture containing 30% slag partial replacement showed a decrease in the slump flow – J-Ring diameter and a J-Ring height difference of 8% and 35%, respectively, when the air content was increased to 5%. Also, the L-Box ratio increased by 92% to 0.8 when increasing the air content up to 7%, well within an acceptable value for SCC. Increasing the air content further to 7% generated no additional improvement in the J-Ring height difference and the L-Box ratio. However, for the 30% partial slag replacement mixture,

the slump flow – J-Ring diameter further decreased by 20% when the air content was increased from 5 to 7%. The segregation factor for both mixtures showed a decreasing trend when the air content was increased. For the 8% silica fume partial replacement mixture, the segregation factor decreased by 48% when the air content was increased to 5% and further decreased by 16% when the air content was increased to 7%. The 30% slag partial replacement mixture showed a large reduction of 99.6% in the segregation factor when the air content was increased from 0 to 5%. Further increasing the air content to 7% yielded no additional decrease in the segregation factor when using 30% partial slag replacement.

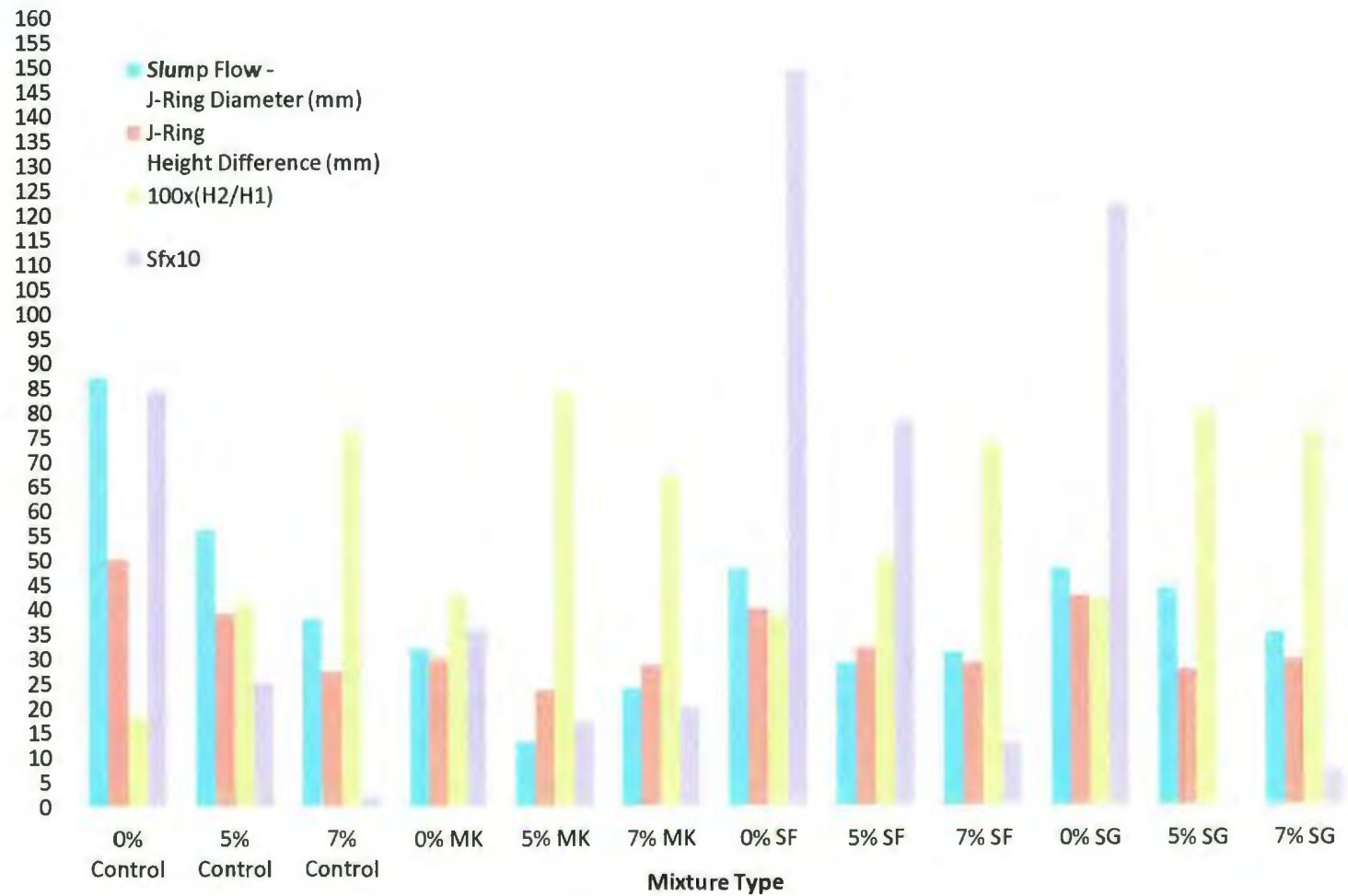


Figure 20 – Passing Ability and Segregation Results for Varying Air Percentages (Units Denoted in Legend)

5.1.3 HRWR Demand

5.1.3.1 Effect of Metakaolin

The HRWR demand results are presented in Figure 21. The HRWR demand was seen to increase as the percentage of metakaolin partial replacement was increased from 0 to 25%. As the partial percentage of metakaolin was increased to 25%, the HRWR demand increased by 148% compared to the control mixture. This result was similar to those of Hassan et al. (2012) and Madandoust et al. (2012), showing that increasing the percentage of metakaolin requires additional HRWR to achieve the desired workability. Using a partial replacement of 8% silica fume showed a higher HRWR demand compared to the control mixture, and a 5% partial metakaolin replacement, while using a partial replacement level higher than 5% metakaolin, resulted in a lower HRWR demand compared to the remaining metakaolin mixtures. The 8% partial silica fume replacement required 47% more HRWR to produce a similar slump flow to that of the control mixture. However, the 30% partial slag replacement had the lowest HRWR demand of any other mixtures and required 35% less HRWR than the control mixture.

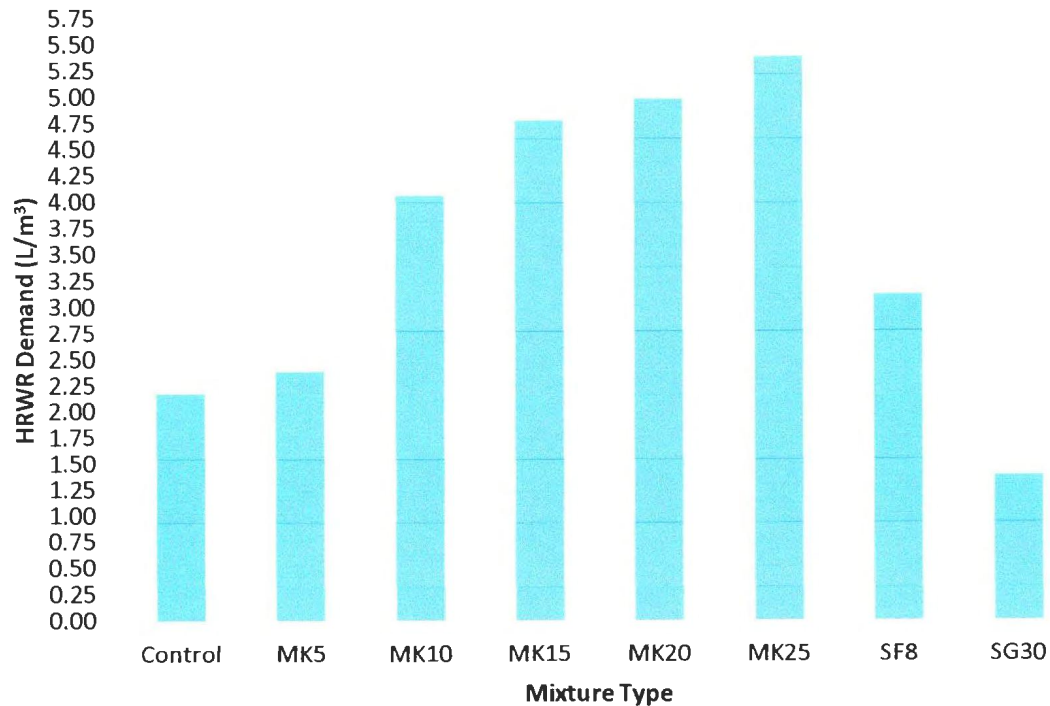


Figure 21 – Effect of Metakaolin on HRWR Demand

5.1.3.2 Effect of C/F Ratio

Figure 22 illustrates that as the C/F ratio was increased from 0.7 to 0.9, the amount of HRWR required for the control mixture to achieve the desired slump flow decreased by 27%. Further increasing the C/F ratio to 1.2 for the control mixture resulted in no additional HRWR. All other mixtures showed a decrease in the HRWR demand as the C/F ratio was increased. The 20% partial metakaolin replacement required 19% less HRWR as the C/F ratio was changed from 0.7 to 1.2. In addition, both the 8% silica fume and 30% slag partial replacements required 9% and 33% less HRWR, respectively. Similar results when increasing the volume of the coarse aggregate were observed by Sonebi et al. (2007). They showed that increasing the coarse aggregate volume and fixing

the dosage of HRWR and the W/B amount led to an increase in the slump. This indicated the presence of free water in the mixture due to the smaller surface area of the larger aggregates compared to the smaller fine aggregates. Thus less HRWR could be added to obtain comparable slump flows.

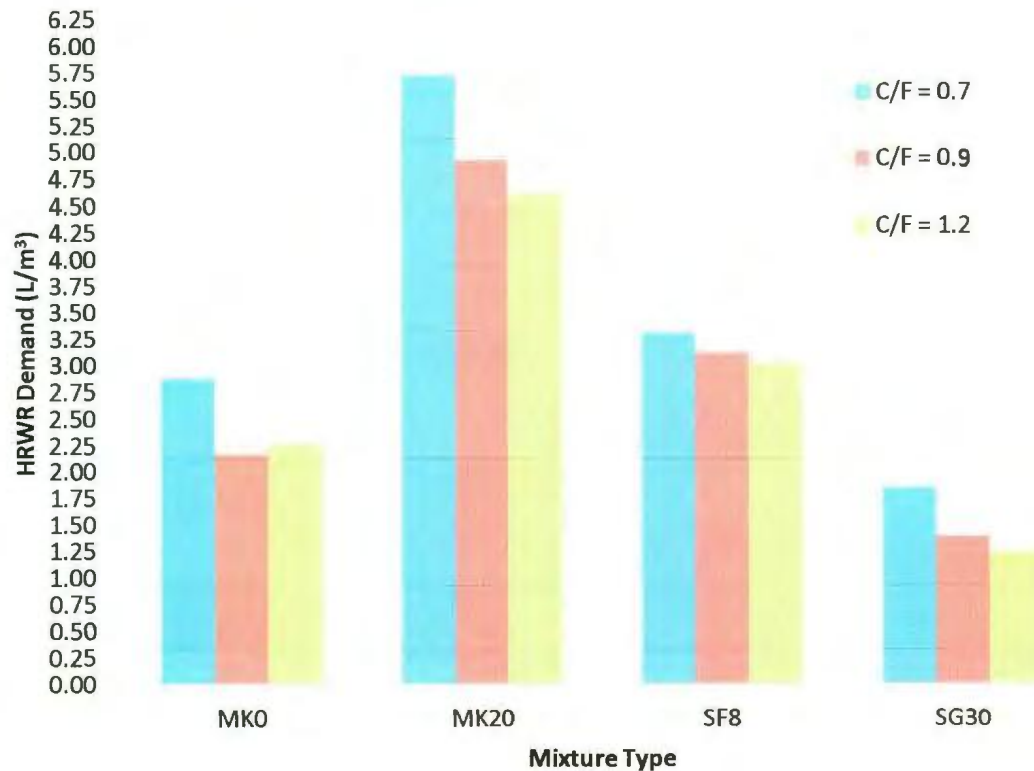


Figure 22 – Effect of C/F Ratio on the HRWR Demand

5.1.3.3 Effect of Coarse Aggregate Size

Figure 23 shows the HRWR demand for varying coarse aggregate sizes. From the figure it can be seen that increasing the size of the coarse aggregate in the mixture decreased the amount of HRWR required to achieve the desired slump flow of 650 ± 50 mm. It has been shown that increasing the coarse aggregate size lowers the water demand

required to achieve a desired workability (Neville 1995). This means that if the W/B is held constant, there is more free water and thus less HRWR is required. The control mixture required 18% less HRWR when using the 20 mm stone compared to the 10 mm stone. In addition, the HRWR demand for the 20% partial metakaolin mixture decreased by 6%. Both 8% silica fume and 30% slag partial replacement mixtures showed a decrease in the HRWR of 13% and 7%, respectively. This is similar to a study carried out by Salman et al. (2008) that showed a slight reduction in the required superplasticizer dosage when increasing the maximum coarse aggregate size.

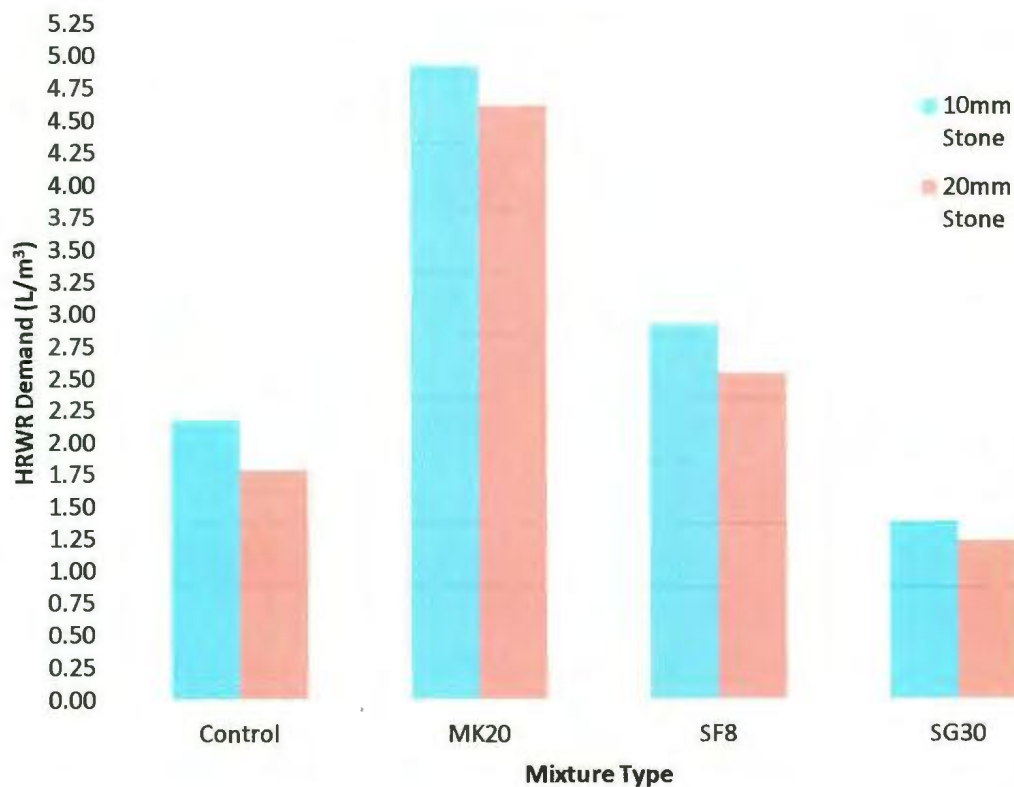


Figure 23 – Effect of Coarse Aggregate Size on HRWR Demand

5.1.3.4 Effect of Binder Content

Figure 24 shows the results for the HRWR demand for varying binder contents. The results show that the HRWR demand for the control, 30% slag, and 8% silica fume partial replacement mixtures were slightly lower when the binder content was increased from 450 to 500 kg/m³. The mixture using 20% partial metakaolin replacement required no additional HRWR to achieve the desired slump flow diameter. The HRWR demand for the control mixture decreased by 9%; however, it required 5% and 18% more HRWR for both 8% silica fume and 30% slag partial replacements when using an increased binder amount. Increasing the binder content has been reported to reduce the HRWR in SCC due to the addition of more fine materials that reduce interparticle friction and water demand (Khayat 2000). Assaad et al. (2005) also showed results that increasing the binder content reduced the HRWR to produce SCC with comparable slump flows.

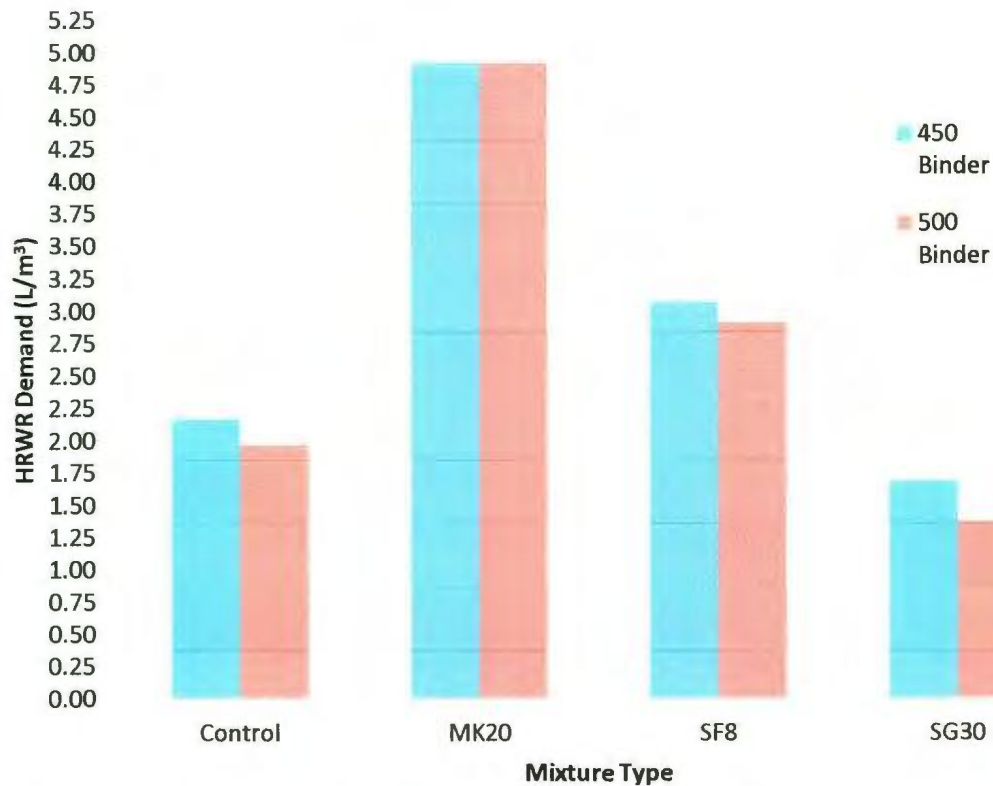


Figure 24 – Effect of Binder Content on HRWR Demand

5.1.3.5 Effect of Air Content

No significant difference in the HRWR demand was noticed for any mixture when the air content was increased from 0 to 7%. Gutmann (1987) found that increasing the air content in concrete resulted in a small decrease in the amount of water required to achieve a similar slump to mixtures containing 2% air content. This small decrease translates to less HRWR required if using a fixed W/B ratio. From Figure 25 it can be seen that the demand decreased by 6% (from 4.92 to 4.62 l/m³) when air content was increased from 0 to 7%, respectively, for the mixture using 20% partial cement replacement with metakaolin. The control mixture showed little to no difference in the amount of HRWR

required, and both 8% silica fume and 30% slag partial replacements required less HRWR. For 8% silica fume partial replacement, the HRWR demand saw around a 1% decrease (from 3.12 to 3.09 l/m³) when the air content was increased from 0 to 7%. And 30% slag partial replacement decreased by 3.6% (from 1.38 to 1.33 l/m³) when the air percentage was increased from 0 to 7%, respectively.

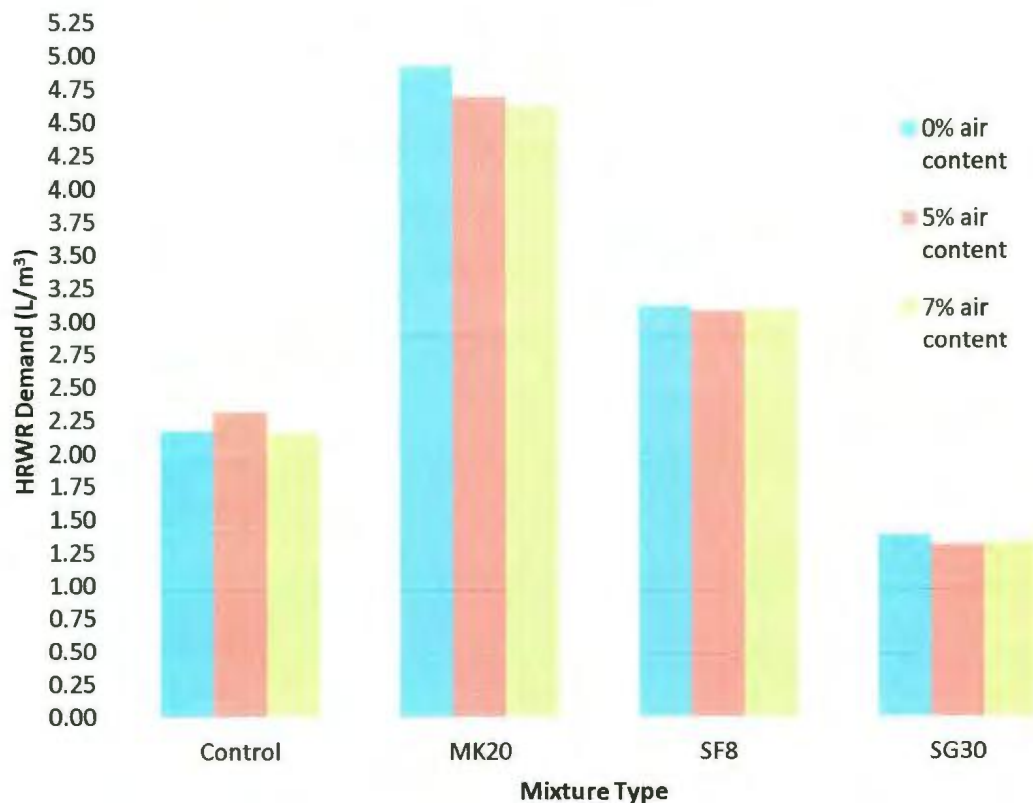


Figure 25 – Effect of Air Content on HRWR Demand

5.2 Mechanical Properties

Table 9 presents the results for the compressive strength at 1-, 3-, 7-, 28- and 90 days, the normalized FS, STS and ME, as well as the modulus of rupture for Stage 1 mixtures. The 1-, 3- and 7- day strength developments for all mixtures are shown in Table 10.

Table 9 – Mechanical Properties for Stage 1 Mixtures

Concrete Type	f'_c , MPa					FS / $\sqrt{f'_c}$	f_r (MPa)	STS / f'_c	ME / $10 \times \sqrt{f'_c}$
	1 Day	3 Day	7 Day	28 Day	90 Day				
Control	7.0	16.8	23.1	31.1	37.9	0.566	1.62	0.092	4.24
MK5	8.4	21.6	31.1	41.3	45.6	0.581	1.66	0.083	4.34
MK10	9.1	23.1	34.0	42.1	48.7	0.602	1.73	0.080	4.54
MK15	7.8	22.8	39.5	47.6	50.6	0.615	1.85	0.073	4.83
MK20	10.0	25.5	38.5	50.6	56.8	0.620	1.96	0.087	4.45
MK25	8.3	23.5	38.2	43.5	52.1	0.675	1.76	0.093	4.25
SF8	9.7	23.1	34.0	44.4	48.6	0.558	1.80	0.096	4.67
SG30	5.5	15.9	27.9	37.0	42.3	0.550	1.71	0.094	4.56

Table 10 - Strength Development for Stage 1 Mixtures

Concrete Type	Strength Development		
	1 Day	3 Day	7 Day
Control	0.22	0.45	0.69

MK5	0.20	0.50	0.76
MK10	0.22	0.55	0.81
MK15	0.18	0.48	0.83
MK20	0.20	0.50	0.77
MK25	0.19	0.54	0.88
SF8	0.22	0.51	0.76
SG30	0.17	0.45	0.72

5.2.1 Strength Development

5.2.1.1 Effect of Metakaolin

To account for the variations in the compressive strengths, the 1-, 3-, and 7-day compressive strengths were divided by their respective 28-day compressive strengths to normalize the results. The normalized 1-, 3-, and 7-day compressive strengths are shown in Figure 26 and Table 10. All metakaolin mixtures (except MK10) had a 1-day strength development lower than the control mixture. The 1-day strength development increased from 5% to 10% in metakaolin replacements, then decreased when the percentage was further increased to 15%, and finally increased as the metakaolin replacement percentage was further increased to 20%. Using a metakaolin replacement of greater than 25% yielded no additional benefits towards the 1-day strength development. These results match those observed by Khatib (2008), who showed that using metakaolin resulted in 1-day strength developments lower than the control mixture. All metakaolin replacement percentages had a higher 1-day strength development than the mixture using 30% slag as

a partial cement replacement. Compared to 8% silica fume, only the 10% metakaolin replacement percentage had a comparable 1-day strength development, while all other metakaolin percentages had a lower 1-day strength development.

The 3-day strength development increased up to 10% metakaolin partial replacement and then decreased when the metakaolin replacement level was increased to 15%. As the metakaolin replacement level was further increased from 15% to 25%, the strength development after 3-days increased. All mixtures using metakaolin as a partial cement replacement showed a higher 3-day strength development than the control mixture. Qian et al. (2001) found similar results when using metakaolin. It was seen that all metakaolin mixtures obtained higher strength developments after 3 days than when not using metakaolin. All metakaolin replacement percentages showed 3-day strength developments greater than those found with 30% slag as a partial cement replacement. Only the 10% and 25% metakaolin replacement levels had a higher 3-day strength development compared to silica fume partial cement replacement.

The 7-day strength development increased with increasing partial replacement with metakaolin up to 15%. Further increasing the partial replacement percentage from 15 to 20% decreased the strength development, while increasing it from 20% to 25% increased the strength development. All metakaolin partial replacement percentages had larger 7-day strength developments compared to the mixtures using no cement replacement. Research done by Wild et al. (1996) had similar results that showed that using metakaolin increased the strength development after 7 days compared to using no metakaolin.

All mixtures using metakaolin, except for 5% partial replacement, showed a higher 7-day strength development when compared to a mixture using 8% silica fume as a partial cement replacement. The 5% partial metakaolin replacement showed a similar 7-day strength to that of silica fume as a partial cement replacement. All metakaolin mixtures showed a 7-day strength development greater than using 30% slag partial replacement.

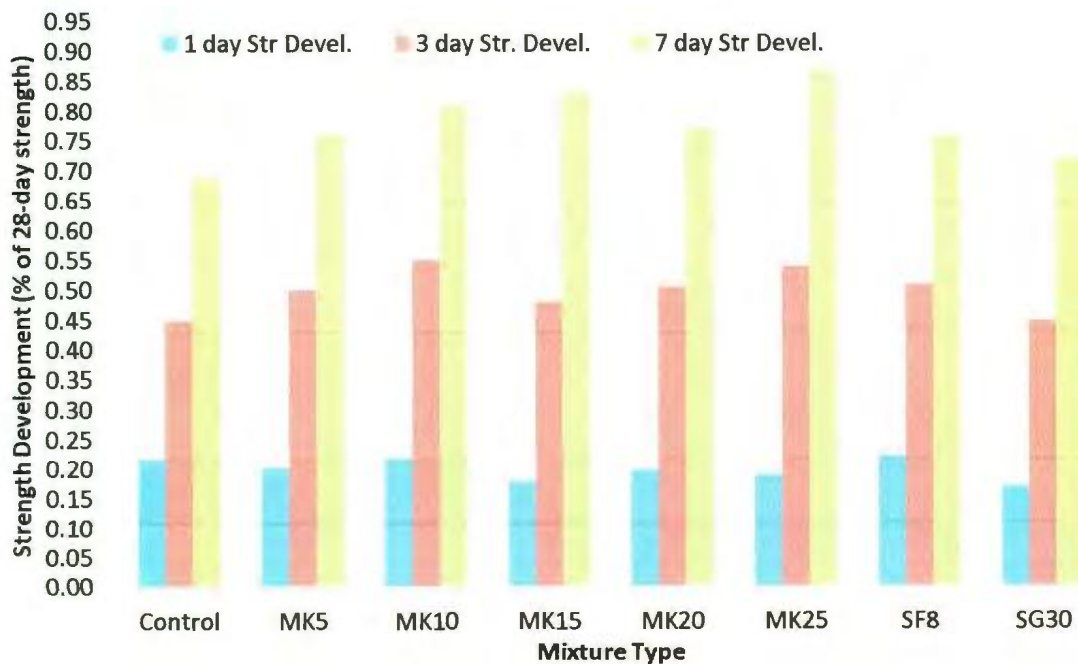


Figure 26 – Strength Development for Stage 1 Mixtures

Table 11 – Mechanical Properties for Varying Mixture Parameters

Concrete Type	f'_c , MPa					f_r (MPa)	STS/ f'_c	ME /10x $\sqrt{f'_c}$
	1-	3-	7-	28-	90-			
	Day	Day	Day	Day	Day			
						FS / $\sqrt{f'_c}$		

0.7C	6.1	13.2	20.7	28.5	33.0	0.56	1.91	0.91	0.44
0.7MK	8.8	20.3	34.1	45.5	53.3	0.58	2.29	0.86	0.451
0.7SF	7.9	18.2	29.0	38.5	45.6	0.55	1.94	0.93	0.472
0.7SG	5.0	13.5	24.3	32.8	38.7	0.55	1.84	0.92	0.471
1.2C	7.4	18.1	23.8	31.6	41.7	0.58	1.56	1.05	0.421
1.2MK	11.2	28.1	42.3	54.9	58.7	0.63	1.76	0.90	0.439
1.2SF	10.1	24.4	35.8	46.8	51.9	0.58	1.74	1.01	0.456
1.2SG	6.9	18.5	31.0	40.9	44.37	0.57	1.50	1.04	0.443
5%C	5.8	15.3	19.8	28.4	35.0	0.57	1.46	0.916	0.420
5%MK	9.4	23.9	33.9	47.0	53.1	0.59	1.83	0.807	0.436
5%SF	8.4	20.8	30.1	40.89	46.6	0.53	1.70	0.867	0.451
5%SG	5.0	13.8	22.3	31.4	37.0	0.51	1.43	0.896	0.451
7%C	5.5	14.0	16.8	25.6	32.6	0.50	1.34	0.856	0.419
7%MK	8.8	21.73	30.4	45.0	51.6	0.52	1.75	0.786	0.439
7%SF	6.7	17.3	24.1	35.2	42.2	0.50	1.54	0.832	0.438
7%SG	4.7	12.6	18.6	27.9	32.8	0.48	1.33	0.883	0.438
20C	8.1	17.6	24.2	32.1	39.1	0.628	1.55	0.993	0.44
20MK	10.8	24.8	40.3	51.9	57.1	0.637	1.79	0.882	0.47
20SF	9.6	22.6	35.0	44.4	48.5	0.640	1.67	0.993	0.49
20SG	6.3	15.9	29.2	38.6	43.3	0.622	1.58	1.05	0.47
500C	10.1	20.1	28.8	37.9	44.1	0.654	2.01	1.05	0.449

500MK	12.5	28.8	43.5	54.7	62.7	0.725	2.34	0.930	0.459
500SF	10.3	24.6	37.2	47.1	52.8	0.685	2.18	1.03	0.472
500SG	8.9	18.6	31.8	41.6	46.7	0.729	2.05	1.02	0.473

Table 12 – Strength Development for Varying Mixture Parameters

Concrete Type	Strength Development		
	1 Day	3 Day	7 Day
0.7C	0.23	0.47	0.70
0.7MK	0.22	0.45	0.69
0.7SF	0.21	0.44	0.68
0.7SG	0.21	0.51	0.81
1.2C	0.21	0.49	0.77
1.2MK	0.19	0.46	0.73
1.2SF	0.17	0.45	0.72
1.2SG	0.17	0.43	0.72
5%C	0.20	0.44	0.68
5%MK	0.19	0.51	0.72
5%SF	0.20	0.51	0.74
5%SG	0.16	0.44	0.71
7%C	0.19	0.43	0.66
7%MK	0.19	0.48	0.68

7%SF	0.19	0.49	0.69
7%SG	0.16	0.45	0.67
20C	0.20	0.44	0.65
20MK	0.19	0.49	0.75
20SF	0.21	0.48	0.74
20SG	0.16	0.42	0.72
500C	0.26	0.51	0.76
500MK	0.22	0.52	0.78
500SF	0.23	0.52	0.77
500SG	0.21	0.46	0.74

5.2.1.2 Effect of C/F Ratio

Table 11 and Figure 27 show the strength development results for varying C/F ratios. From Figure 27 it can be seen that as the C/F ratio increased, the 1-, 3-, and 7-day strength development decreased for all mixtures. The mixture using metakaolin as a partial replacement had a 4.8%, 7.3%, and 6.5% decrease in the 1-, 3-, and 7-day strength developments when the C/F ratio was increased from 0.7 to 1.2. Raising the C/F ratio from 0.7 to 1.2 decreased the 1-, 3-, and 7-day strength developments by 5.7%, 6.5%, and 3%, respectively, for the control mixture. The 8% silica fume and 30% slag mixtures also showed a similar trend as those of the control and metakaolin mixtures, where the 1-, 3-, and 7-day strength developments decreased as the C/F ratio was increased from 0.7 to 1.2. As the C/F ratio was increased the total volume of the coarse aggregate in the mixture

was increased. The mechanical properties of concrete are related to the ITZ that forms between the coarse aggregate and the cement matrix. This transition zone has low-density cement grains and contributes to the reduction in the overall strength and porosity of the concrete (Larbi 1993). As the volume of the coarse aggregate was increased, the total volume of the interfacial zone increased, which reduced the quality of the concrete and the strength development.

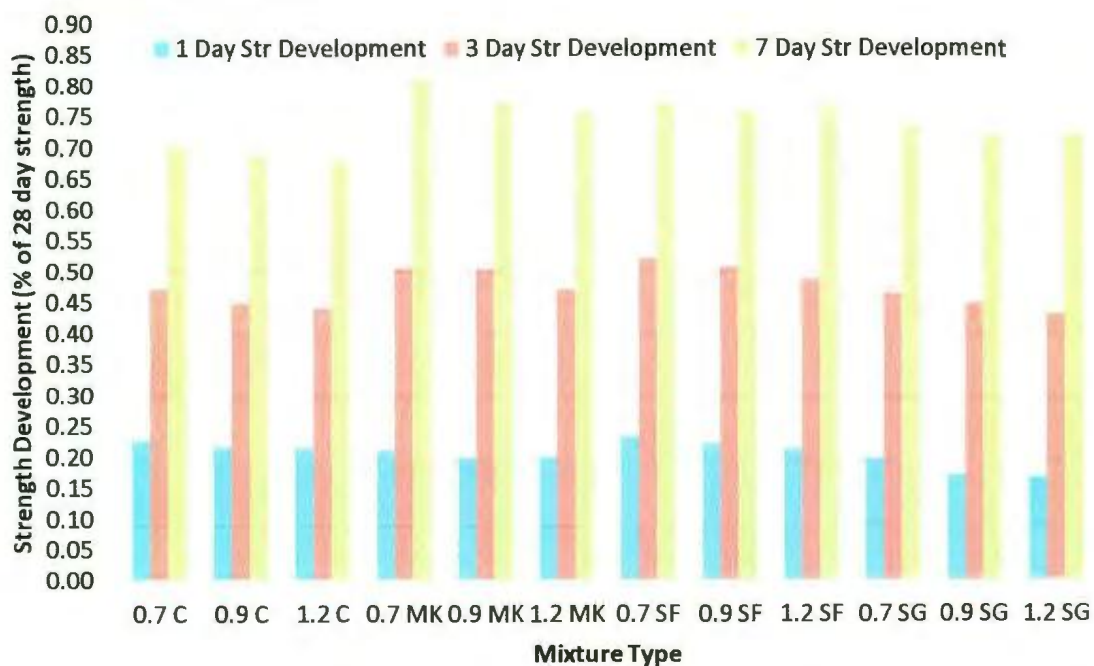


Figure 27 – Effect of C/F Ratio on Strength Development

5.2.1.3 Effect of Coarse Aggregate Size

The strength development results for varying coarse aggregate sizes are shown in Table 12 and Figure 28. From Figure 28 it can be seen that increasing the coarse aggregate size from 10 to 20 mm, the 1-, 3-, and 7-day strength developments for all mixtures decreased. The 1-, 3-, and 7-day strength developments for mixtures using

metakaolin as a partial cement replacement had a decrease of 4%, 2.7%, and 3%, respectively, as the aggregate size was increased from 10 to 20 mm. As well, increasing the coarse aggregate size from 10 to 20 mm for the control mixture showed a decrease of 6.5%, 2.1%, and 5.2% in the 1-, 3-, and 7-day strength developments, respectively. Mixtures using 8% silica fume as a partial replacement showed decreases of 5.2%, 6%, and 2.7% for 1-, 3-, and 7-day strength development, respectively, while 30% slag as a partial replacement showed decreases of 4.1%, 6.3%, and 0.44% for the 1-, 3-, and 7-day strength developments, respectively, when using a 20 mm coarse aggregate. Yaqub et al. (2006) observed that increasing the coarse aggregate size from 10 to 25 mm decreased the strength development of normal concrete after 7 and 14 days.

This decrease in the strength development could be a contribution to the interaction of the ITZ, as previously described. As the coarse aggregate size was increased (while holding the C/F ratio constant), the thickness of the ITZ increased (Larbi 1993), which contributed to the reduction in the strength development of the concrete.

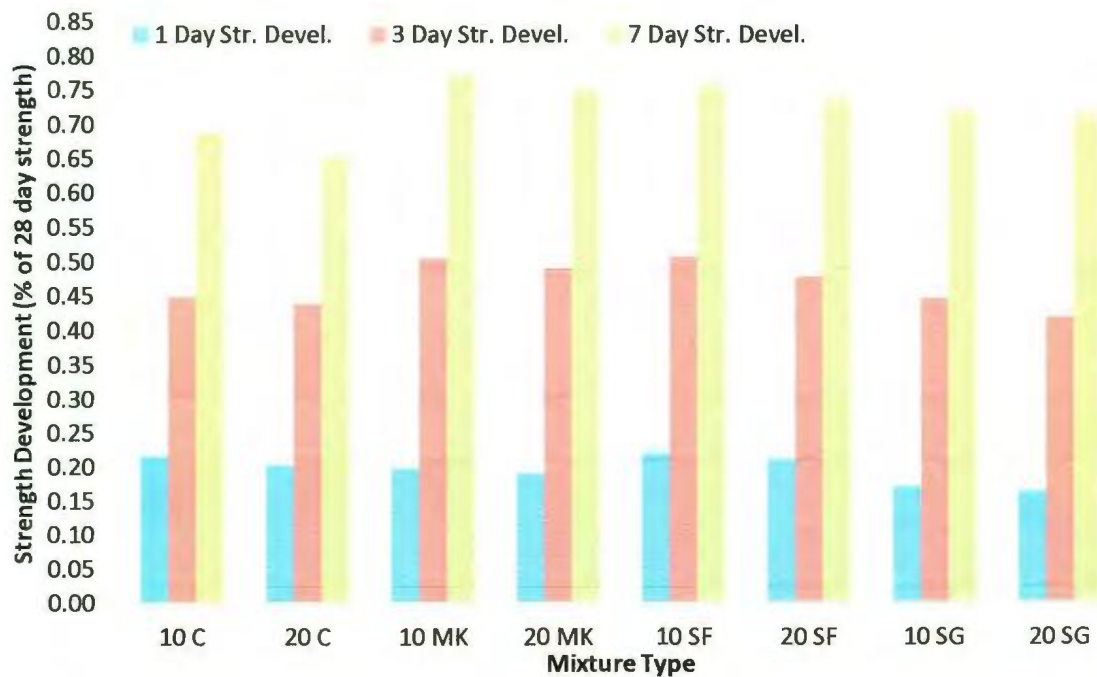


Figure 28 - Effect of Coarse Aggregate Size on Strength Development

5.2.1.4 Effect of Binder Content

Increasing the binder from 450 to 500 kg/m³ increased the 1-day strength development for all mixtures. From Figure 29 and Table 12 it can be seen that the control mixture showed an increase in the 1-day strength development of 20.3%, while using metakaolin as a partial cement replacement showed an increase of 10.6%. Both 8% silica fume and 30% slag as partial replacements had increases of 4.1% and 21.7%, respectively. The 3-day strength development for all mixtures increased as the binder content was increased from 450 to 500 kg/m³. The 3-day strength development rose by 14% for the control mixture and by 2.4% when using 20% metakaolin as a partial cement replacement. Both 8% silica fume and 30% slag partial replacements had increases in the 3-day strength development with the increased binder content. All mixtures had an

increase in their 7-day strength development when the binder was increased from 450 to 500 kg/m³. Using 20% metakaolin as a partial replacement increased the strength development by 1.0%, from 0.774 to 0.782, while the control mixture increased by 10.6%, from 0.687 to 0.760. Both 8% silica fume and 30% slag as a partial cement replacement showed increases of 1.5% and 3.1%, respectively, for their 7-day strength developments with the increased binder content.

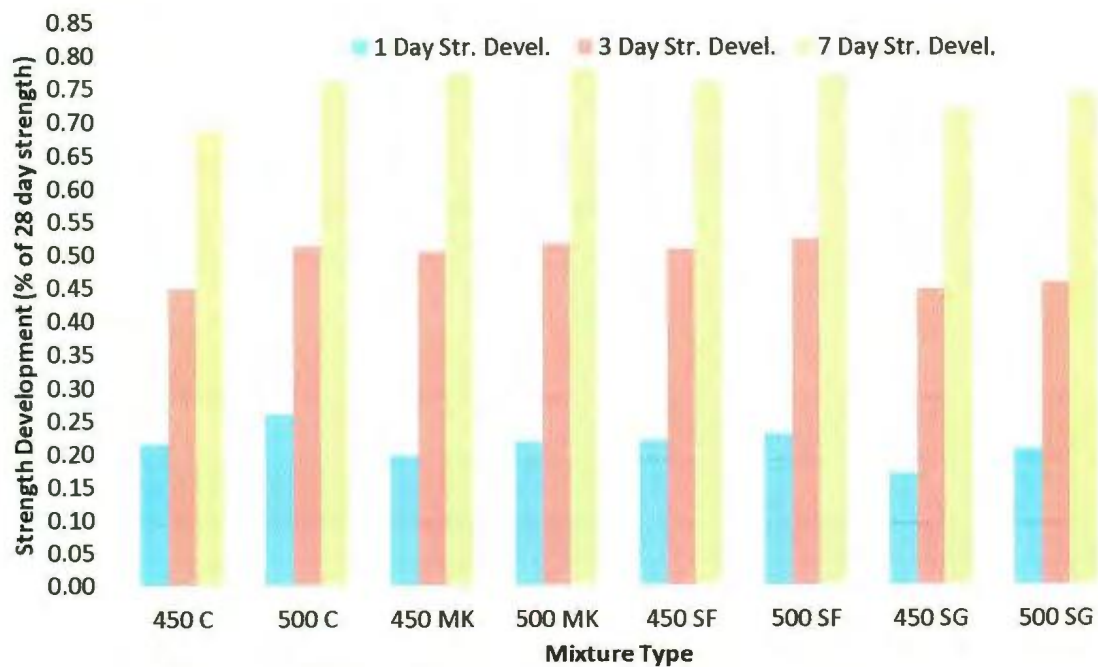


Figure 29 – Effect of Binder Content on Strength Development

5.2.1.5 Effect of Air Content

Figure 30 and Table 12 show the results for 1-, 3-, and 7-day strength developments for varying air percentages. From this figure it can be seen that as the air percentage was increased from 0 to 7%, the 1-, 3-, and 7-day strength developments decreased. The control mixture decreased by 10.6% as the air content was increased from

0 to 7%. Using 20% metakaolin partial replacement showed a decrease of 2% in the 1-day strength development when increasing air content up to 7%. And using 8% silica fume as a partial replacement had a decrease of 14% in the 1-day strength development, while the 30% slag mixture had a decrease of 7.1% in the 1-day strength development when the air content was increased from 0 to 7%. The 3-day strength development decreased by 4% for the control mixture, by 4.2% for the 20% metakaolin as a partial cement replacement mixture, by 5.8% for the 8% partial replacement of cement with silica fume, and by 1.3% using 30% slag partial replacement when the air content was increased from 0 to 7% for each mixture. The 7-day strength development for all four mixtures decreased with increasing air content: the control mixture showed a decrease of 4.2%, the 20% metakaolin as a partial replacement had a decrease of 12.8%, and both 8% silica fume and 30% slag as a partial replacement had decreases of 9.5% and 7.2%, respectively, as the air content increased from 0 to 7%. Gutmann (1987) showed similar results where increasing the air content resulted in decreased strength developments after 1, 3, and 7 days when increasing the air content from 1.9 to 3.75%.

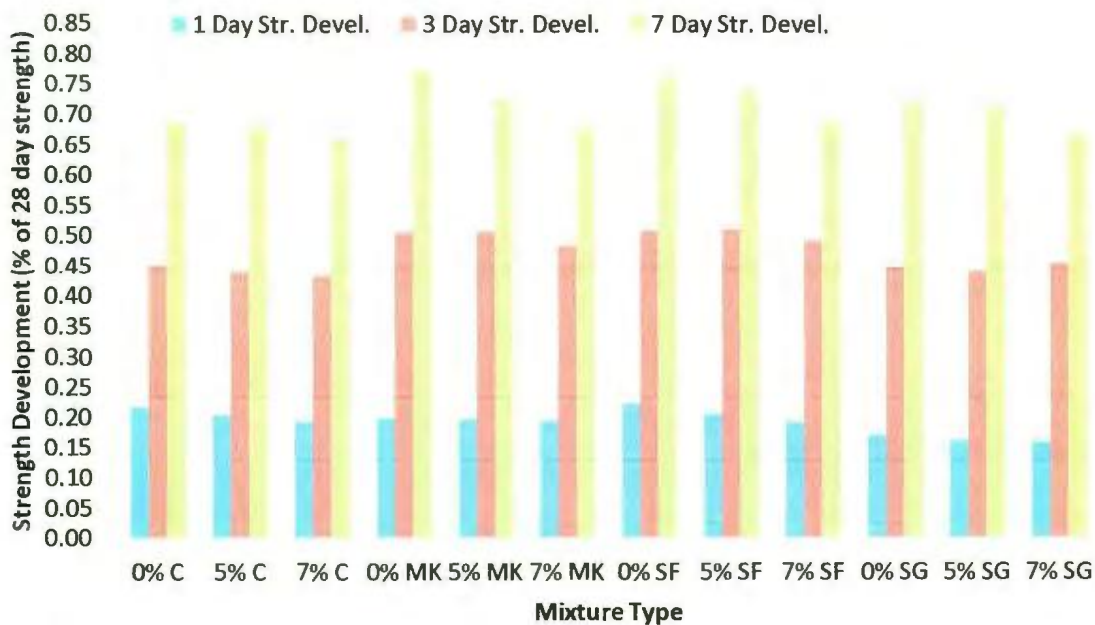


Figure 30 – Effect of Air Content on Strength Development

5.2.2 28- and 90-Day Compressive Strengths

5.2.2.1 Effect of Metakaolin

Figure 31 and Table 9 show the 28- and 90-day compressive strengths for all metakaolin partial replacement percentages. From this figure it can be seen that the 28-day compressive strength increased by 29.8% as the metakaolin replacement level was increased to 20%. Madandoust et al. (2012) also showed that using any percentage of metakaolin (5 to 20%) increased the 28-day compressive strength with more noticeable improvements with larger amounts of metakaolin. Further increasing the metakaolin replacement level from 20 to 25% decreased the 28-day strength by 13.4%. All partial metakaolin replacement percentages obtained a higher 28-day compressive strength

compared to the control mixture. This agrees with multiple researchers who have shown similar results. Qian et al. (2001) showed a large increase of 84% in the 28-day compressive strength with the inclusion of 15% metakolin. Also, all partial metakaolin replacement levels had a higher 28-day compressive strength compared to 30% slag replacement, while only the 15%, 20%, and 25% partial metakaolin replacements had a 28-day compressive strength that was higher compared to 8% silica fume as a partial replacement. The 10% partial metakaolin replacement showed a similar 28-day compressive strength to 8% partial silica fume replacement.

The 90-day compressive strength increased by 24.7% as the metakaolin partial replacement level was increased to 20%. As the metakaolin partial replacement was further increased to 25%, the 90-day compressive strength decreased by 3.9%. All partial metakaolin replacement percentages obtained a higher 90-day compressive strength compared to the control mixture, which was expected when using metakaolin. Wild et al. (1996) found the same conclusions when using metakaolin, but they showed that using a 5% metakaolin percentage resulted in a slightly lower 90-day compressive strength compared to the control mixture. However, this result differs from the results shown in Figure 30, although 5% metakaolin showed a small increase of 2.07 MPa over the control mixture. Using a partial metakaolin replacement percentage less than 15% resulted in a 90-day compressive strength that was lower compared to a mixture using 8% silica fume as a partial cement replacement. All partial metakaolin replacement levels investigated had a higher 90-day compressive strength compared to 30% partial slag replacement.

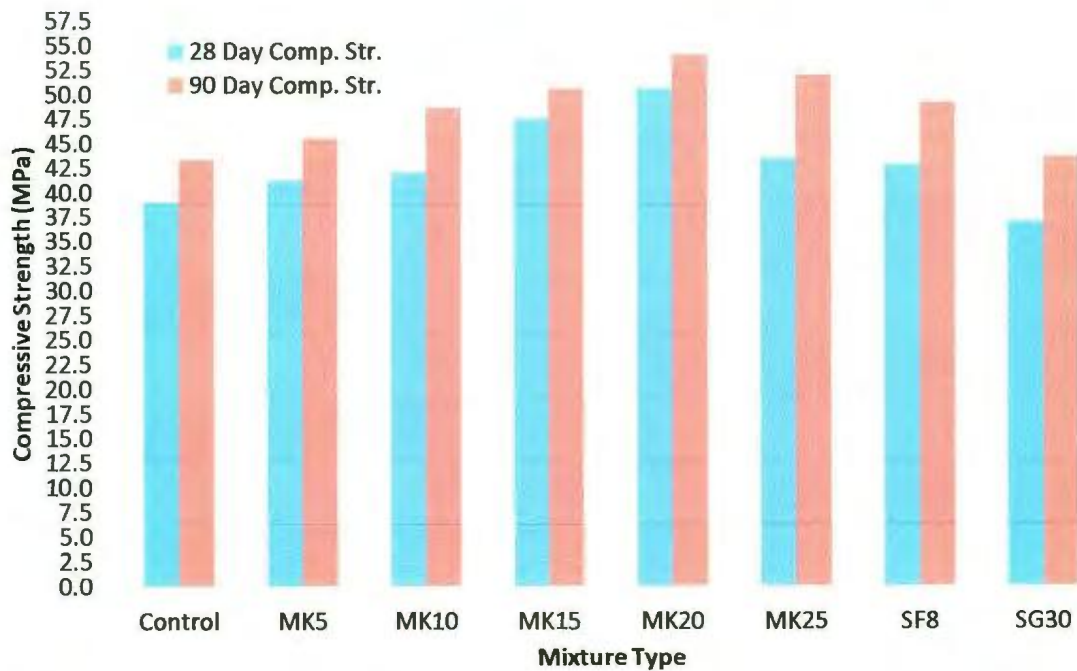


Figure 31 – Effect of Metakaolin on 28- and 90-Day Compressive Strength

5.2.2.2 Effect of C/F Ratio

Figure 32 and Table 11 show the results for the 28- and 90-day compressive strengths for varying C/F ratios. It can be seen from this figure that both the 28- and 90-day compressive strengths decreased as the C/F ratio was changed from 0.7 to 1.2. Examining the control mixture, there was a 6.5% and 6% decrease in the 28- and 90-day compressive strengths, respectively, as the C/F ratio was increased from 0.7 to 1.2. When using the 20% metakaolin mixture, the 28- and 90-day compressive strengths decreased by 6.3% and 5.8%, respectively, as the C/F ratio was increased from 0.7 to 1.2. Both 8% silica fume and 30% slag as partial cement replacements showed decreases of 6.4% and 3.8% for the 28-day compressive strength, while the 90-day compressive strengths had a decrease of 4.2% and 4.9%, respectively, as the C/F ratio was increased from 0.7 to 1.2.

The mechanical properties of concrete are related to the ITZ that forms between the coarse aggregate and the cement matrix. This transition zone has low-density cement grains and contributes to an overall reduction in the strength and porosity of the concrete (Larbi 1993). As the volume of the coarse aggregate was increased, the total volume of the interfacial zone increased, which reduced the quality of the concrete and the compressive strength.

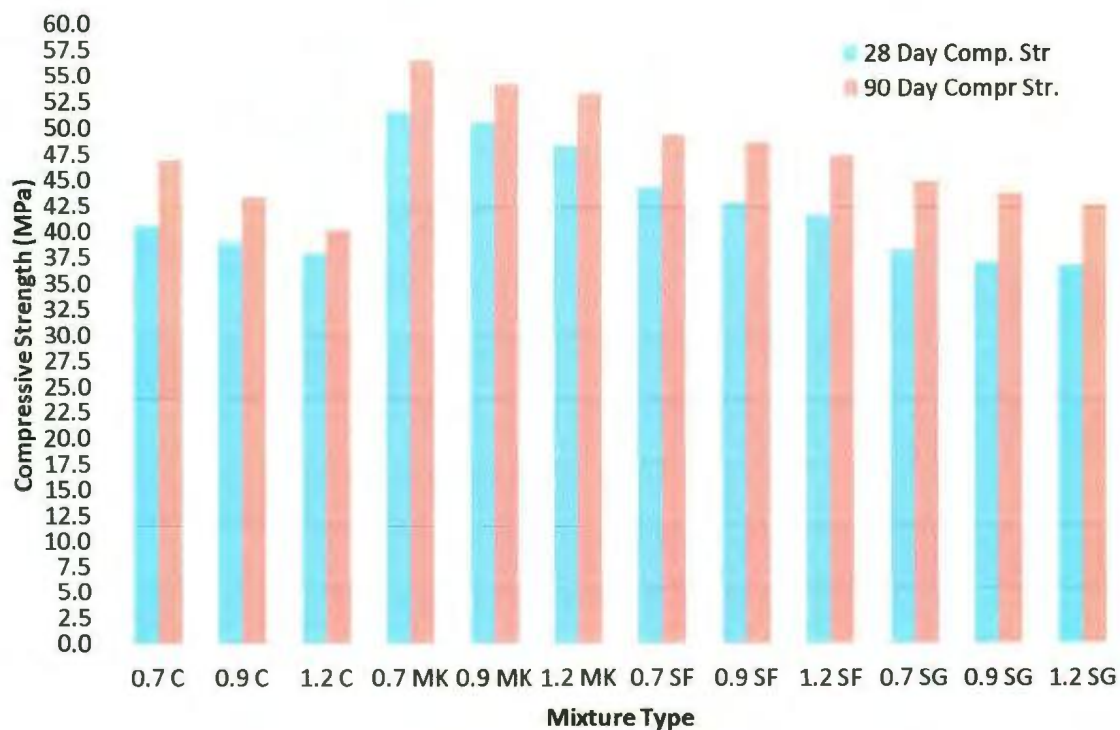


Figure 32 - Effect of C/F on 28- and 90-Day Compressive Strengths

5.2.2.3 Effect of Coarse Aggregate Size

Figure 33 and Table 11 show the results for the 28- and 90-day compressive strengths when using a 20 mm coarse aggregate. The 28-day compressive strength for the control mixture decreased by 5.6% when the coarse aggregate size was increased from 10

mm to 20 mm. The 20% metakaolin mixture also had a decrease of 6.7% in the 28-day compressive strength, from 50.63 to 47.22 MPa, when the coarse aggregate size was increased. The 8% silica fume mixture had a decrease of 7.6% in the 28-day compressive strength with increased coarse aggregate size, while the 30% slag mixture had a decrease of 8.9%. The 90-day compressive strength for the control mixture fell by 4.1% when using the 20 mm coarse aggregate. Using 20% metakaolin as a partial replacement showed a small decrease of 2.7% in the 90-day compressive strength when the coarse aggregate size was increased to 20 mm. 8% silica fume as a partial replacement also showed a small decrease of 2.2% in the 90-day compressive strength when using the 20 mm coarse aggregate. 30% slag as a partial replacement showed a 1.0% decrease in the 90-day compressive strength when the size of the coarse aggregate was increased from 10 to 20 mm. When studying the effect of increasing the coarse aggregate size from 25, 50, to 63 mm in normal concrete, Loannides et al. (2006) also recorded a decrease in the 28-day compressive strength when the coarse aggregate size was increased. Yaqub et al. (2006) noted similar observations when they reported a loss in the 28-day compressive strength as the maximum coarse aggregate size increased. This decrease in the strength development could be a contribution to the interaction of the ITZ, as previously described. As the coarse aggregate size was increased (while holding the C/F ratio constant), the thickness of the ITZ was increased (Larbi 1993), which contributed to a reduction in the strength of the concrete.

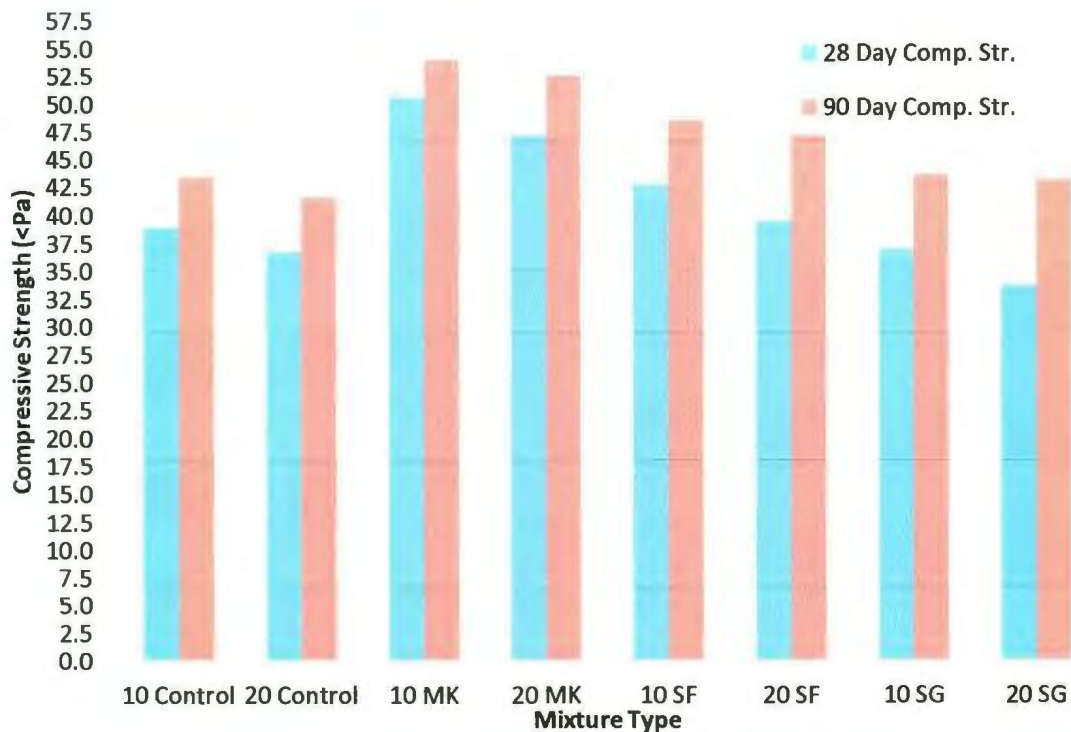


Figure 33 – Effect of Coarse Aggregate Size on 28- and 90-Day Compressive Strengths

5.2.2.4 Effect of Binder Content

Figure 34 and Table 11 show the results for the effect that binder content had on the 28- and 90-day compressive strengths. Figure 34 shows that all mixtures had an increase in the 28-day compressive strength when the binder content was increased from 450 to 500 kg/m³. This is an expected result, that increasing the binding volume increased the compressive strength, and was shown by Su et al. (2001). The control mixture had an increase from 39.00 to 49.54 MPa (a 27% increase), and the 20% metakaolin mixture had an increase in the 28-day compressive strength from 50.63 to 65.64 MPa (a 29.6% increase). The 28-day compressive strengths for both the 8% silica fume and 30% slag

mixtures had increases of 31.4% and 33.9%, respectively, when the binder content was increased from 450 to 500 kg/m³. Marar et al. (2011) found that increasing the cementing materials in a mixture increased the compressive strength. All mixtures also showed increases in their respective 90-day compressive strengths with increasing binder content. The control mixture had an increase of 21.6%, while the 20% metakaolin mixture showed an advancement of 38.7% with increasing binder content. Both 8% silica fume and 30% slag mixtures showed increases of 29.6% and 28.1%, respectively, in their 90-day compressive strengths.

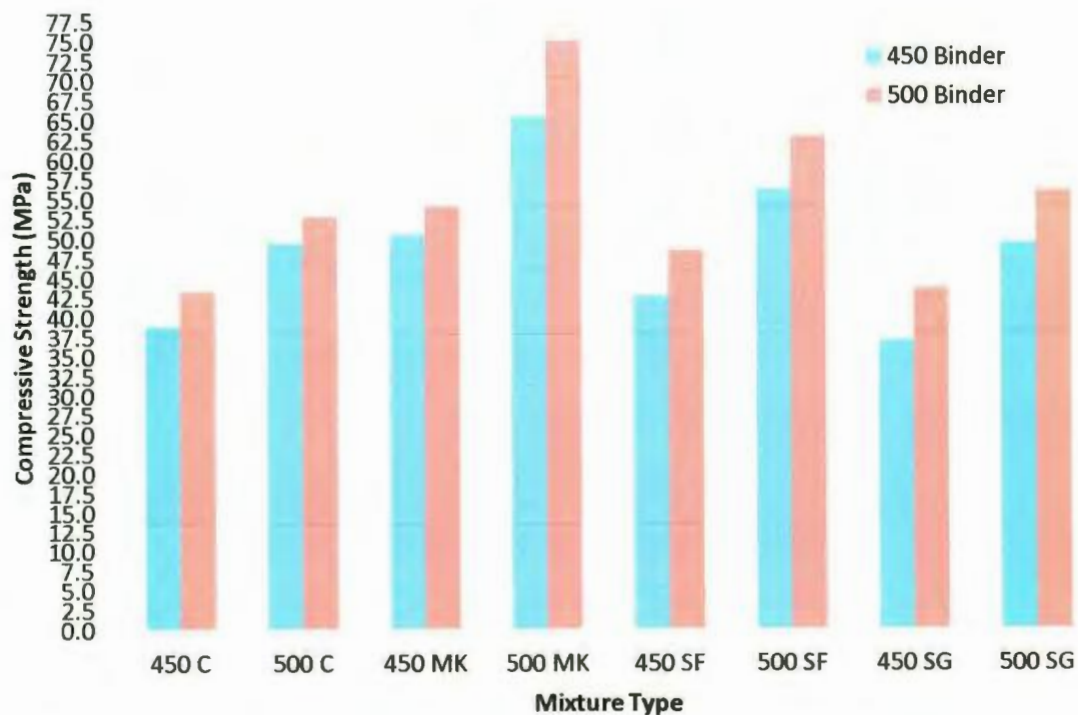


Figure 34 – Effect of Binder Content on 28- and 90-Day Compressive Strengths

5.2.2.5 Effect of Air Content

Table 11 and Figure 35 show the results for the 28- and 90-day compressive strengths for varying air contents. From this figure it can be seen that as the percentage of air was increased from 0 to 7%, the 28- and 90-day compressive strengths decreased. The 20% metakaolin mixture showed a decrease of 11.1% and 4.6% in the 28- and 90-day compressive strengths, respectively. The control mixture had a 21.2% and 9.9% decrease in the 28- and 90-day compressive strengths, respectively, when the air content was increased from 0 to 7%. Both the 8% silica fume and 30% slag mixtures had decreases of 17.8% and 24.7% for the 28-day compressive strengths, respectively, while both showed decreases of 13.2% and 24.9%, respectively, in their 90-day compressive strengths when the air content was increased from 0 to 7%. Gutmann (1987) found similar results when using air entrainment to increase the air content. Gutmann (1987) showed that the addition of air decreased the 28-day compressive strength when the W/B ratio was constant. Beaupre et al. (1999) reported similar results that showed a lower 28-day compressive strength when using air entrainment compared to non-air entrained concrete.

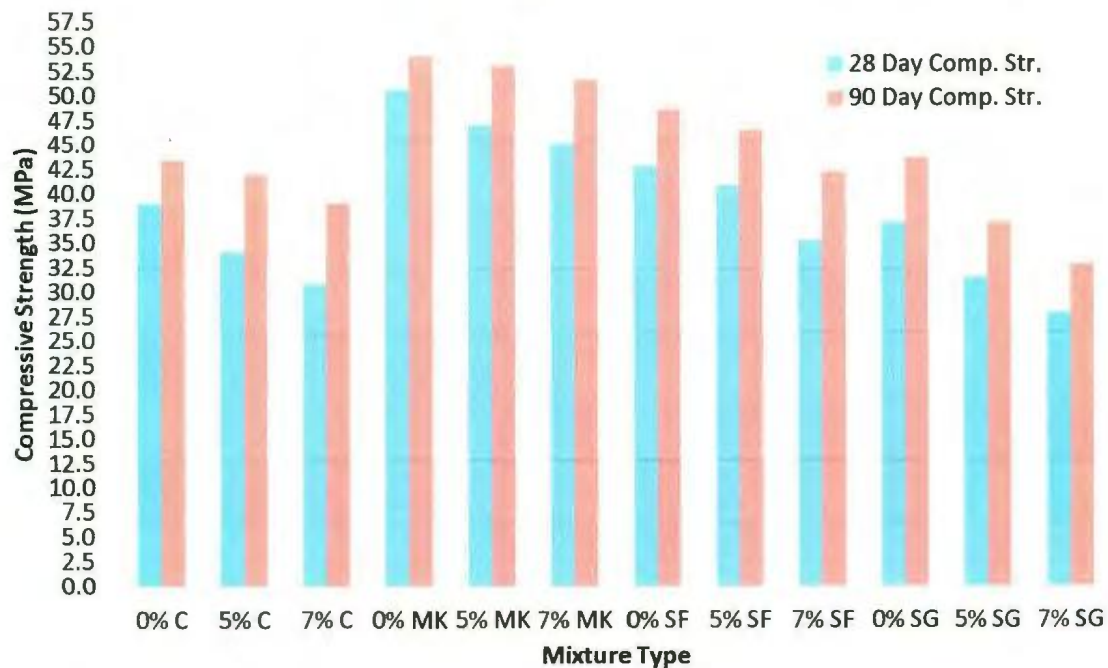


Figure 35 – Effect of Air Content on 28- and 90-Day Compressive Strengths

5.2.3 Flexural Strength

5.2.3.1 Effect of Metakaolin

The flexural strength (FS) for all mixtures was normalized to account for differences in the compressive strength. Since the FS is proportional to the square root of the compressive strength, all FS values were divided by the square root of the 28-day compressive strength. This was done so that a comparison could be made between various SCM types. From Table 9 and Figure 36 it can be seen that using a 20% or greater partial metakaolin replacement percentage resulted in a normalized FS that is higher compared to using 8% silica fume partial cement replacement. 30% slag partial cement replacement exhibited a higher normalized FS compared to 5, 10, 15 and 20% partial metakaolin

replacements and had a similar normalized FS compared to using a 25% partial metakaolin replacement level.

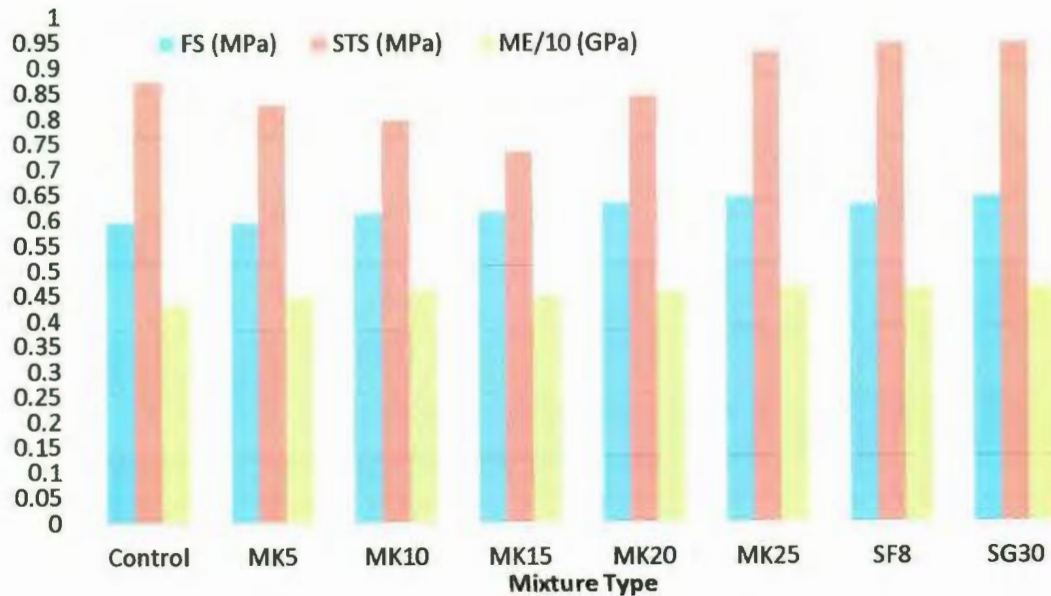


Figure 36 – Effect of Metakaolin Partial Replacement on the Normalized FS, STS, and ME

Figure 37 shows the FS for all mixtures. From this figure it can be seen that the FS increased as the partial metakaolin replacement percentage was increased from 0 to 20%. Nita et al. (2004) studied the effect of using metakaolin up to 15% to increase the Modulus of Rupture of the mixture compared to using no metakaolin. Figure 37 shows that the FS increased by 20.9% when the partial metakaolin replacement percentage was increased to 20%. Further increasing the partial replacement level from 20 to 25% resulted in a 10% decrease in the FS. Using 8% metakaolin in SCC was shown to increase the flexural strength compared to SCC containing no metakaolin (Justice et al. 2007).

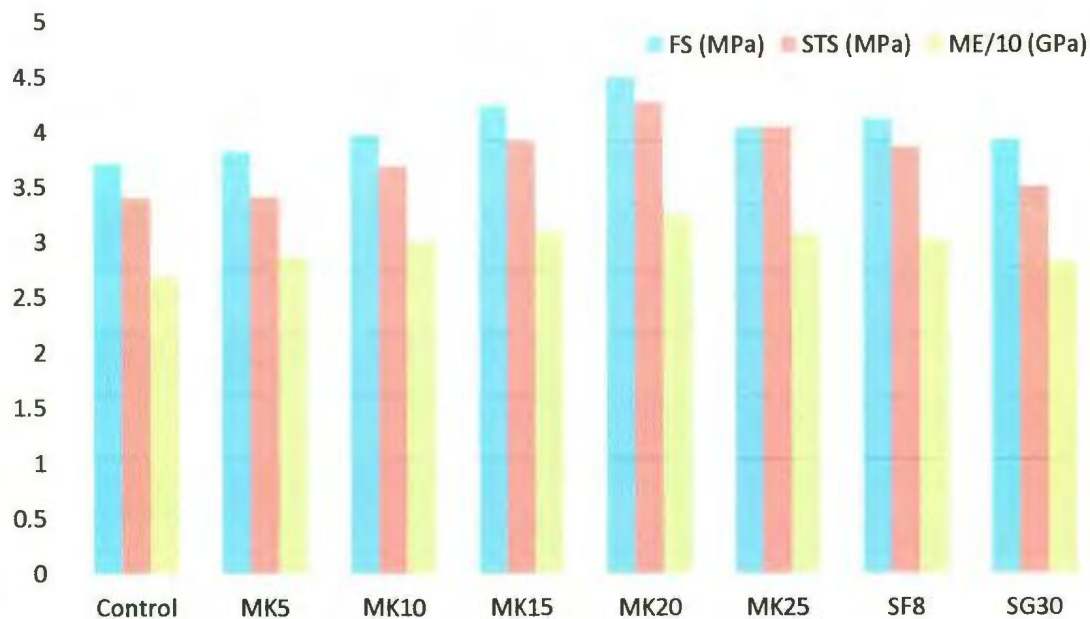


Figure 37 – FS, STS, and ME for Mixtures Containing Metakaolin

5.2.3.2 Effect of C/F Ratio

Figure 38 and Table 11 show the FS results for varying C/F ratios. From Figure 38 it can be seen that the FS decreased for all mixtures as the C/F aggregate ratio was increased from 0.7 to 1.2. A similar result was reported by Dhonde et al. (2007); when increasing the C/F ratio from 0.99 to 1.5 the FS of SCC decreased. Zhenshuang et al. (2011) also came to similar conclusions when the coarse aggregate content was increased. Using 20% metakaolin as a partial replacement showed a large decrease in the FS of 23% with an increase of the C/F ratio from 0.7 to 1.2. SCC containing no SCMs had a decrease in the FS of 18.2% with an increase of the C/F ratio from 0.7 to 1.2. Both partial replacements with 8% silica fume and 30% slag showed decreases in the FS of 10.3% and 18.6% with an increase of the C/F ratio from 0.7 to 1.2.

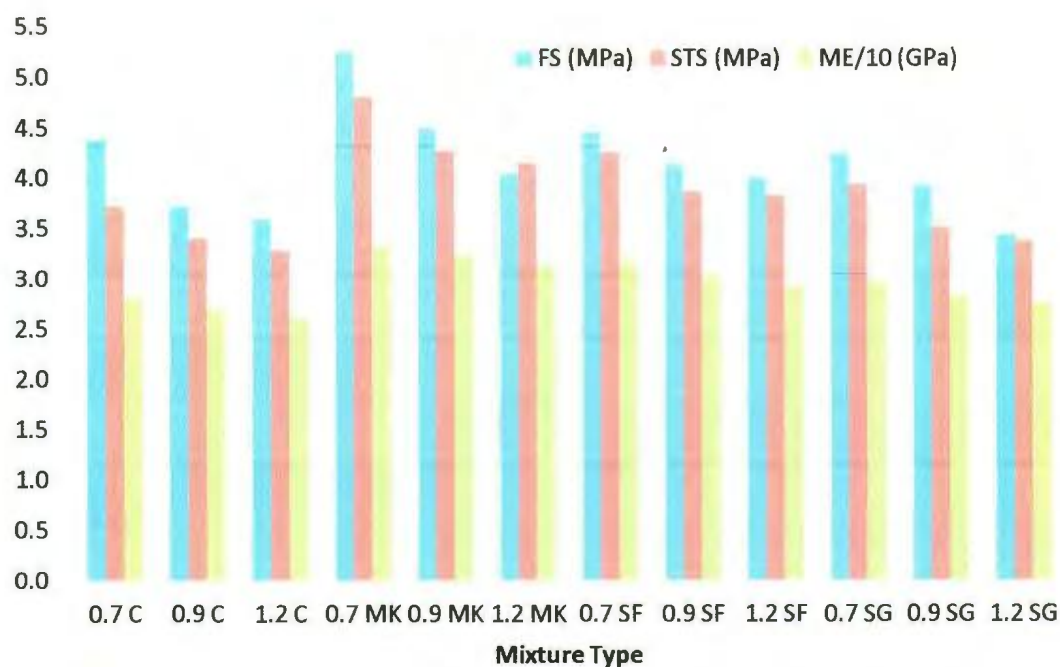


Figure 38 – Effect of C/F Ratio on FS, STS, and ME

5.2.3.3 Effect of Coarse Aggregate Size

Table 11 and Figure 39 show the FS results for varying coarse aggregate sizes. From this figure it can be seen that using a larger coarse aggregate size of 20 mm decreased the FS for all four mixtures. Neptune et al. (2010) showed that increasing the maximum nominal aggregate size on average decreased the FS of the mixture in normal concrete. The control mixture had a decrease of 4.3% and partial replacement of cement with 20% metakaolin showed a decrease of 8.9%. Using 8% silica fume and 30% slag as partial replacements also showed decreases in the FS of 6.7% and 7.9%, respectively, when the coarse aggregate size was increased from 10 mm to 20 mm.

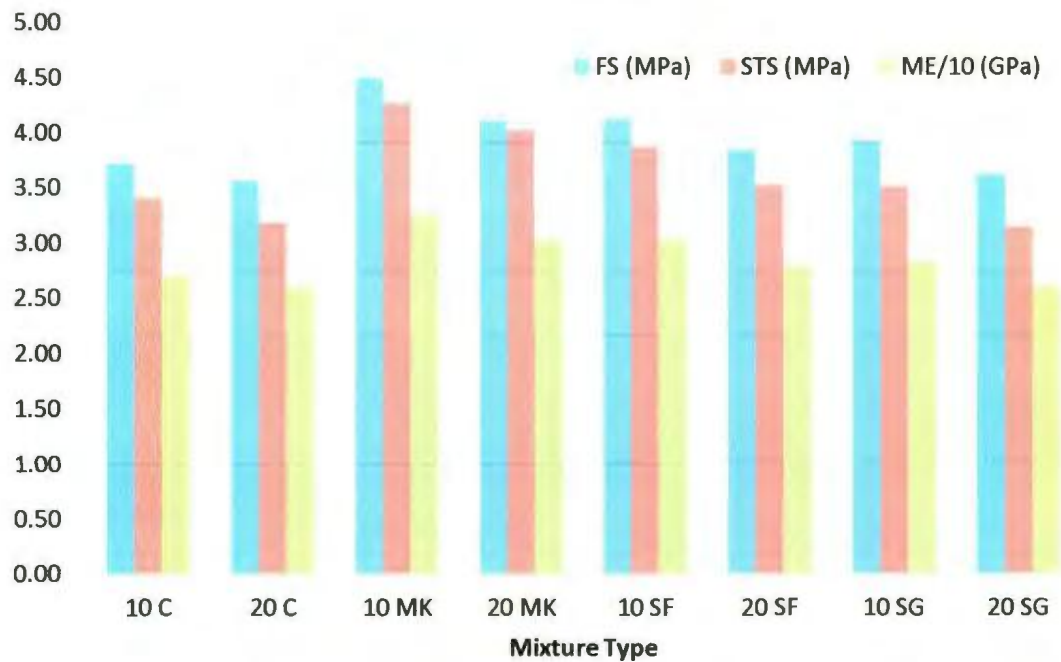


Figure 39 – Effect of Coarse Aggregate Size on FS, STS, and ME

5.2.3.4 Effect of Binder Content

Figure 40 and Table 11 show the FS results for varying binder contents. From Figure 40 it can be seen that all FS increased with increasing binder content. 20% metakaolin as a partial replacement showed an increase in the FS of 19.1% when the binder was increased to 500 kg/m^3 . The FS of the control mixture increased by 23.6%, with the increased binder content. Both 8% silica fume and 30% slag as partial replacements gained 21.4% and 19.6% in their respective FS when the binder content was increased from 450 to 500 kg/m^3 . An increase in the FS was also seen in fibre-reinforced concrete, regardless of the fibre percentage, when the amount of binder was increased (Gencel et al. 2011).

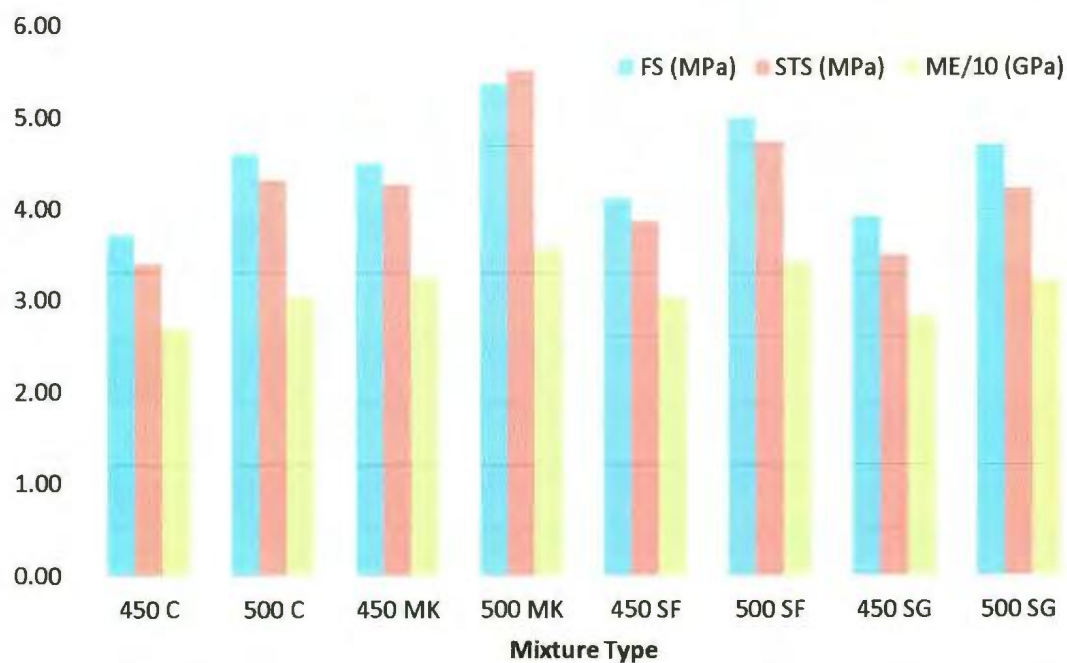


Figure 40 – Effect of Binder Content on FS, STS, and ME

5.2.3.5 Effect of Air Content

Figure 41 and Table 11 show the FS results for varying air contents. From this figure it can be seen that increasing the air content from 0 to 7% decreased the FS for all mixtures. The control mixture showed a 17.5% decrease in the FS with increasing air content up to 7%; 20% partial replacement with metakaolin had a 10.9% drop in the FS with the addition of 7% air; and both partial replacements with 8% silica fume and 30% slag showed reductions of 14.1% and 22.1%, respectively, when the air content was increased from 0 to 7%. Lee et al. (1977) reported a large decrease in the Modulus of Rupture in normal concrete as the air content rose from 2.8 to 10.2%.

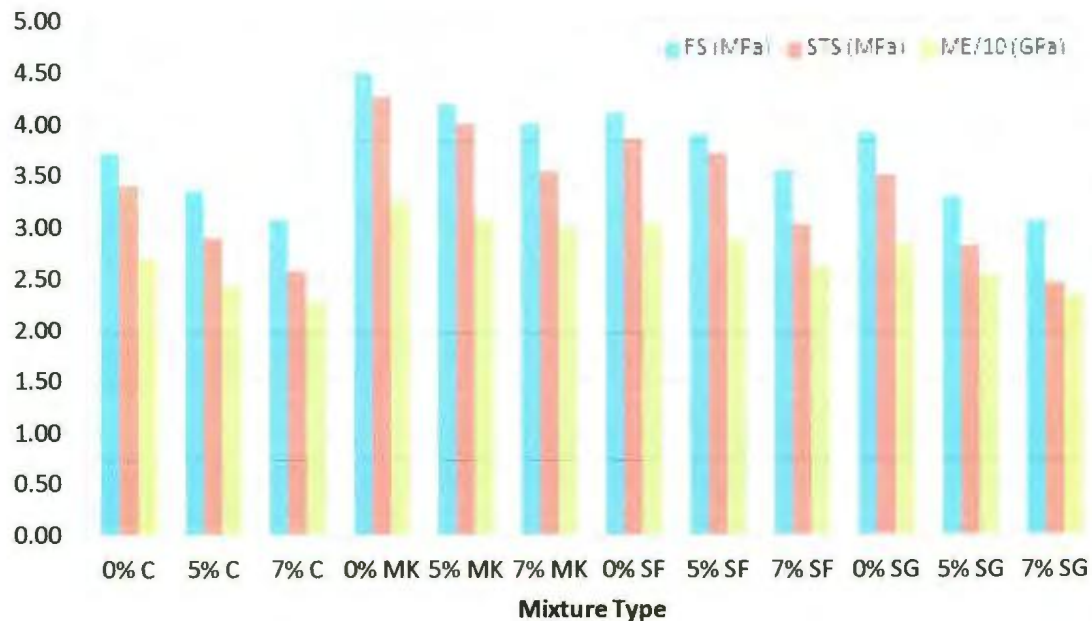


Figure 41 – Effect of Air Content on FS, STS, and ME

5.2.4 Splitting Tensile Strength

5.2.4.1 Effect of Metakaolin

Figure 36 and Table 9 show the results of the normalized Splitting Tensile Strength (STS) for the effect of partial cement replacement with metakaolin on SCC. From this figure it can be seen that when using 8% silica fume and 30% slag as partial cement replacements, these mixtures resulted in a higher normalized STS compared to all partial metakaolin replacement mixtures used.

Figure 37, which shows the results for the STS of all mixtures, shows that increasing the partial metakaolin percentage from 0 to 20% increased the STS. Using 20% metakaolin as a partial cement replacement resulted in an increase of 25.4% in the

STS. Further increasing the metakaolin replacement from 20 to 25% slightly decreased the STS by 5.2%. However, all partial cement replacements with metakaolin resulted in a higher STS when compared to the control mixture. Similar results were observed by Qian et al. (2001), where up to a 15% metakaolin replacement was studied and shown to produce a larger STS compared to the control mixture.

5.2.4.2 Effect of C/F Ratio

Figure 38 and Table 11 show the STS results for varying C/F ratios. This figure shows that increasing the C/F ratio from 0.7 to 1.2 reduced the STS for all mixtures. The control mixture had a reduction of 11.8% and using 20% metakaolin partial replacement resulted in a decrease of 13.8% when the C/F ratio increased from 0.7 to 1.2. The 8% silica fume and 30% slag partial replacements experienced a drop of 9.9% and 14%, respectively, as the C/F ratio was varied from 0.7 to 1.2. In a study performed by Dhonde et al. (2006), increasing the C/F ratio was shown to decrease the STS of SCC.

5.2.4.3 Effect of Coarse Aggregate Size

Figure 39 and Table 11 show the STS results of varying coarse aggregate sizes. From this figure it can be seen that increasing the coarse aggregate size from 10 mm to 20 mm decreased the STS for all mixtures. The control mixture showed a 6.2% decrease in the STS and the 20% partial replacement with metakaolin showed a 5.6% decrease in the STS with the use of the 20 mm coarse aggregate. In addition, both 8% silica fume and 30% slag partial replacements showed decreases in the STS of 8.8% and 10%, respectively, with the 20 mm coarse aggregate. Akcaoglu et al. (2002) reported a loss in

the tensile strength in normal concrete with an increasing coarse aggregate size. It was observed that the bond in the interfacial transition was the governing factor for the tensile strength of concrete.

5.2.4.4 Effect of Binder Content

Figure 40 shows the effect that varying the binder content has on the STS. It can be seen in the figure that increasing the binder from 450 to 500 kg/m³ increased the STS for all mixtures. These results are in agreement with those of Gencil et al. (2011), which showed an increase in the STS in concrete as the binder content rose from 470 to 570 kg/m³, irrespective of the use of fibre reinforcement. The control mixture had an increase in the STS of 27.1%, and 20% metakaolin as a partial cement replacement showed an increase of 29.3% with an increased binder content. In addition, when using 8% silica fume 30% slag partial replacements, increasing the binder content to 500 kg/m³ increased the STS by 22.8% and 20.9%, respectively.

5.2.4.5 Effect of Air Content

Table 11 and Figure 41 show the STS results for varying air contents. It can be seen from the figure that all mixtures exhibited a loss in the STS as the air content was increased from 0 to 7%. The control showed a decrease in the STS of 24.1% and the 20% metakaolin as a partial cement replacement mixture showed a decrease in the STS of 17.1%. Both 8% silica fume and 30% slag as partial replacements showed decreases of 21.8% and 29.7%, respectively, when the air content rose from 0 to 7%.

5.2.5 Modulus of Elasticity

5.2.5.1 Effect of Metakaolin

Figure 36 and Table 9 show the results for the normalized Modulus of Elasticity (ME) for the effect of metakaolin partial cement replacements on SCC. Similar to the FS and STS results, the ME was normalized by dividing it by its respective compressive strength. Figure 36 shows that using a 10% or 25% partial metakaolin replacement resulted in a similar or higher normalized ME when compared to the use of 8% silica fume as a partial cement replacement. When using 30% partial cement replacement with slag, only 25% partial cement replacement with metakolin resulted in a slightly higher normalized ME. All other replacement percentages resulted in a lower normalized ME when compared to the use of 30% slag partial replacement.

The results for the ME are shown in Figure 37. These values were not normalized in order to show the effect of metakaolin partial replacement on the ME of SCC. This figure shows that increasing the partial metakaolin percentage from 0 to 20% increased the ME. The ME increased by 20.8% with the addition of 20% metakaolin as a partial cement replacement. As the metakaolin partial replacement percentage was further increased from 20% to 25%, the ME decreased by 5.3%. Similar results were obtained and confirmed by Qian et al. (2001). Their study used up to 15% metakaolin partial replacement and demonstrated that the addition of metakaolin up to 15% increased the ME. Justice et al. (2007) also reported a 5 to 19% increase in the ME when using 8% metakaolin compared to concrete containing no metakaolin.

5.2.5.2 Effect of C/F Ratio

Figure 38 and Table 11 show the ME results when varying the C/F ratio. From this figure it can be seen that as the C/F ratio was increased from 0.7 to 1.2 for all mixtures, the ME decreased. The control mixture had a decrease of 6.8%; the 20% metakaolin as a partial cement replacement had a decrease in the ME of 5.4%; and both partial cement replacements with 8% silica fume and 30% slag showed decreases in the ME of 8.2% and 7.4%, respectively, when the C/F ratio was increased from 0.7 to 1.2.

5.2.5.3 Effect of Coarse Aggregate Size

Figure 39 and Table 11 show the ME results for varying coarse aggregate sizes. The figure shows that all mixtures experienced a decrease in the ME when the coarse aggregate size was increased from 10 mm to 20 mm. 20% metakaolin partial replacement showed a 7.1% decrease in the ME when using a larger coarse aggregate size; the control mixture showed a 3.6% decrease in the ME when using a 20 mm coarse aggregate; and the 8% silica fume and 30% slag partial cement replacements had decreases in their respective MEs of 7.8% and 8.0% as the coarse aggregate size was increased from 10 mm to 20 mm. These results are typical when the coarse aggregate size is increased, as indicated by Filho et al. (2010) who reported that SCC mixed with larger coarse aggregates showed lower values for ME.

5.2.5.4 Effect of Binder Content

Table 11 and Figure 40 show the ME results for varying binder contents. From this figure it can be seen that increasing the binder content increased the ME for all

mixtures. Using 500 kg/m^3 resulted in an increase in the ME of 13.0% for the control mixture, and a 9.9% increase in the ME for 20% metakaolin partial replacement. Both partial cement replacements of 8% silica fume and 30% slag had increases of 12.9% and 13.9% in their respective MEs when using a larger binder content. Similar results were presented by Gencel et al. (2011).

5.2.5.5 Effect of Air Content

Figure 41 shows the ME results for varying air contents. The figure shows that the ME for all mixtures decreased with increasing air content. This is a similar result as that observed by Lee et al. (1977) when increasing the percentage of air in the mixtures. The figure shows that when the air content increased from 0 to 7%, the ME decreased by 15.3% for the control mixture, by 8.0% for 20% metakaolin partial replacement, and by 13.8% and 17.3%, respectively, for both 8% silica fume and 30% slag partial replacement mixtures. Browning (2011) concluded that an increase in the air content in concrete leads to a 2.5% reduction in the ME for every 1% increase of air content.

5.3 Optimal SCC Mixture

After examining the effect of metakaolin and the mixture design on SCC, the optimal metakaolin percentage, along with the most desirable mixture design, can be concluded. From Stage 1, it was shown that according to the V-Funnel and T_{50} tests increasing the metakaolin replacement percentage increased the viscosity of SCC. However, increasing the metakaolin content, up to a 20% replacement, assisted in the passing ability of the mixture (seen from the L-Box, J-Ring, and V-Funnel tests) and reduced the segregation factor. The HRWR demand continuously increased with increasing metakaolin content from 0 to 25%. From these results, 20% metakaolin was deemed to be the most beneficial cement replacement, compared to any other replacement percentage, for the fresh properties of SCC. It was noted that when using a C/F of 0.9, the SCC mixtures resulted in less than acceptable H2/H1 ratios and required an investigation into the effect of the mixture needed to improve the fresh property results. The results for the mechanical properties showed similar results, that using 20% metakaolin cement replacement was the most beneficial. Using 20% metakaolin replacement obtained the highest 28- and 90-day compressive strengths, although the 7-day strength development was the lowest compared to the other replacement percentages. The FS, STS, and ME results showed that 20% metakaolin replacement was the most optimal compared to the other metakaolin replacement percentages. Overall, for the fresh and mechanical properties, 20% metakaolin replacement was deemed the most optimal replacement percentage.

From Stage 2, it was shown that using a lower C/F ratio of 0.7, increasing the coarse aggregate size to 20 mm, increasing the total binder content to 500 kg/m³, and using air entrainment up to 7% all helped to improve the flowability, viscosity, and passing ability of SCC, regardless of the SCMs used. However, when using a lower C/F ratio of 0.7, the HRWR demand increased for all mixtures, while all other design parameters reduced the HRWR demand. Examining the mechanical properties, it was seen that using either a lower C/F ratio of 0.7 or increasing the binder content to 500 kg/m³ improved all mechanical properties. However, increasing the coarse aggregate size to 20 mm or increasing the air entrainment to 7% resulted in a reduction in all the mechanical properties. Therefore, using lower C/F ratios, a smaller coarse aggregate size, and an increased binder content were more beneficial when using SCC, while air entrainment and larger coarse aggregate sizes should be avoided.

5.4 Shear of SCC Beams

Table 13 – Compressive Strengths, Failure Loads, and Load at First Diagonal Crack

Beam	f'_c	Failure	Failure	Shear	Normalized	First
Type	(MPa)	Type	Load	failure	Shear	Diagonal
			(kN)	capacity	capacity	Crack (kN)
				(kN)	(kN/ \sqrt{MPa})	
B1	34.0	Shear	197.36	98.68	16.92	157.0
B2	29.3	Shear	145.86	72.93	13.47	108.0
B3	27.3	Shear	147.66	73.83	14.14	98.0
B4	30.39	Shear	224.61	112.30	20.37	150.0
B5	29.0	Shear	152.92	76.46	14.20	94.0
B6	29.5	Shear	170.12	85.06	15.66	102.0
B7	72.0	Shear	241.57	120.79	14.24	140.0
B8	70.0	Shear	242.29	121.14	14.48	128.0
B9	69.7	Shear	252.01	126.40	15.09	142.0
B10	68.8	Shear	241.03	120.86	14.53	132.0

5.4.1 Beam Loading Results

5.4.1.1 Fresh Properties of SCC Beams

The T_{50} , slump flow diameter, and HRWR demand for all ten beam types are shown in Figure 42. For beams 1 through 6 the slump flow diameter was set to 750 ± 50

mm, while beams 7 through 10 had a target slump flow of 650 ± 50 mm, by using enough HRWR to obtain the desired slump flow diameters. It can be seen from Figure 42 that the HRWR demand decreased with an increasing C/F ratio and decreased with an increasing stone size. This was confirmed early in the fresh property sections, and a more detailed discussion can be found there. Also, a general increasing trend in the T_{50} time was observed as the C/F ratio was increased from 0.7 to 1.2. In addition, the T_{50} times showed a general decreasing trend as the coarse aggregate size was increased from 10 to 20 mm, which was also seen in beams 7 through 10. Also, the replacement of cement with 20% metakaolin showed an increase in the HRWR demand as well as the T_{50} times (a more detailed discussion of this can be found in the fresh properties section).

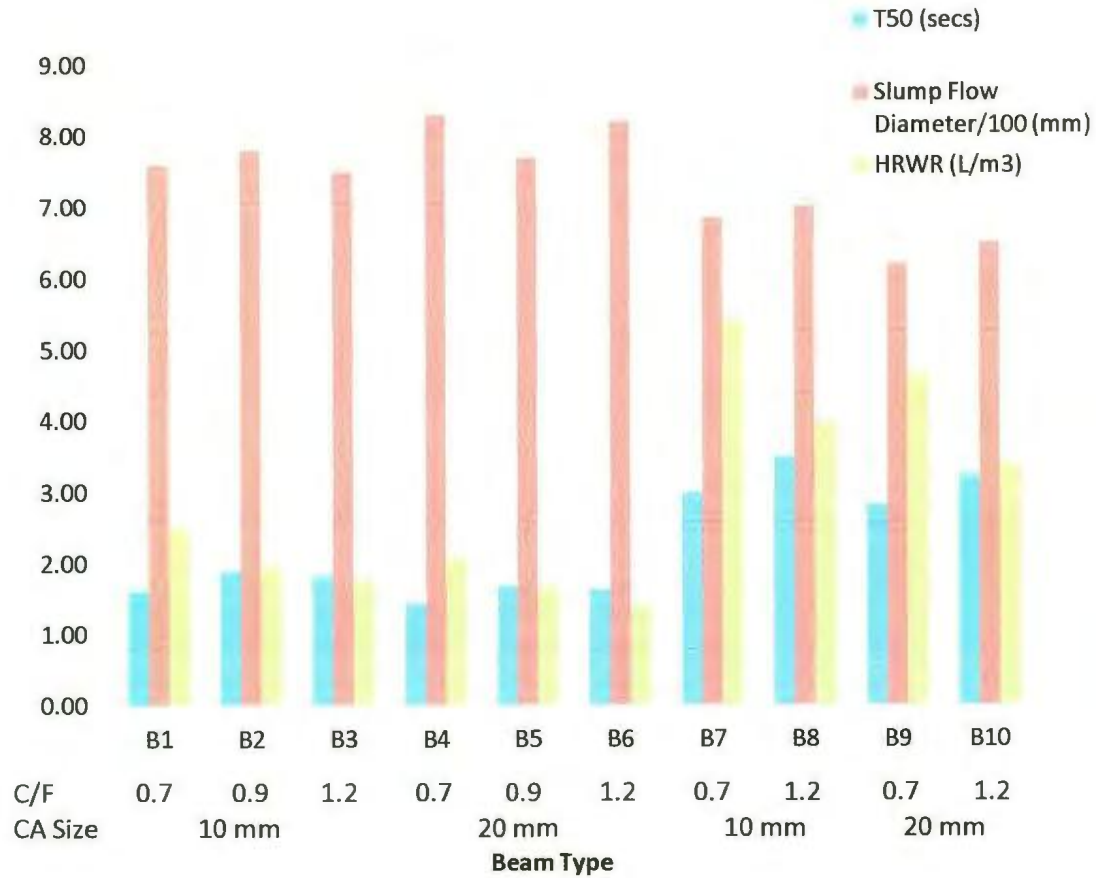


Figure 42 – T₅₀, Slump Flow Diameters, and HRWR Demand for the 10 SCC Beams

5.4.1.2 Twenty Eight and 90-Day Compressive Strength Results

Beams 1 through 6 were designed with a total binder of 500 kg/m³ and used 60% fly ash as a partial cement replacement in order to produce a 28-day compressive strength of 30 ± 5 MPa. The high-strength SCC beams used the same total binder content but used 20% metakaolin as a partial cement replacement in order to obtain a higher strength of 70 ± 5 MPa (high-strength concrete). The results for the 28- and 90-day compressive strength tests are shown in Table 13 and Figure 43. From this figure it can be seen that for

the normal-strength and high-strength SCC beams, the 28-day compressive strengths were all within the target range. Also, as previously discussed in the mechanical properties section, the compressive strength decreased with an increasing C/F ratio and decreased as the coarse aggregate size was increased from 10 to 20 mm. A similar effect was observed in the high-strength SCC beams, but it was more noticeable in the normal-strength SCC beams. The use of 20% metakaolin as a partial cement replacement greatly increased the 28- and 90-day compressive strengths compared to the normal-strength SCC beams (previously discussed and shown in Figure 43).

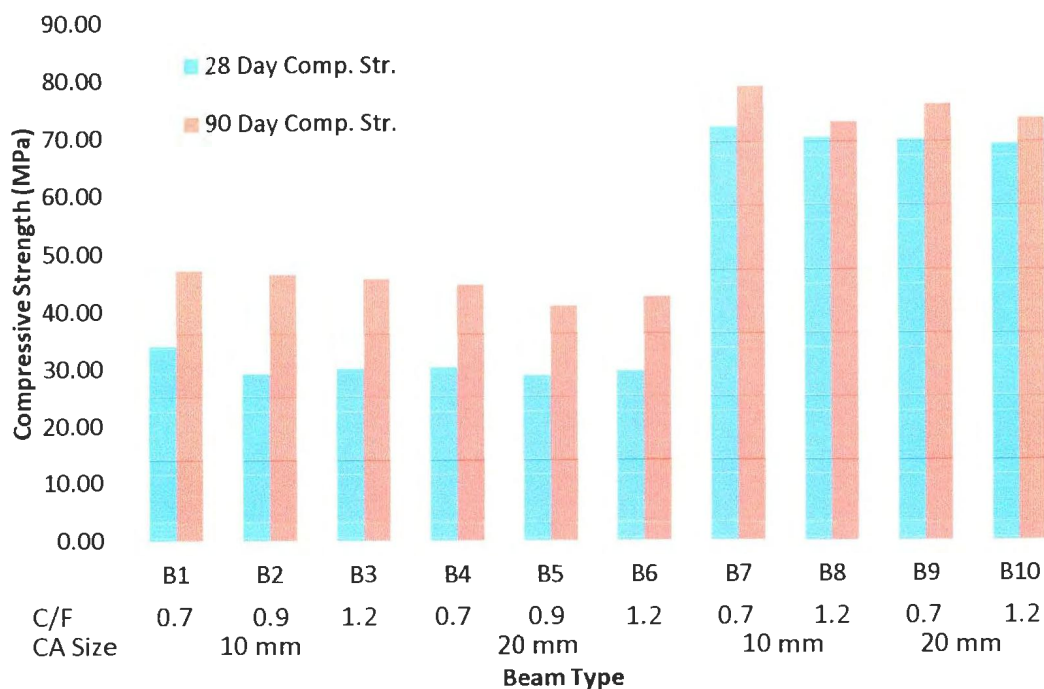


Figure 43 – 28- and 90-Day Compressive Strengths for SCC Beams

5.4.2 Shear Failure Capacity of SCC Beams

5.4.2.1 Failure Modes

As seen in Figures A1 through A10 in Appendix A, it is clear that all the beams failed in shear (as expected), and the failure happened after the formation of one major diagonal crack starting from one point of at the support and then moving towards the loading application at an angle ranging between 26 and 31°. During the first stage (in which the load was applied to 50% of the theoretical failure load) of loading, thin vertical flexural cracks appeared almost on the mid-span of the beam. By increasing the load in the second stage (in which the load was applied to 75% of the theoretical failure load), more flexural cracks were formed away from the mid-span on the two sides. Finally, by further increasing the load, the flexural-shear cracks spread diagonally towards the loading point, and new diagonal cracks were formed along the beam length.

5.4.2.2 Effect of C/F Ratio

Figure 44 and Table 13 show the normalized shear failure capacity for all 10 SCC beams. To account for the variation in the concrete strength of all 10 SCC beams, the shear failure capacity for all beams was normalized by dividing the shear failure capacity load by the square root of the compressive strength for each beam, respectively. From this figure it can be seen that as the C/F ratio for the normal-strength SCC beams was increased from 0.7 to 1.2, the normalized shear failure capacity decreased. This decrease in the normalized shear failure capacity with increasing C/F ratio was seen regardless of the coarse aggregate size used (10 or 20 mm). When using a 10 or 20 mm coarse

aggregate size, the normalized shear failure capacity decreased by 16.4% and 23.1%, respectively, as the C/F ratio was increased to 1.2.

It should be noted that although the effect of aggregate interlock increased (which enhanced the shear resistance), the total volume of the ITZ around the coarse aggregate also increased as the C/F ratio increased. At this zone the water traps around the aggregate, which results in a larger porosity at this area compared to the surrounding matrix. This forms a weak chain in the concrete around the aggregate (Jennings et al. 2008). It is believed that the increased volume of the transition zone at higher C/F ratios had more effect on reducing the shear capacity compared to the improvement of the aggregate interlock. Therefore, increasing the volume of coarse aggregate in the beam weakened the concrete and reduced its shear capacity.

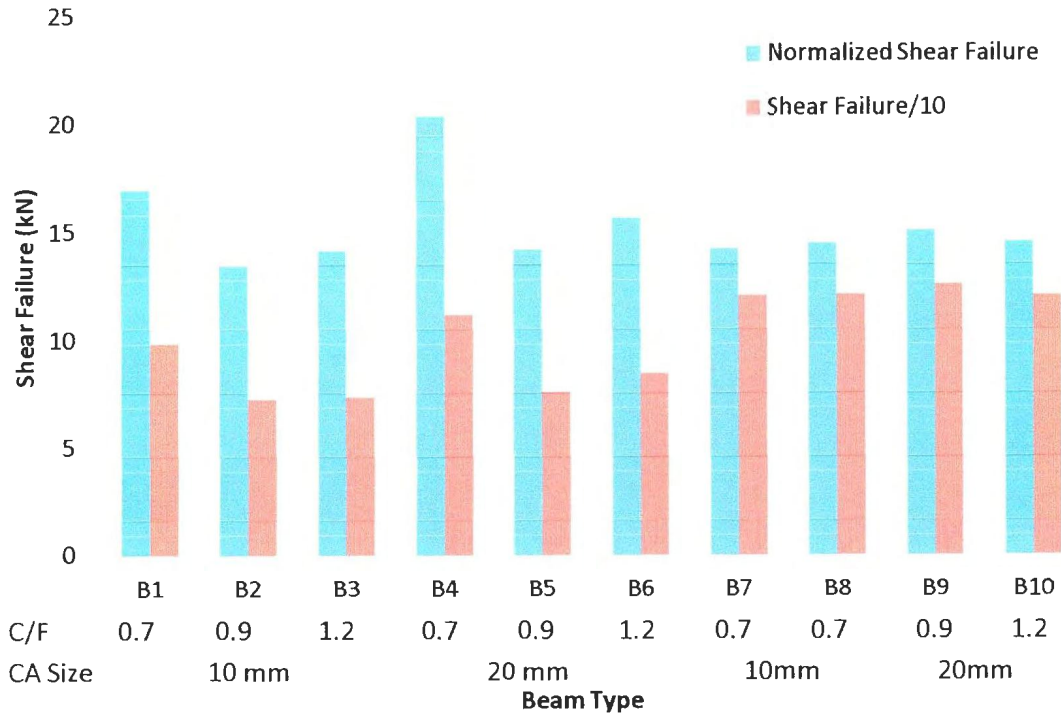


Figure 44 – Shear Failure Capacity and Normalized Shear Failure Capacity for SCC Beams

5.4.2.3 Effect of Coarse Aggregate Size

From Figure 44 and Table 13 it can be seen that for the normal-strength SCC beams the average normalized shear failure capacity, when using a 10 mm coarse aggregate size, was 29.7. Using a larger coarse aggregate size of 20 mm increased the average normalized shear failure capacity to 33.5, or a 12.8% increase. An increase in the failure shear stress of concrete beams, as the coarse aggregate size was increased, was also reported by Sherwood et al. (2007). Table 14 shows the results for the crack angles for the two different coarse aggregates sizes for varying C/F ratios. To obtain the average

crack failure angle for each aggregate size the average crack angle failure was averaged using the three C/F ratios (0.7, 0.9 and 1.2) for each aggregate size and an average failure angle obtained. Using a 10 mm coarse aggregate resulted in an average crack failure angle of 29.8° , while using a larger 20 mm coarse aggregate produced an average crack failure angle of 29.0° . This shows that when using a larger coarse aggregate size of 20 mm, there was no significant difference in the crack failure angles. Using larger aggregates increased the thickness of the ITZ, which caused a weakness in the hardened concrete mixture in which failure can occur (Koehler et al. 2007). The thickness of the interfacial zone increased as the size of the coarse aggregate was increased, which reduced the quality of the concrete and the compressive strength and reduced the shear failure capacity. However, using a larger coarse aggregate size increased the aggregate interlock, and this effect was more pronounced than the reduction caused by the ITZ.

5.4.2.4 Effect of High-Strength Concrete

The normalized shear failure capacity results can be seen in Table 13 and Figure 44. This figure shows that, contrary to normal-strength concrete, the shear failure capacity for high-strength concrete was not highly dependent on the C/F ratio. This could be due to the high quality of the paste matrix in high-strength concrete compared to normal-strength concrete, which warrants a stronger ITZ. Therefore, increasing the total volume of the ITZ at higher C/F ratios did not significantly reduce the shear capacity of the beam. As well, the figure shows that the average normalized shear failure capacity when using the 10 mm coarse aggregate was 14.36, while the average normalized shear failure capacity when using the 20 mm coarse aggregate was 14.81. There was, again, very little

difference and no apparent effect of the coarse aggregate size on the shear failure capacity of high-strength SCC beams. This could be due to the increase in the strength of the paste matrix, which reduced the role of the ITZ in reducing the shear capacity. In addition, the expected increase of the aggregate interlock (which increases the shear capacity) was not a factor in high-strength concrete because in high-strength concrete the failure crack penetrates the paste and the coarse aggregate forms a smoother failure surface. This matches results that show that the aggregate in high-strength SCC beams does not affect the aggregate interlock due to the fracturing of the coarse aggregate, creating smoother surfaces along the diagonal crack failure, which in turn reduces the effect of the aggregate interlock (Kim et al. 2010). Also, the average normalized shear failure capacity for the normal-strength SCC beams was 14.84 and 16.74 when using the 10 and 20 mm coarse aggregates, respectively. Note, these values were obtained by averaging the normalized shear failure capacity for SCC beams using C/F ratios of 0.7, 0.9 and 1.2 when using a 10 mm coarse aggregate and similarly when using a 20 mm coarse aggregate. This shows that the high-strength SCC beams had a lower normalized shear failure capacity when compared to the normal-strength SCC beams. However, the shear failure capacity for high-strength SCC beams was higher compared to all normal-strength SCC beams. An increase in the nominal shear strength of concrete beams was reported by Shin et al. (1999) as the compressive strength of the mixture increased.

5.4.3 Crack Development

5.4.3.1 Post Diagonal Cracking

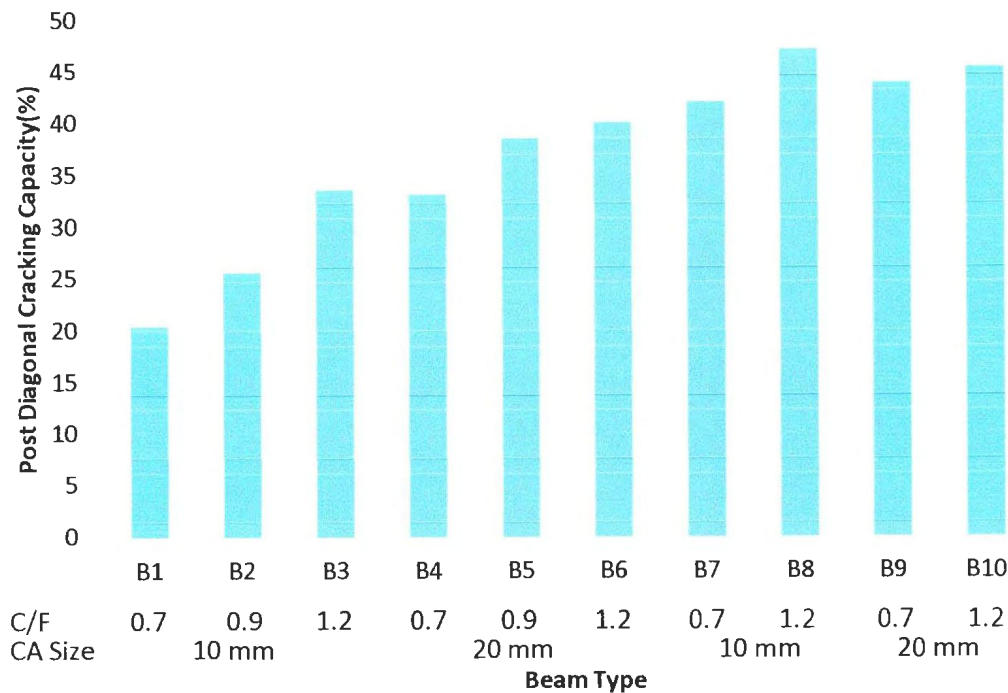


Figure 45 – Post Diagonal Cracking Capacity Percentages

As mentioned previously, the first diagonal cracking load was visually observed and confirmed using the Load versus Deflection and Strain versus Loading graphs. To account for the variations in the shear failure capacity for all 10 beams, the first diagonal cracking load was used to determine the post load percentage the beam withstood after the first diagonal crack occurred. Figure 45 shows the post diagonal crack failures for all 10 SCC beams. To calculate the post diagonal cracking capacity, the load at the first diagonal crack was observed during tests and confirmed using the LVDT and strain gauge data. Equation 5 was then used to calculate the post diagonal cracking capacity.

$$\text{Post Cracking Capacity} = \frac{(\text{Max Failure Load} - \text{Load at First Diagonal Crack})}{\text{Max Failure Load}} \times 100\% \quad (\text{Equation 5})$$

5.4.3.3.1 Effect of C/F Ratio

From Figure 45 it can be seen that increasing the C/F ratio from 0.7 to 1.2 in normal-strength SCC beams increased the post diagonal cracking resistance, regardless of the coarse aggregate size used. When using a 10 mm coarse aggregate, the post diagonal cracking resistance increased by 64.4% as the C/F ratio was increased from 0.7 to 1.2. Increasing the C/F ratio in normal concrete increased the volume of the coarse aggregate, which resulted in longer and more complicated cracking paths (higher aggregate interlock). This is due to the fact that in normal-strength concrete the cracks travelled through the ITZ around the aggregate (Joseph 2010).

Using a 20 mm coarse aggregate and increasing the C/F ratio from 0.7 to 1.2 showed an increase of 20.6% in the post diagonal cracking resistance. The increase in the coarse aggregate size means the crack had more area to travel around the aggregates (Joseph 2010). Lachemi et al. (2005) found similar results in which the increase in the volume of coarse aggregates led to an improvement in the post-cracking shear transfer.

5.4.3.3.2 Effect of Coarse Aggregate Size

Examining Figure 45 shows that as the coarse aggregate size was increased in normal-strength SCC beams, the post diagonal cracking resistance was greatly improved. When using a 10 mm coarse aggregate, the average post diagonal cracking resistance was 26.7%, and while using a 20 mm coarse aggregate the average was 37.3%, which amounts to an average increase of 39.7% with an increasing coarse aggregate size. The

increase in the post diagonal cracking resistance can be contributed to the aggregate interlock by using a larger coarse aggregate, which increased the resistance by producing rougher crack surfaces (Sherwood et al. 2007).

5.4.3.3.3 Effect of High-Strength Concrete

Figure 45 shows the results for the post diagonal cracking resistances for high-strength SCC beams. From this figure it can be seen that there was an increase in the post diagonal cracking resistance regardless of the coarse aggregate size or C/F ratio used. When using a 10 mm coarse aggregate, there was an 11.9% increase in the post diagonal cracking resistance as the C/F ratio was increased from 0.7 to 1.2. Using a 20 mm coarse aggregate showed a small increase of only 3.5% in the post diagonal cracking behaviour as the C/F ratio was increased from 0.7 to 1.2. Using a 10 or 20 mm coarse aggregate in high-strength SCC beams resulted in an average increase of the post diagonal cracking resistance of 44.6%, for each.

The increase in the post diagonal capacity increased much more than that seen in normal-strength concrete, even though the effect of aggregate interlock was minimal in this area. This could be due to a higher stiffness, which means less deflection and therefore smaller crack widths, as seen in Table 12 with high-strength concrete.

5.4.3.3.4 Crack Failure Angles and Maximum Crack Width

The crack angle and maximum failure crack widths were measured during the test and sketched to scale (see Appendix A for beam crack drawings (Figure A1 to A10)). The results for the crack angles and crack widths are shown in Table 14. The results show that

increasing the C/F ratio had little effect on the crack failure angle for both normal- and high-strength SCC beams. In addition to increasing the C/F ratio, using a larger coarse aggregate size of 20 mm showed a slight change in the average crack angle failure in normal-strength SCC beams and showed no difference in high-strength SCC beams. Increasing the coarse aggregate size from 10 mm to 20 mm in normal-strength SCC beams resulted in a 2.8% decrease in the average crack angle from 29.8° to 29°. However, there was a noticeable difference in the crack failure angle between high-strength and normal-strength SCC beams. All high-strength SCC beams showed an average crack failure angle of 27°, while normal-strength SCC beams had an average failure angle of 29°. This resulted in a decrease in the average crack angle of 7% and could account for the increase in the shear failure capacity due to the increase in the shearing area from the reduced angle.

From Table 14 it can be seen that increasing the C/F ratio from 0.7 to 1.2 in normal-strength concrete beams reduced the maximum crack width at each loading stage, due to the increase in the volume of the coarse aggregate, which contributed to the aggregate interlock. Lin et al. (2012) found similar results and came to the conclusion that increasing the amount of coarse aggregate enhances the aggregate interlock and thus reduces the crack widths.

Table 14 – Beam Cracking Results

Beam Type	Failure Type	Number of Cracks	Crack at	Angle Failure	Maximum Crack Width (mm)		
					50%*	75%*	100%*

(deg.)						
B1	Shear	7	31	0.1270	0.2159	5.0
B2	Shear	6	28	0.1143	0.2032	3.0
B3	Shear	6	30.5	0.1143	0.1778	4.0
B4	Shear	9	28	0.1016	0.1905	3.2
B5	Shear	7	30	0.1016	0.1905	5.0
B6	Shear	8	29	0.1143	0.1651	4.0
B7	Shear	7	27	0.0762	0.1524	0.5715
B8	Shear	7	27	0.0889	0.1270	2.5
B9	Shear	9	26	0.1016	0.1524	3.0
B10	Shear	7	28	0.0889	0.1397	1.5

5.4.4 Deflection versus Load

The deflection versus loading curves for the 10 SCC beams can be found in Appendix B (Figures B1 through B10). The deflection of the beam was measured in three locations, as previously discussed. Increasing the C/F ratio from 0.7 to 1.2 showed a slight increase in the ductility of normal-strength SCC beams. Lin et al. (2012) reported that the shear ductility, where the shear is spread out through a wider zone, resulting in less brittle behaviour of SCC beams was affected by the volume of the coarse aggregate in the mixture. Increasing the coarse aggregate size from 10 to 20 mm resulted in an increase in the ductility of the beams.

6. Conclusions

1. Increasing the percentage of metakaolin replacement in SCC mixtures from 0 to 25% was shown to increase the viscosity, passing ability, HRWR demand, and segregation factor, while the flowability of the mixture decreased. Comparing metakaolin with other SCMs, SCC mixtures with 30% slag had a lower viscosity and improved flowability than all SCC mixtures with metakaolin. SCC with 8% silica fume showed a better viscosity compared to SCC mixtures containing metakaolin; however, using 10% or greater metakaolin showed an improved segregation factor and passing ability. Meanwhile, using a metakaolin replacement of 10% or less resulted in a better SCC flowability compared to silica fume.
2. Using metakaolin as a partial cement replacement in SCC seemed to slightly decrease the 1-day strength development compared to SCC using no SCMs. Compared to SCC mixtures with 8% silica fume, the addition of metakaolin appeared to show a slightly lower 1-day strength development. When compared to SCC mixtures with 30% slag as a partial cement replacement, all metakaolin mixtures showed a slightly higher 1-day strength development. All SCC mixtures containing metakaolin obtained higher 3-day strength developments compared to SCC containing silica fume and slag as a partial cement replacement. All SCC mixtures containing metakaolin showed a higher 7-day strength development compared to SCC using no SCMs or SCC using 30% slag partial replacement. Using 10% or more metakaolin replacement resulted in a higher 7-day strength development compared to 8% silica fume.

3. Increasing the partial cement replacement with metakaolin up to 20% showed an increase in the 28- and 90-day compressive strengths of the mixtures compared to SCC mixtures using no SCMs and SCC using 30% partial slag replacement. Using a 15% or greater metakaolin partial replacement resulted in higher 28- and 90-day compressive strengths compared to SCC with 8% silica fume.
4. Using 20% or greater metakaolin in SCC mixtures resulted in a higher normalized FS than using 8% silica fume. In addition, using 30% slag resulted in a higher normalized FS compared to SCC using 20% or less metakaolin. SCC using no SCMs resulted in a lower FS compared to SCC containing metakaolin. The FS increased as the metakaolin content increased up to 20%, and further increasing the metakaolin content reduced the FS in SCC.
5. The normalized STS when using 8% silica fume was higher than all SCC mixtures using metakaolin. Using 30% partial cement replacement with slag resulted in a higher normalized STS compared to the any SCC mixtures using metakaolin. Increasing the amount of metakaolin in SCC increased the FS up to 20% partial cement replacement, while further increasing the metakaolin content up to 25% decreased the STS. All SCC mixtures using metakaolin obtained a higher STS compared to SCC using no SCMs.
6. The normalized ME for SCC containing 8% silica fume, was comparable to SCC mixtures using 10% and 25% partial metakaolin replacements. All other metakaolin percentages had a lower ME compared to 8% silica fume partial replacement. In addition, using 30% partial cement replacement with slag resulted in a higher

normalized ME compared to using 20% or less metakaolin. The normalized ME for SCC when using 30% slag was higher compared to SCC containing 20% or less metakaolin. Increasing the amount of metakaolin in SCC increased the ME up to 20% partial cement replacement, while further increasing the metakaolin content up to 25% decreased the ME for SCC. Compared to SCC using no SCMs, all metakaolin partial replacement percentages resulted in a higher ME.

7. Increasing the C/F ratio from 0.7 to 0.9 reduced the flowability, passing ability, and HRWR demand, and increased the viscosity and segregation factor of all tested SCC mixtures. Further increasing the C/F to 1.2 was found to adversely affect the viscosity of all SCC mixtures and adversely affect the passing ability and segregation factors of some SCC mixtures, depending on the type of SCM used. Increasing the C/F ratio in SCC was found to negatively affect the mechanical properties of the mixtures. The 1-, 3-, and 7-day strength developments decreased as the C/F ratio increased from 0.7 to 1.2, regardless of the SCC mixture. Also, as the C/F ratio was increased, the 28- and 90-day compressive strengths, FS, STS, and ME for all SCC mixtures were found to decrease.
8. Using a larger coarse aggregate size (20 mm compared to 10 mm) decreased the viscosity, segregation factor, and HRWR demand, while the passing ability and flowability (except for SCC with metakaolin) increased for all tested SCC mixtures. Increasing the coarse aggregate size in SCC mixtures was also found to reduce the 1-, 3-, and 7-day strength developments, the 28- and 90-day compressive strengths, FS, STS, and ME for all tested SCC mixtures.

9. Increasing the binder content from 400 to 500 kg/m³ decreased the viscosity, flowability, and HRWR demand, and it increased the passing ability and segregation factor for all tested SCC mixtures. Increasing the binder content also increased the 1-, 3-, and 7-day strength developments, the 28- and 90-day compressive strengths, FS, STS, and ME for all tested SCC mixtures.
10. All SCC mixtures experienced decreases in the viscosity, segregation factor, and HRWR demand, when increasing the air content to 7%. However, the flowability and passing ability increased as the air content was increased from 0 to 7%, while the 1-, 3-, and 7-day strength developments, 28- and 90-day compressive strengths, FS, STS, and ME were reduced.
11. In general, the fresh properties of SCC greatly improved when the C/F ratio was decreased or the binder content/air content were increased. A decrease in the C/F ratio from 1.2 to 0.7 produced SCC that obtained successful L-Box ratios more favourable v-funnel times, according to the standards and produced in SCC. In addition, an increase in the binder content from 450 kg/m³ to 500 kg/m³ or increasing the air content from 0 to 7% resulted in SCC using SCMs that obtained L-Box ratios, V-funnel times, slump flow times and J-Ring measurements in accordance with SCC standards for acceptable SCC.
12. For normal-strength SCC beams, increasing the C/F ratio from 0.7 to 1.2 decreased the normalized shear strength by 16.4 and 23.1% when using 10 mm and 20 mm coarse aggregates, respectively. The normalized shear strength for normal-strength

SCC beams increased by an average of 12.8% when the coarse aggregate size was increased from 10 to 20 mm.

13. When using high-strength SCC beams, it was shown that the normalized shear failure capacity did not significantly change as the C/F ratio was increased from 0.7 to 1.2. As well, increasing the coarse aggregate size from 10 to 20 mm did not show any significant variation in the normalized shear failure capacity.
14. In normal-strength SCC beams, the post diagonal cracking resistance increased as the C/F ratio was increased. As the C/F ratio was increased from 0.7 to 1.2, the post diagonal cracking resistance of normal-strength concrete increased by 64.4% and 20.6% when using a 10 mm and 20 mm coarse aggregate, respectively. Increasing the coarse aggregate size in normal-strength SCC beams from 10 to 20 mm resulted in an average increase of 39.7% in the post diagonal cracking resistance. For high-strength SCC beams, increasing the C/F ratio from 0.7 to 1.2 increased the post diagonal cracking resistance by 11.9% and 3.5% when using a 10 mm and 20 mm coarse aggregate, respectively. However, increasing the coarse aggregate size in high-strength SCC beams showed no change in the average post diagonal cracking resistance.
15. The failure crack angle in normal-strength SCC beams was not affected by the C/F ratio in the mixture. However, increasing the coarse aggregate size in normal-strength SCC beams from 10 to 20 mm showed a reduction in the average failure crack angle by 2.8%. High-strength SCC beams showed no differences in the crack failure angle when the C/F ratio increased from 0.7 to 1.2 or when the coarse

aggregate size increased from 10 to 20 mm. In general, there was a decrease in the average crack failure angle of 7.6% when comparing high-strength to normal-strength SCC beams.

16. Increasing the C/F ratio for normal- and high-strength SCC beams showed an increase in their ductility, and using a larger coarse aggregate size (20 mm compared to 10 mm) showed an increase in the ductility of all tested SCC beams.

7. References

- Admixtures and Ground Slag for Concrete*. Transportation Research Board, National Research Council, 1990.
- Aggarwal, P. et al. "Self-Compacting Concrete – Procedure for Mix Design." *Leonardo Electronic Journal of Practices and Technologies* 12 (2008): 15–24.
- Akcaoglu, T., M. Tokyay, and T. Celik. "Effect of Coarse Aggregate Size on Interfacial Cracking Under Uniaxial Compression." *Materials Letters* 57 (2002): 828–833.
- Assaad, J., and K.H. Khayat. "Kinetics of Formwork Pressure Drop of Self-Consolidating Concrete Containing Various Types and Contents of Binder." *Cement and Concrete Research* 35 (2005): 1522–1530.
- Beaupre, D., P. Lacombe, and K.H. Khayat. "Laboratory Investigation of Rheological Properties and Scaling Resistance of Air Entrained Self-Consolidating Concrete." *Materials and Structures* 32 (1999): 235–240.
- Brooks, J.J., and M.A.M. Johari. "Effect of Metakaolin on Creep and Shrinkage of Concrete." *Cement and Concrete Composites* 23.6 (2001): 495–502.
- Browning, G.A. "Optimum Air Content Range in the Plastic and Hardened State for TDOT Class D Portland Cement Concrete." BiblioBazaar, 2012.
- Concrete in Practice: What, Why & How?* National Ready Mixed Concrete Association, 2000.
- CIP 16 - Flexural Strength Concrete.
- Concrete Manual – Properties and Mix Designations. Minnesota Department of Transportation, 2003.

- Detwiler, R.J., and P.K. Mehta. "Chemical and Physical Effects of Silica Fume on the Mechanical Behavior of Concrete." *Materials Journal* 86.6 (1989): n. pag.
- Dhonde, H.B. et al. "Fresh and Hardened Properties of Self-Consolidating Fibre-Reinforced Concrete." *ACI Materials Journal* 104.5 (2007): 491–500.
- Ding, J., and Z. Li. "Effects of Metakaolin and Silica Fume on Properties of Concrete." *ACI Materials Journal* 99.4 (2002): 393–398.
- El-Chabib, H., and M. Nehdi. "Effect of Mixture Design Parameters on Segregation of Self-Consolidating Concrete." *ACI Materials Journal* 103.5 (2006): 374–383.
- Filho, A.F.M. et al. "Hardened Properties of Self-Compacting Concrete – A Statistical Approach." *Construction and Building Materials* 24 (2010): 1608–1615.
- Gencel, O. et al. "Mechanical Properties of Self-Compacting Concrete Reinforced with Polypropylene Fibres." *Materials Research Innovations* 15.3 (2011): 216–225.
- Grace Construction. "An Introduction to Self-Consolidating Concrete (SCC)." 2005: n. pag.
- Guneyisi, E., M. Gesoglu, and Erdogan Ozbay. "Permeation Properties of Self-Consolidating Concretes with Minerals Admixtures." *ACI* 108.2 (2011): 150–158.
- Gutmann, P.F. "Bubble Characteristics as they Pertain to Compressive Strength and Freeze-Thaw Durability." *ACI Materials Journal* 5 (1988): 361–366.
- Hassan, A.A.A., M. Lachemi, and K.M.A. Hossain. "Behaviour of Full-Scale Self-Consolidating Concrete Beams in Shear" *Cement & Concrete Composites* 30 (2008): 588-596.
- Hassan, A.A.A., M. Lachemi, and K.M.A. Hossain. "Structural Assessment of Corroded Self-Consolidating Concrete Beams." *Cement & Concrete Composites* 32 (2010): 874-885.

- Hassan, A.A.A., M. Lachemi, and K.M.A. Hossain. "Strength, Cracking and Deflection Performance of Large-Scale Self-Consolidating Concrete Beams Subjected to Shear Failure." *Cement & Concrete Composites* 32 (2010): 1262-1271.
- Hassan, A.A.A., M. Lachemi, and K.M.A. Hossain. "Effect of Metakaolin and Silica Fume on Rheology of Self-Consolidating Concrete." *ACI Materials Journal* 109.6 (2012): 657–664.
- Hinczak, I. "Alternative Cements – The Blue Circle Experience." Vol. 3. 1990. 1–21.
- Hu, J., and K. Wang. "Effect of Coarse Aggregate Characteristics on Concrete Rheology." *Construction and Building Materials* 25.3 (2011): 1196–1204.
- Jawahar, J.G. et al. "Effect of Coarse Aggregate Blending on Fresh Properties of Self-Compacting Concrete." *International Journal of Advances in Engineering & Technology* 3.2 (2012): 456–466.
- Jennings, H.M. et al. "Characterization and Modeling of Pores and Surfaces in Cement Paste: Correlations to Processing and Properties." *Journal of Advanced Concrete Technology* 6.4 (2008): 5–29.
- Joseph, D. *Influence of Aggregate on Fracture Properties of Concrete*. Department of Civil Engineering College of Engineering Trivandrum, 2010.
- Justice, J.M. et al. "Comparison of Two Metakaolins and a Silica Fume Used as Supplementary Cementitious Materials." Washington D.C., 2005.
- Justice, J.M., and K.E. Kurtis. "Influence of Metakaolin Surface Area on Properties of Cement-Based Materials." *Journal of Materials in Civil Engineering* 19.9 (2007): 762–771.

- Khatib, J.M. "Metakaolin Concrete at a Low Water to Binder Ratio." *Construction and Building Materials* 22 (2008): 1691–1700.
- Khayat, K. "Workability, Testing and Performance of Self-Consolidating Concrete." *ACI Materials Journal* 96.3 (1999): 346–353.
- Khayat, K.H. "Optimization and Performance of Air-Entrained, Self-Consolidating Concrete." *ACI Materials Journal* 97.5 (2000): 526–535.
- Khayat, K.H., and J. Assaad. "Air-Void Stability in Self-Consolidating Concrete." *ACI Materials Journal* 99.4 (2002): 408–416.
- Khayat, K.H., P. Paultre, and S. Tremblay. "Structural Performance and In-Place Properties of Self-Consolidating Concrete Used for Casting Highly Reinforced Columns." *ACI Materials Journal* 98.5 (2001): 371–378.
- Kim, Y.H. et al. "Shear Characteristics and Design for High-Strength Self-Consolidating Concrete." *Journal of Structural Engineering* 136.8 (2010): 989–1000.
- Koehiler, E.P. "Aggregates in Self-Consolidating Concrete." 2007: n. pag.
- Kosmatka, S.H., Kerkhoff, B., Panarese, W.C. "Design and Control of Concrete Mixtures." *Portland Cement Association*. Chap 3: 57-72.
- Lachemi, M., K.M.A. Hossain, and V. Lambros. "Shear Resistance of Self-Consolidating Concrete Beams – Experimental Investigations." *Canadian Journal of Civil Engineering* 32.6 (2005): 1103–1113.
- Larbi, J.a. *Microstructure of the Interfacial Zone Around Aggregate Particles in Concrete*. Stevin-Laboratory of the Fac. of Civil Engineering, Delft University of Technology, 1993.

- Lee, D.Y., F.W. Klaiber, and J.W. Coleman. *Fatigue Behavior of Air-Entrained Concrete*. IOWA: Department of Civil Engineering Research Institute IOWA State University, 1977.
- Li, A. Assih, J. And Delmas, Y. "Shear Strengthening of RC Beams with Externally Bonded CFRP Sheets" *Journal of Structural Engineering*. Vol 127(4). 2001. 374-380.
- Lin, C.H., and J.H. Chen. "Shear Behaviour of Self-Consolidating Concrete Beams." *ACI Structural Journal* 109.3 (2012): 307–316.
- Loannides, A.M., and J.C. Mills. Effect of Larger Sized Coarse Aggregates on Mechanical Properties of Portland Cement Concrete Pavements and Structures. Ohio Department of Transportation Office of Research and Development, 2006.
- MacGregor, J.G., and F.M.P. Bartlett. *Reinforced Concrete: Mechanics and Design*. Prentice Hall Canada, 2000.
- Madandoust, R., and S.Y. Mousavi. "Fresh and Hardened Properties of Self-Compacting Concrete Containing Metakaolin." 35 (2012): 752–760.
- Marar, K., and O. Eren. "Effect of Cement Content and Water/Cement Ratio on Fresh Concrete Properties Without Admixtures." *International Journal of the Physical Sciences* 6.24 (2011): 5752–5765.
- Mehta, P.K., and P.J.M. Monteiro. *Concrete: Structure, Properties and Materials*. 2nd ed. Prentice Hall, 1993.
- "*Metakaolin Application and Benefits*." Advanced Cement Technologies, LLC n. pag.
- Mindess, S., J.F. Young, and D. Darwin. *Concrete*. 2nd ed. NJ: Prentice, 2003.

- Nanthagopalan, P., and M. Santhanam. "Experimental Investigations on the Influence of Paste Composition and Content on the Properties of Self-Compacting Concrete." *Construction and Building Materials* 23 (2009): 3443–3449.
- Neptune, A.I., and B.J. Putman. "Effect of Aggregate Size and Gradation on Pervious Concrete Mixtures." *ACI Materials Journal* 107.6 (2010): 625–631.
- Neville, A.M. *Properties of Concrete. 4th and Final Edition*. 4th ed. Longman Group UK Limited, 1995.
- Nita, C. et al. "Effect of Metakaolin on the Performance of PVA and Cellulose Fibres Reinforced Cement." 2004: n. pag.
- Ozkul, M.H., and U.A. Dogan. "Rheological Properties and Segregation Resistance of SCC Prepared by Portland Cement and Fly Ash." *Measuring, Monitoring and Modeling Concrete Properties*. 94 vols. 2006. 463–468.
- Qian, Xiaoqian, and Zongjin Li. "The Relationships Between Stress and Strain for High-Performance Concrete with Metakaolin." *Cement and Concrete Research* 31 (2001): 1607–1611.
- Razak, H.A., and Wong, H.S. "Effect of Incorporating Metakaolin on Fresh and Hardened Properties of Concrete." *ACI Special Publication* 200.19 (2000): 309-324.
- Safiuddin, M. "Development of Self-Consolidating High Performance Concrete Incorporating Rich Husk Ash." 2008: n. pag.
- Salman, M.M., and Z.M.A. Hussian. "Production of Self-Compacting Concrete by Using Finer Aggregate Not Conforming to Local Specification." *International Journal of Civil Engineering* (2008): 65–88.

“Self-Consolidating High Performance Concrete: SCC Self-Consolidation and Highly Flowable Concrete.” Web. 11 Dec. 2012.

“Self-Consolidating Concrete Defined – The Concrete Network.” *ConcreteNetwork.com*. Web. 17 Dec. 2012.

Sherwood, E.G., E.C. Bentz, and M.P. Collins. “Effect of Aggregate Size on Beam-Shear Strength of Thick Slabs.” *ACI Structural Journal* 104.2 (2007): 180–190.

Shetty, M.S. *Concrete Technology: Theory and Practice*. 2nd ed. Chand (S.) & Co Ltd, 1987.

Shin, S.W. et al. “Shear Strength of Reinforced High-Strength Concrete Beams with Shear Span-to-Depth Ratios Between 1.5 and 2.5.” *ACI Structural Journal* 96.4 (1999): 549–556.

Sonebi, M., S. Grunewald, and J. Walraven. “Filling Ability and Passing Ability of Self-Consolidating Concrete.” *ACI Materials Journal* 104.2 (2007): 162–170.

Standard Practice for Selecting Proportions for Normal, Heavyweight, and Mass Concrete (ACI 211.1-91). ACI Committee 211, 2002.

Standard Test Method for Flexural Strength of Concrete (Using Simple Beam With Center-Point Loading). ASTM.

Standard Test Method for Passing Ability of Self-Consolidating Concrete by J-Ring. ASTM.

Standard Test Method for Slump Flow of Self-Consolidating Concrete. ASTM.

Standard Test Method for Splitting Tensile Strength of Cylindrical Concrete Specimens. ASTM.

Standard Test Method for Static Modulus of Elasticity and Poisson’s Ratio of Concrete in Compression. ASTM.

- Struble, L.J., and Q. Jiang. "Effects of Air Entrainment on Rheology." *ACI Materials Journal* 101.6 (2003): 448–456.
- Su, J.K. et al. "Effect of Sand Ratio on the Elastic Modulus of Self-Compacting Concrete." *Journal of Marine Science and Technology* 10.1 (2002): 8–13.
- Su, N., K.C. Hsu, and H.W. Chai. "A Simple Mix Design Method for Self-Compacting Concrete." *Cement and Concrete Research* 31 (2001): 1799–1807.
- Symon, Keith. *Mechanics*. 3rd ed. Addison-Wesley Publishing Company, 1971.
- Taylor, H.P.J. Investigation of the Forces Carried Across Cracks in Reinforced Concrete Beams in Shear by Interlock of Aggregate. London, 1970.
- "Tensile Test on Concrete." *Building Research Institute (P) Ltd., BREINS*. Web. 11 Dec. 2012.
- The European Guidelines for Self-Compacting Concrete. European Project Group, 2005.
- Uysal, M., and K. Yilmaz. "Effect of Mineral Admixtures on Properties of Self-Compacting Concrete." *Cement and Concrete Composites* 33.7 (2011): 771–776.
- Vejmelkova, E. et al. "Properties of Self-Compacting Concrete Mixtures Containing Metakaolin and Blast Furnace Slag." *Construction and Building Materials* 25 (2011): 1325–1331.
- Walraven, J.C. Aggregate Interlock: A Theoretical and Experimental Analysis. Delft University Press, 1980.
- Wild, S., J.M. Khatib, and A. Jones. "Relative Strength, Pozzolanic Activity and Cement Hydration in Superplasticised Metakaolin Concrete." *Cement and Concrete Research* 26.10 (1996): 1537–1544.

Yaqub, M., and I. Bukharu. "Effect of Size of Coarse Aggregate on Compressive Strength of High Strength Concrets." Singapore: CI-Premier PTE LTD, 2006.

Zhenshuang, W. et al. "Optimization of Coarse Aggregate Content Based on Efficacy Coefficient Method." *Journal of Wuhan University of Technology-Materials Science Edition* 26.2 (2011): 329–334. Zhu, W., and P.J.M. Bartos. "Permeation Properties of Self-Compacting Concrete." *Cement and Concrete Research* 33 (2003): 921–926.

8.1 Appendix A -- Crack Development Figures for 10 SCC Beams

Note: Crack Widths are in mm

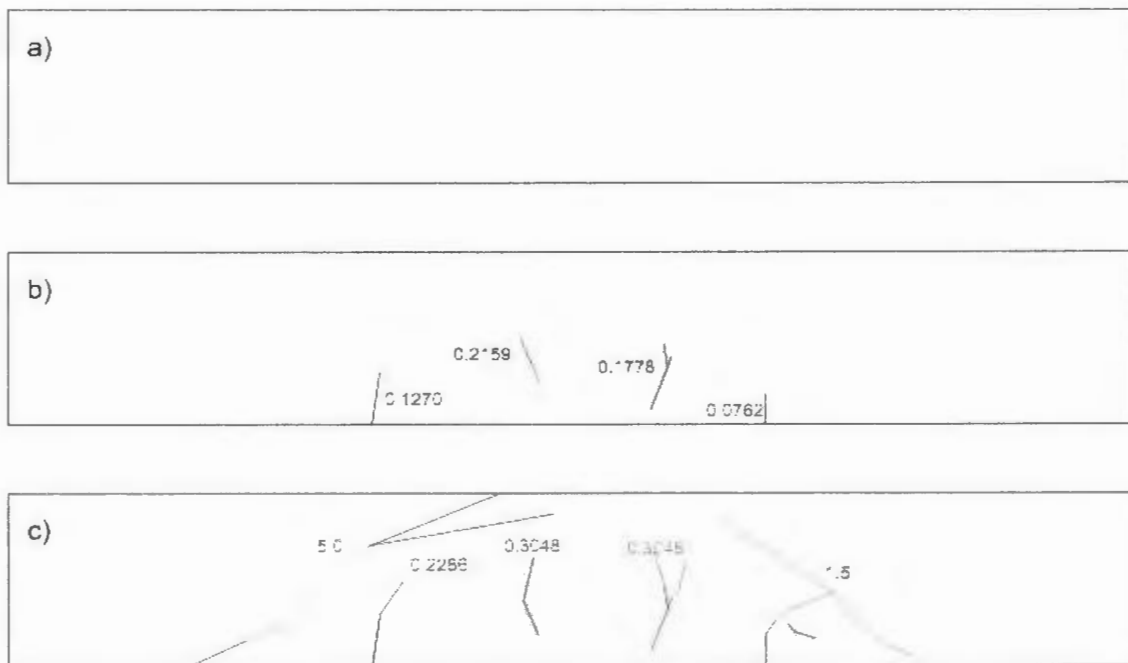


Figure A1 – Crack Development for a) 50%, b) 75% and c) 100% of Max Load

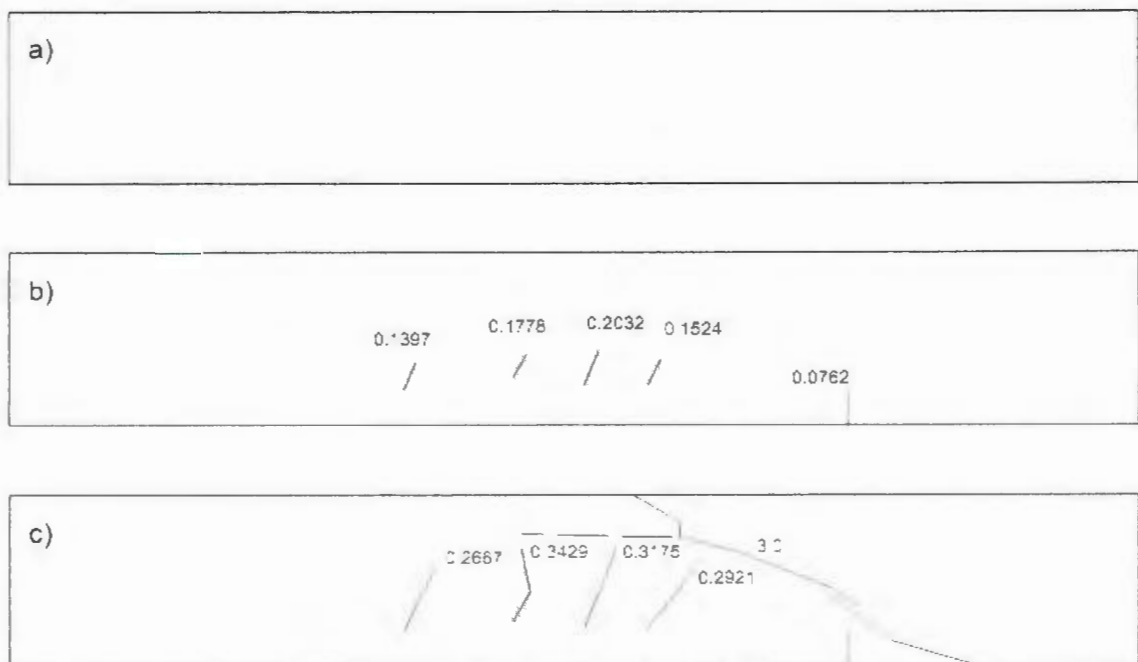


Figure A2 – Crack Development for a) 50%, b) 75% and c) 100% of Max Load

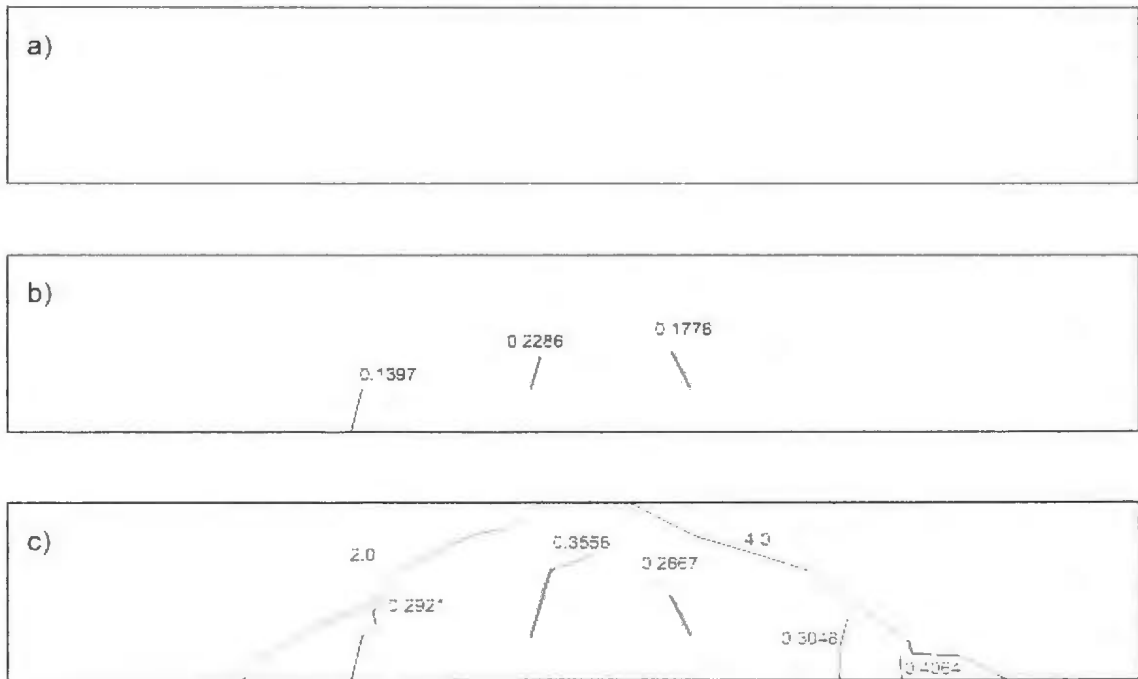


Figure A3 – Crack Development for a) 50%, b) 75% and c) 100% of Max Load

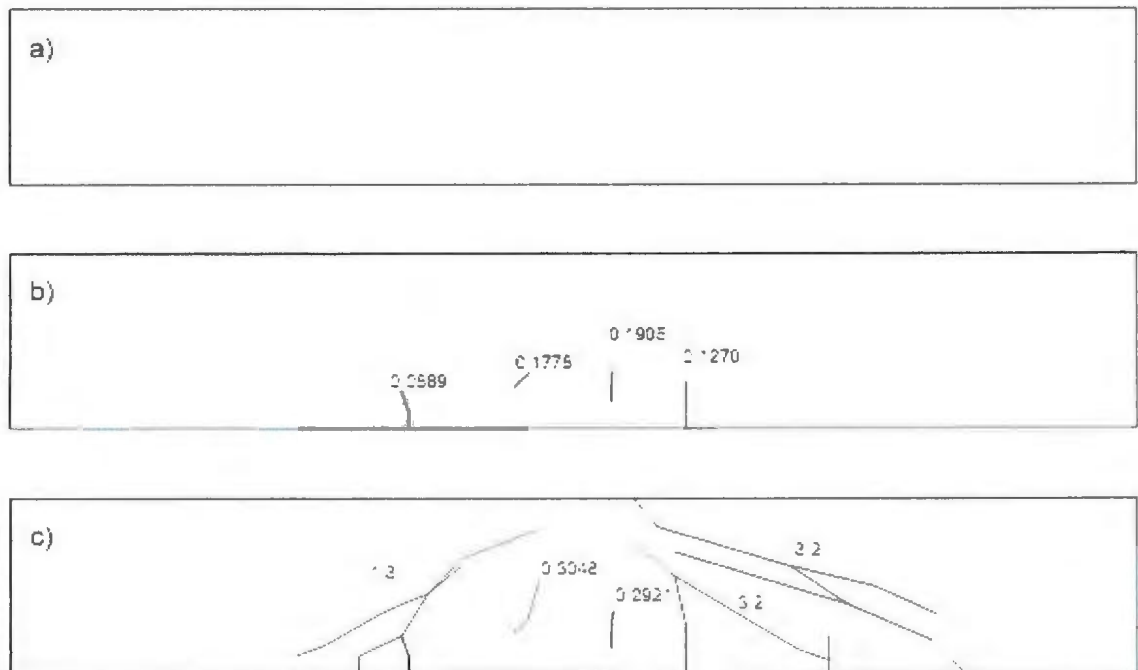


Figure A4 – Crack Development for a) 50%, b) 75% and c) 100% of Max Load

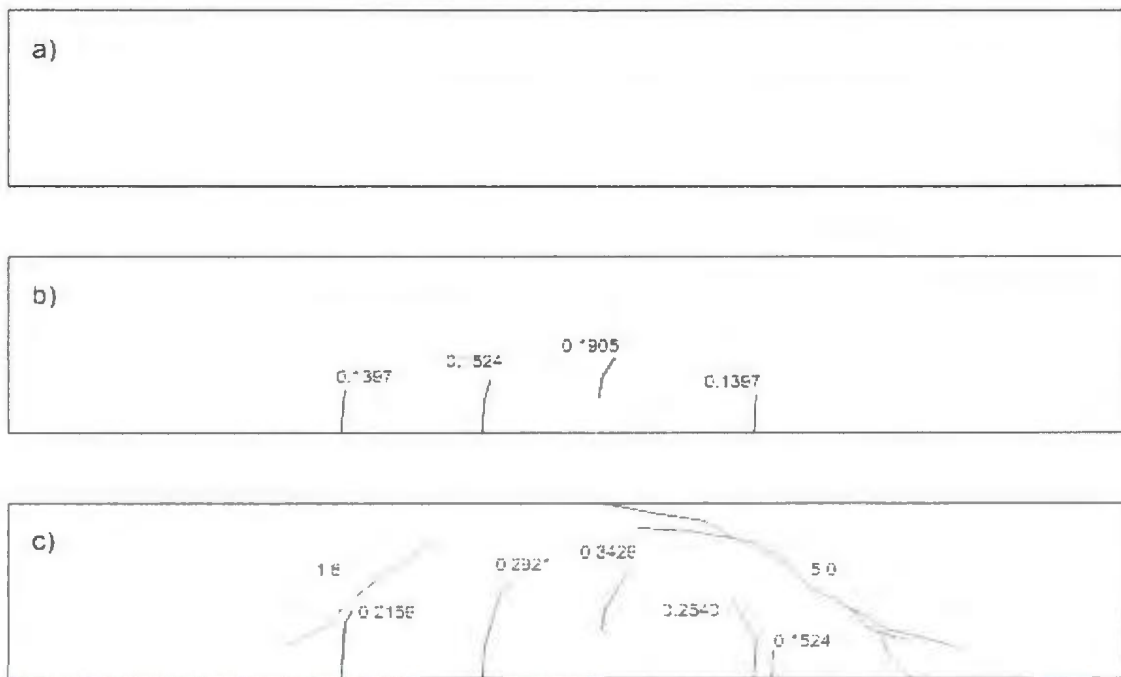


Figure A5 – Crack Development for a) 50%, b) 75% and c) 100% of Max Load

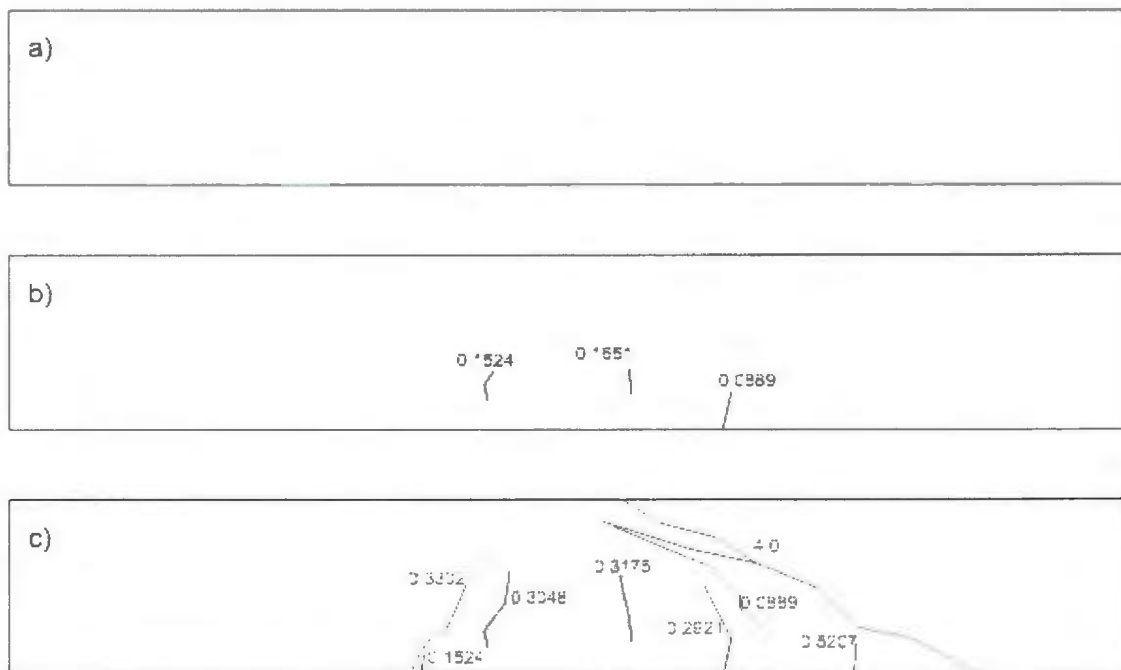


Figure A6 – Crack Development for a) 50%, b) 75% and c) 100% of Max Load

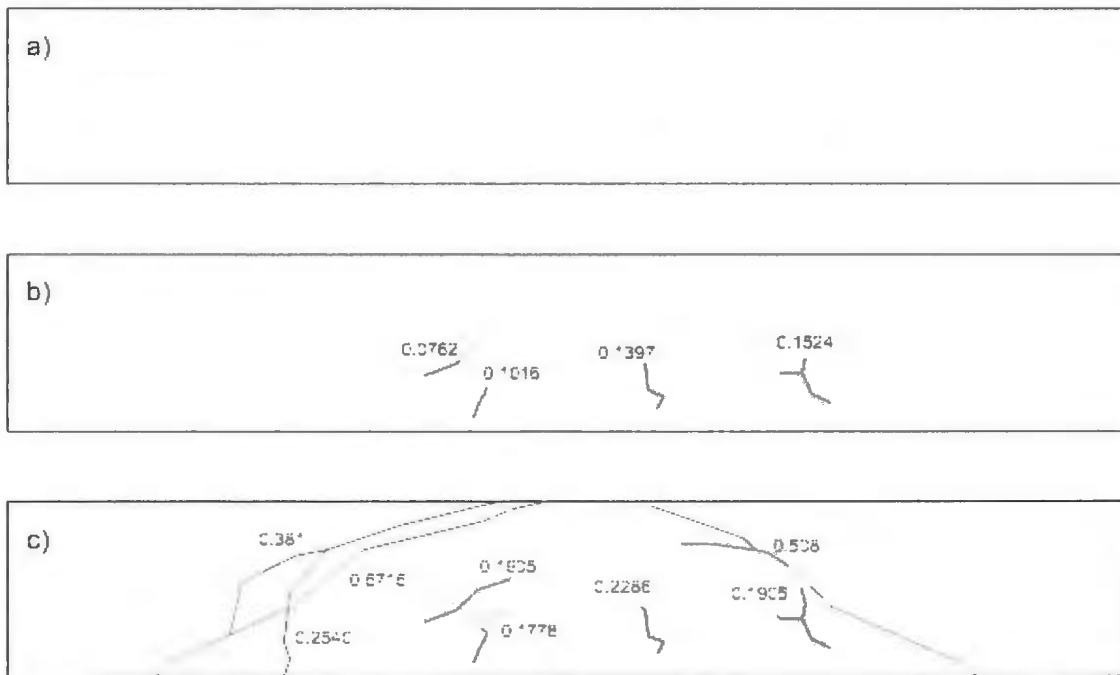


Figure A7 – Crack Development for a) 50%, b) 75% and c) 100% of Max Load

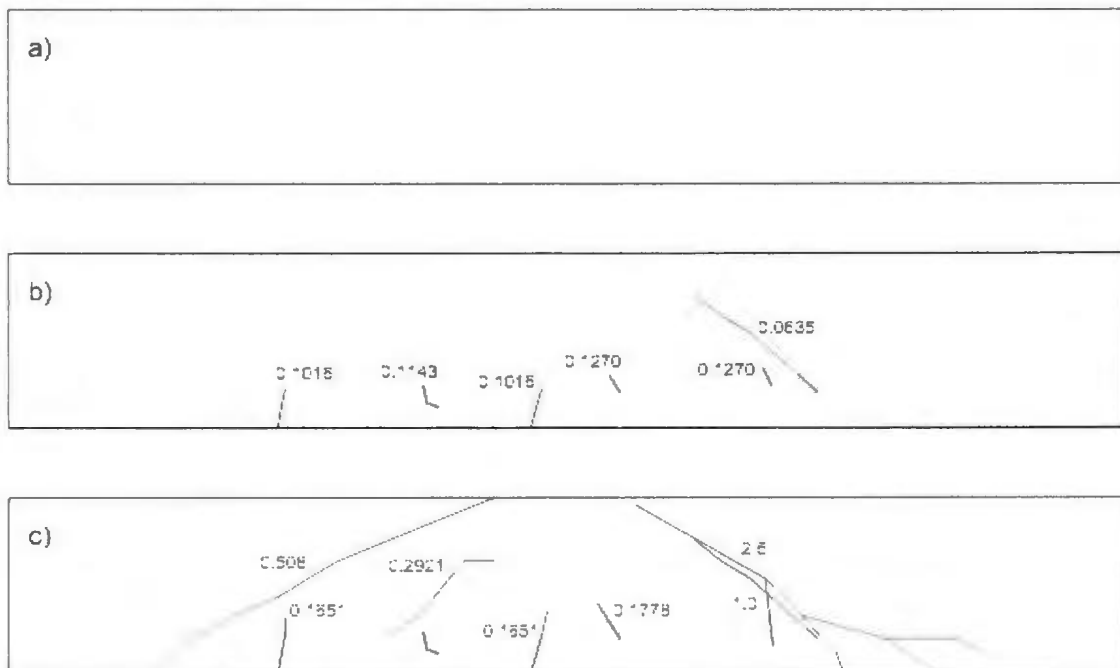


Figure A8 – Crack Development for a) 50%, b) 75% and c) 100% of Max Load

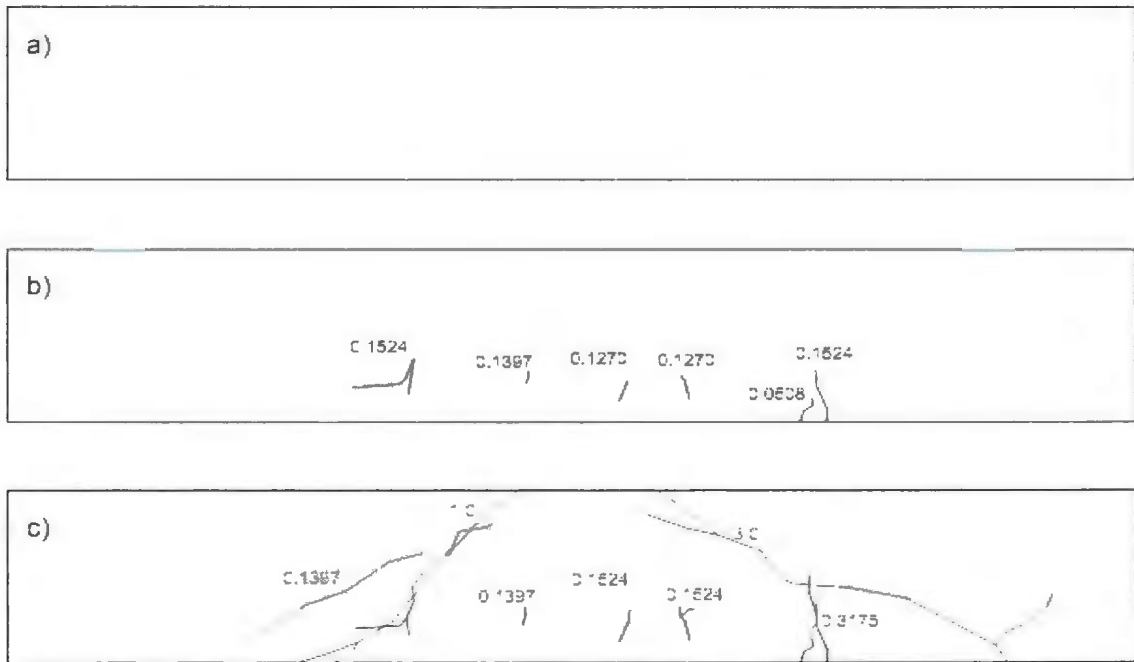


Figure A9 – Crack Development for a) 50%, b) 75% and c) 100% of Max Load

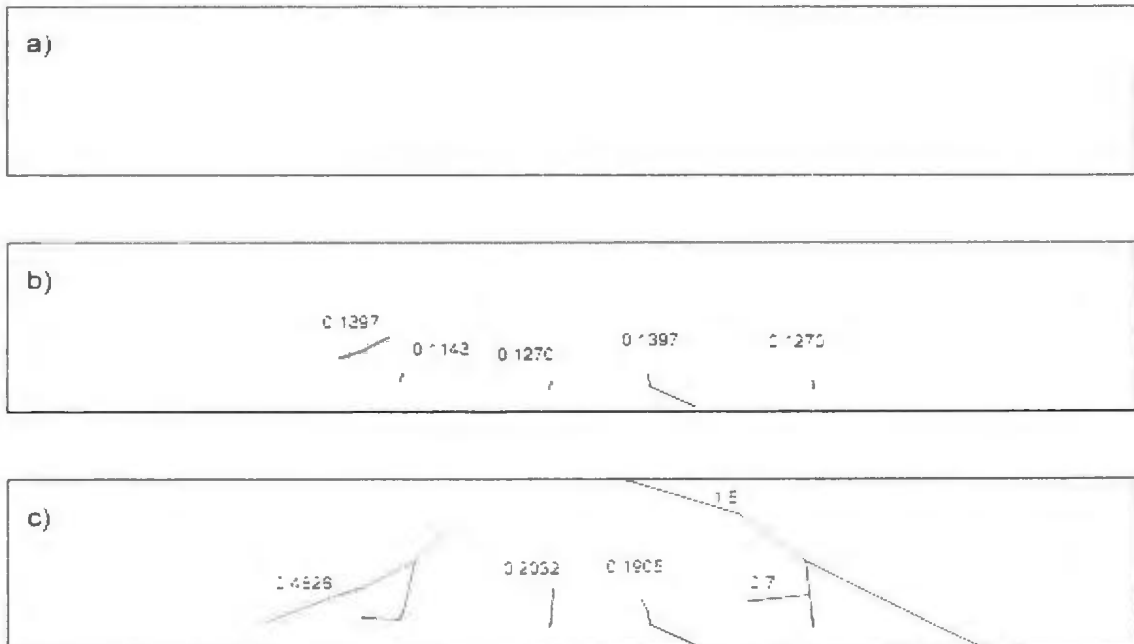


Figure A10 – Crack Development for a) 50%, b) 75% and c) 100% of Max Load

8.2 Appendix B - LVDT Deflection Graphs for 10 SCC Beams

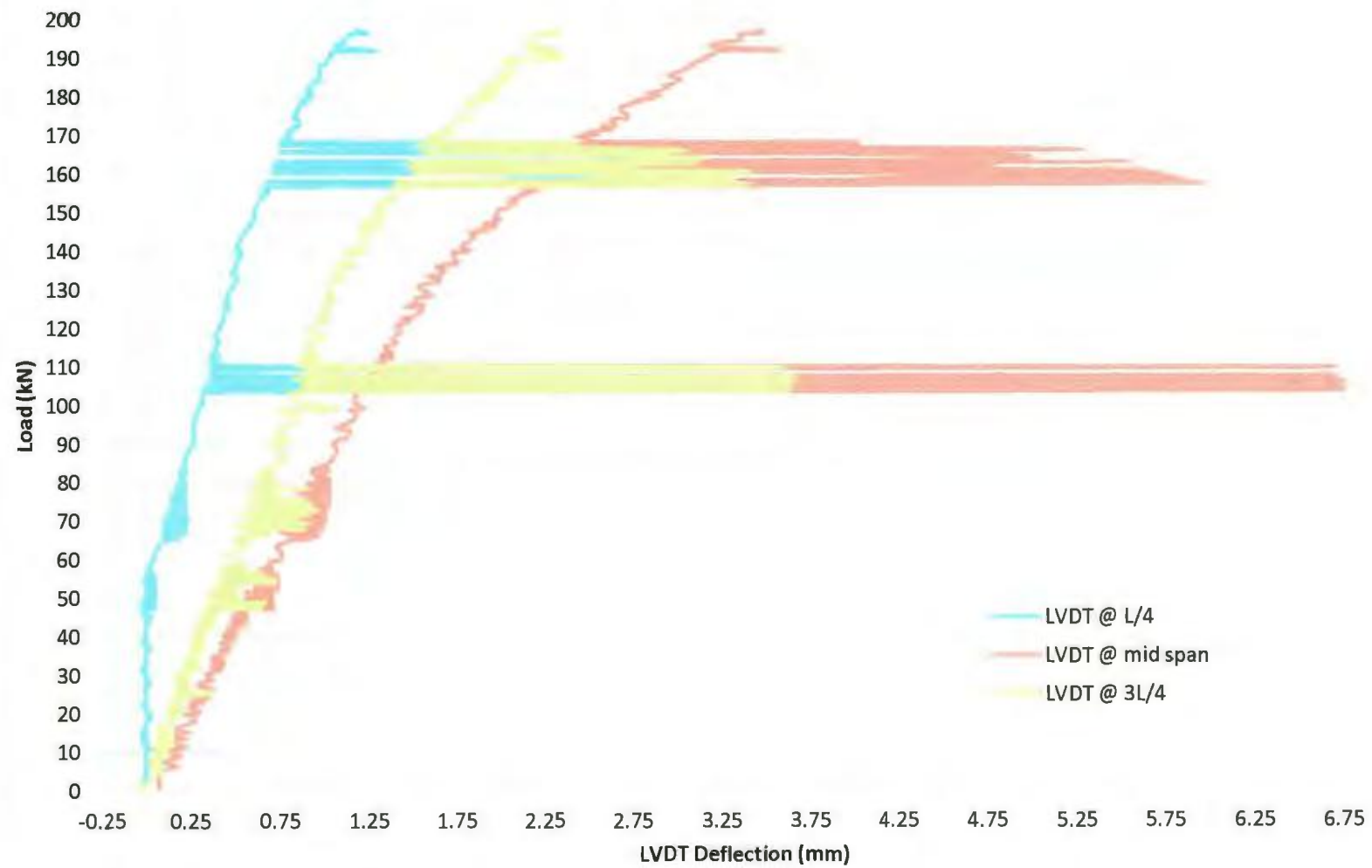


Figure B2 – LVDT Deflection vs. Loading for Beam 1

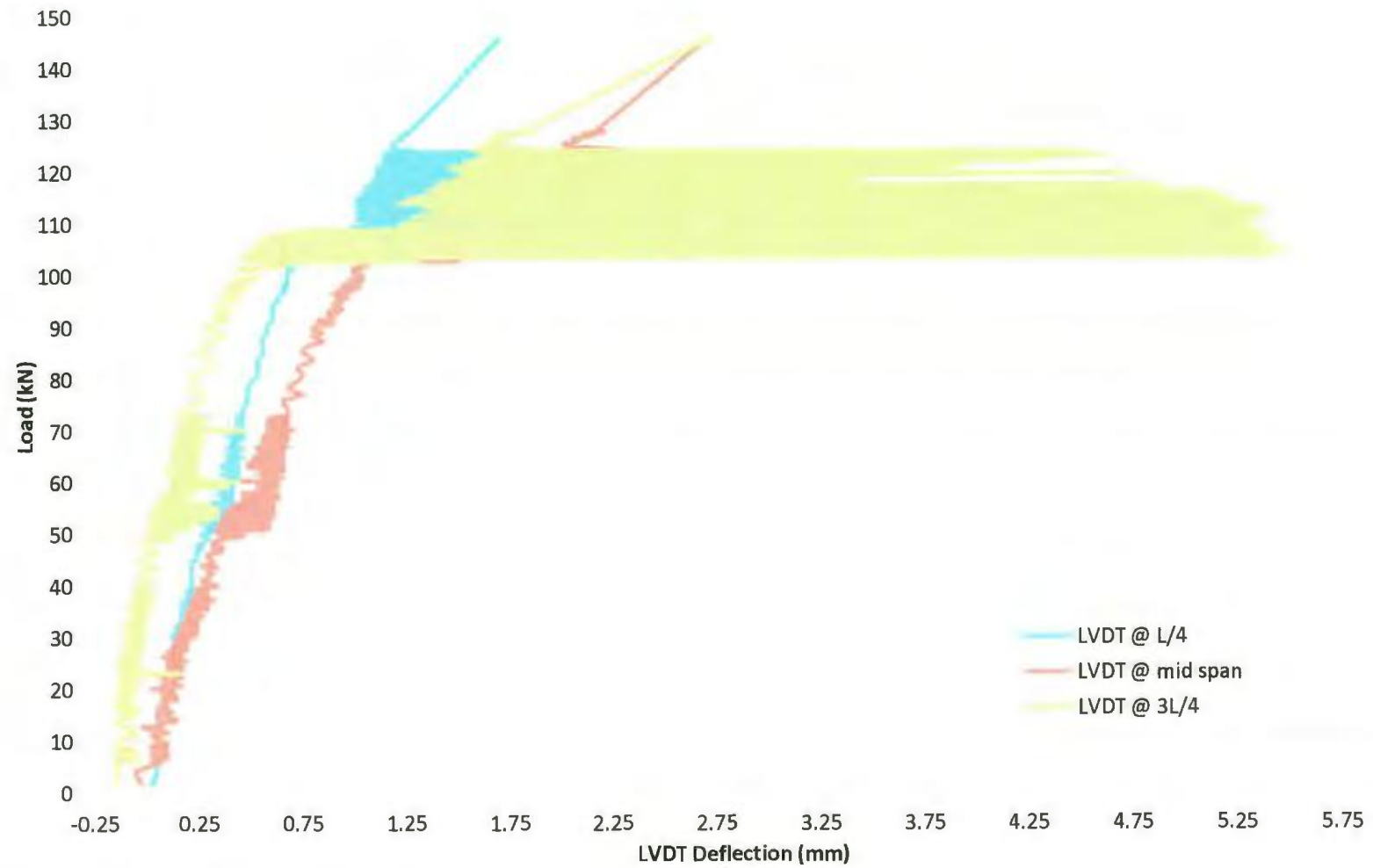


Figure B3 – LVDT Deflection vs. Loading for Beam 2

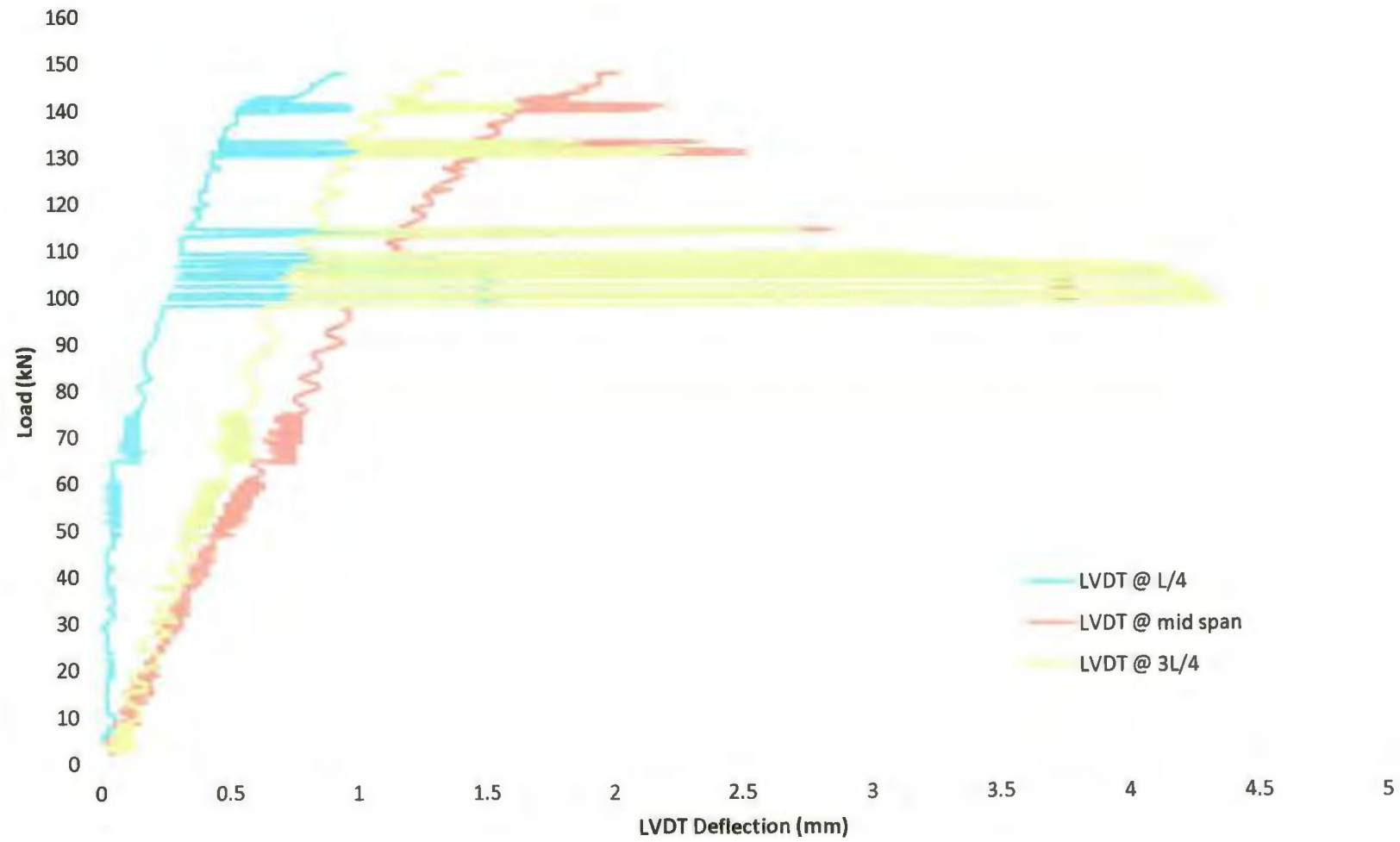


Figure B3 – LVDT Deflection vs. Loading for Beam 3

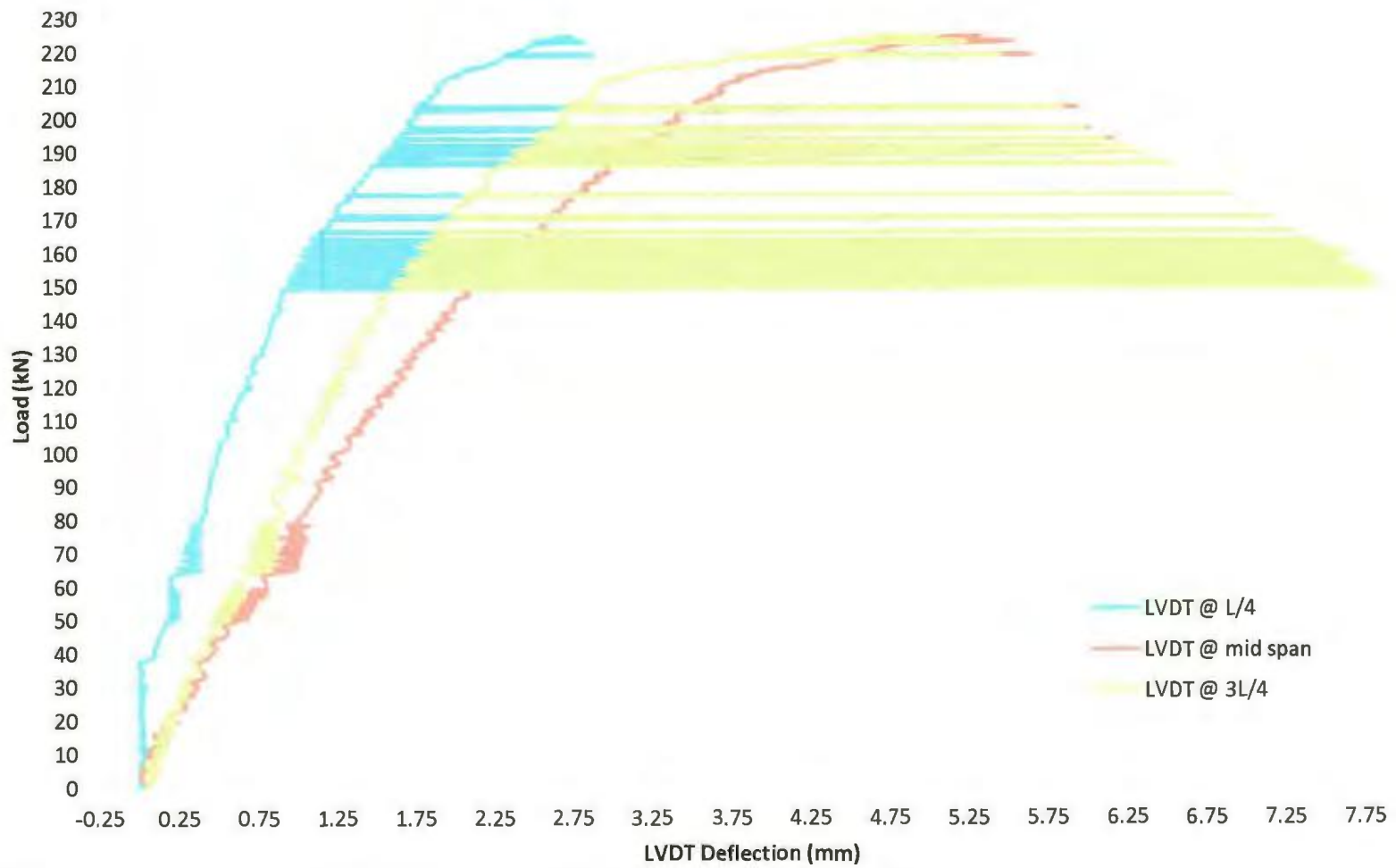


Figure B4 – LVDT Deflection vs. Loading for Beam 4

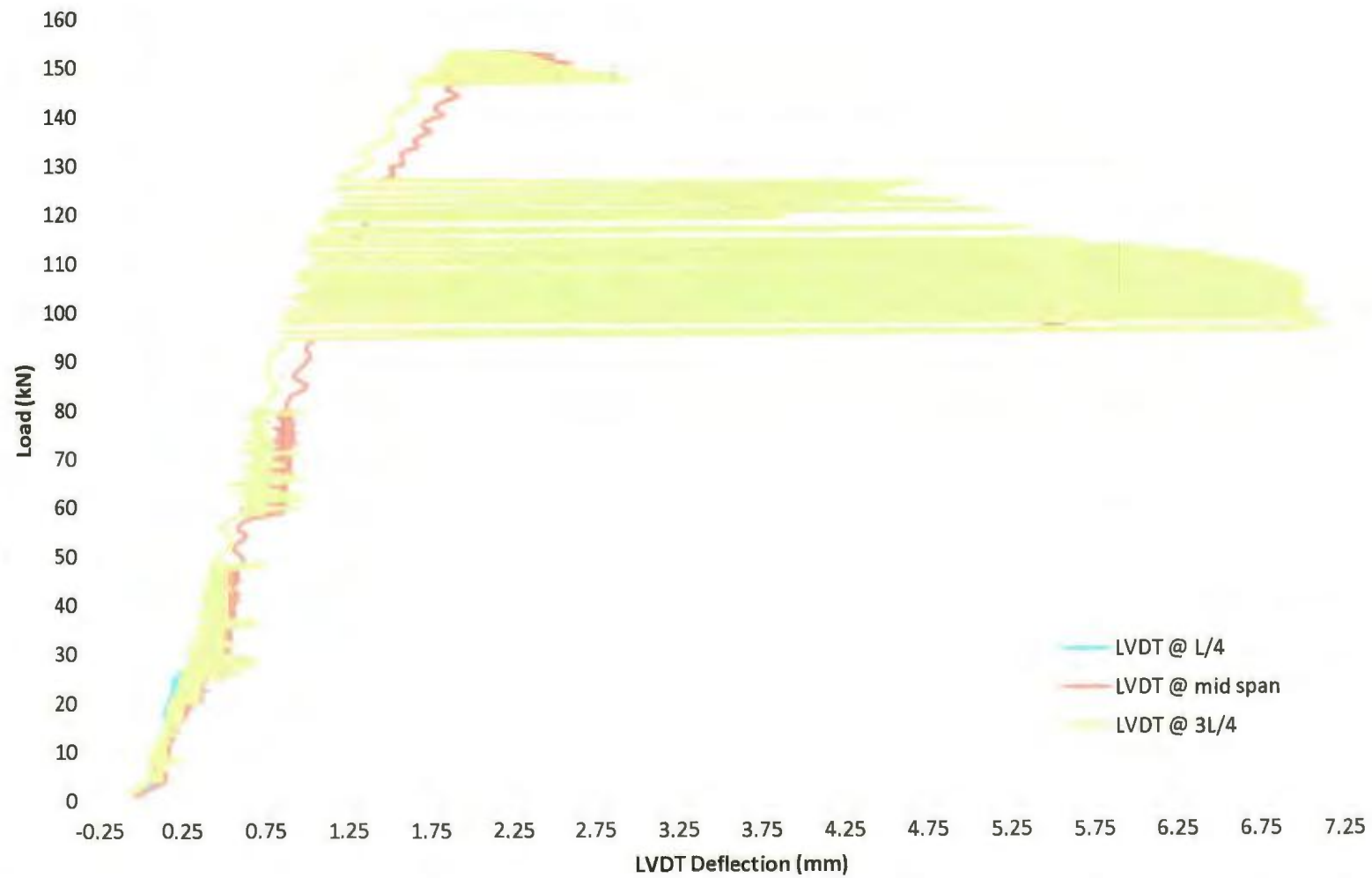


Figure B5 – LVDT Deflection vs. Loading for Beam 5

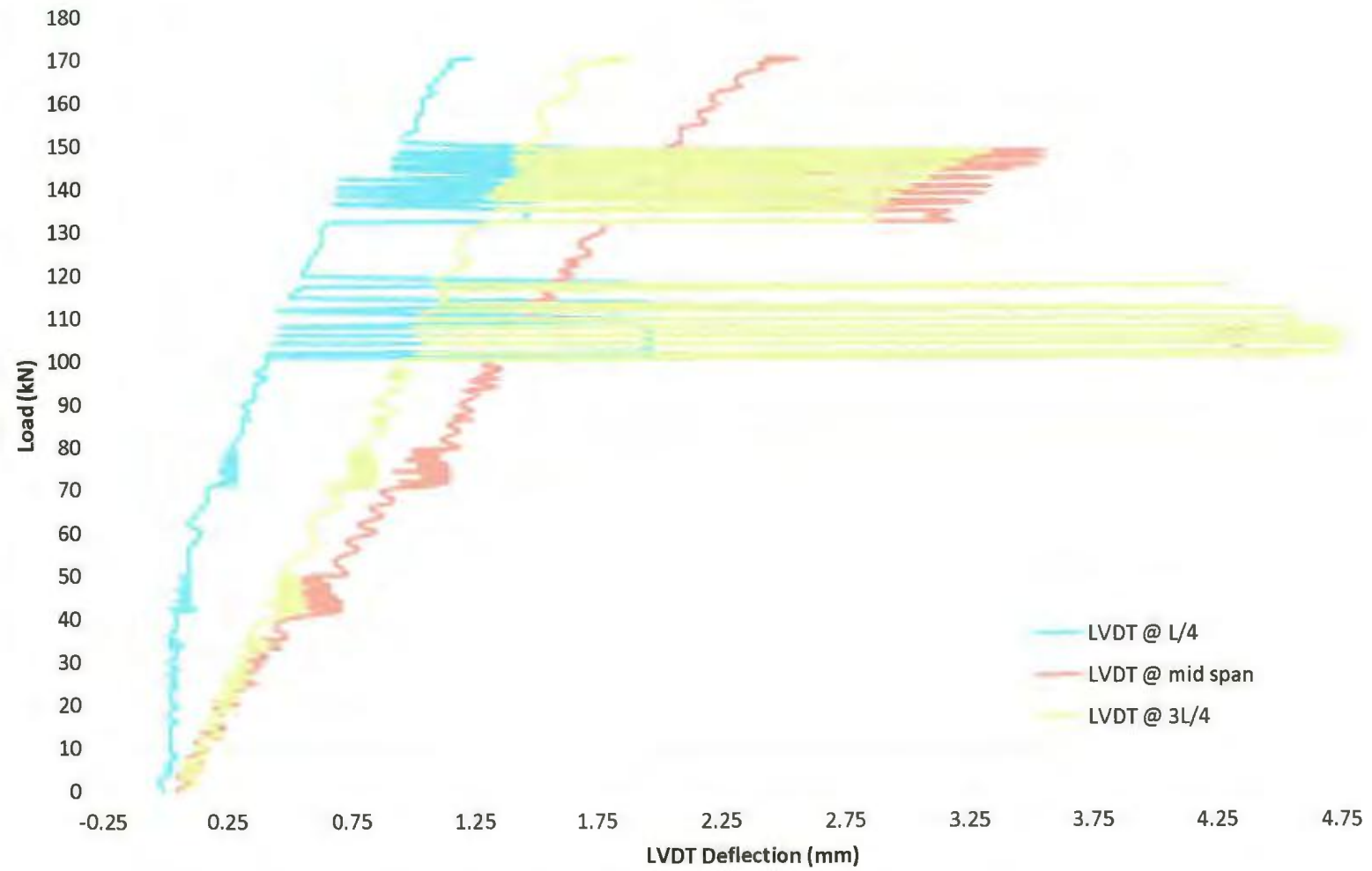


Figure B6 – LVDT Deflection vs. Loading for Beam 6

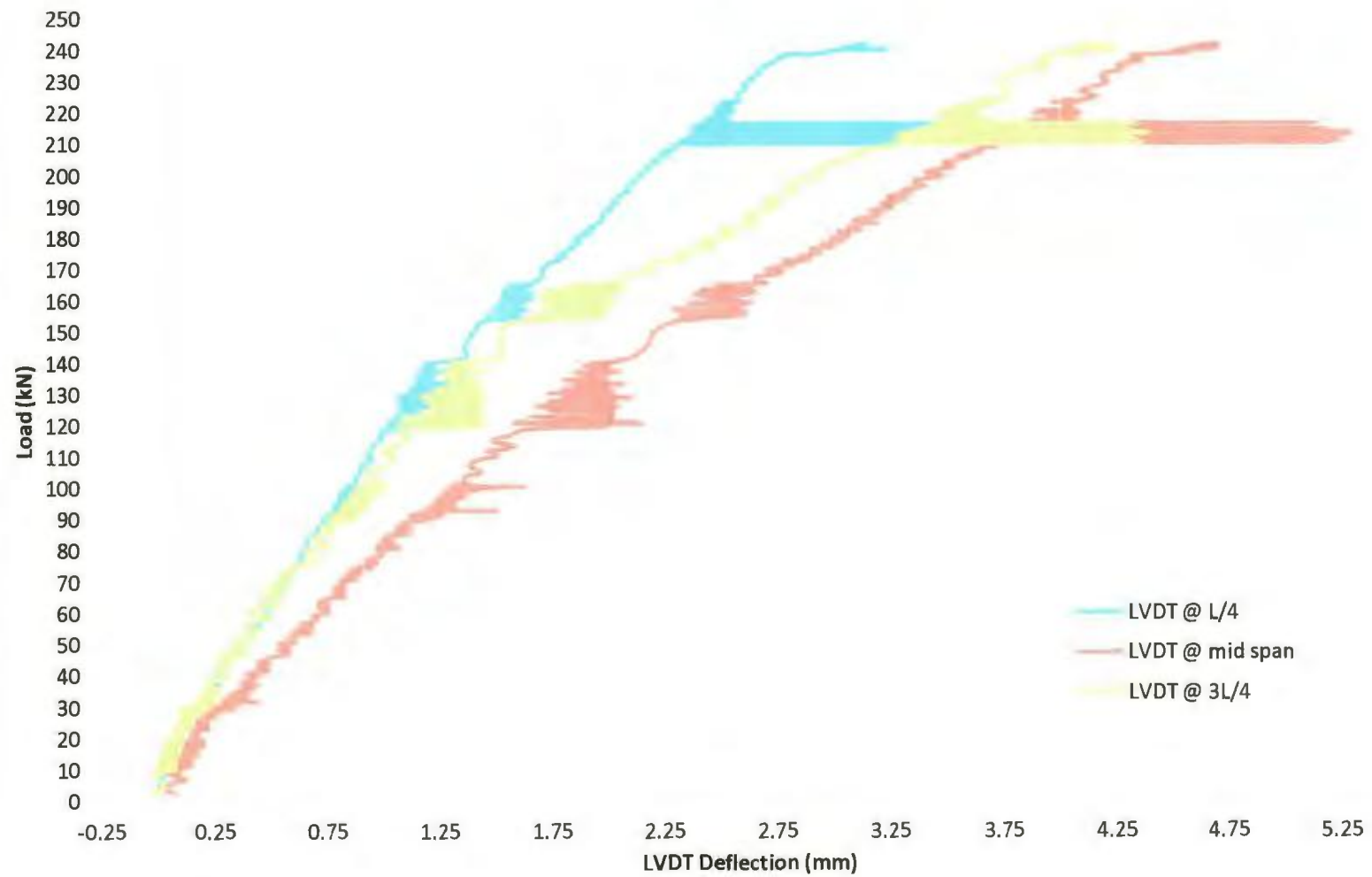


Figure B7 – LVDT Deflection vs. Loading for Beam 7

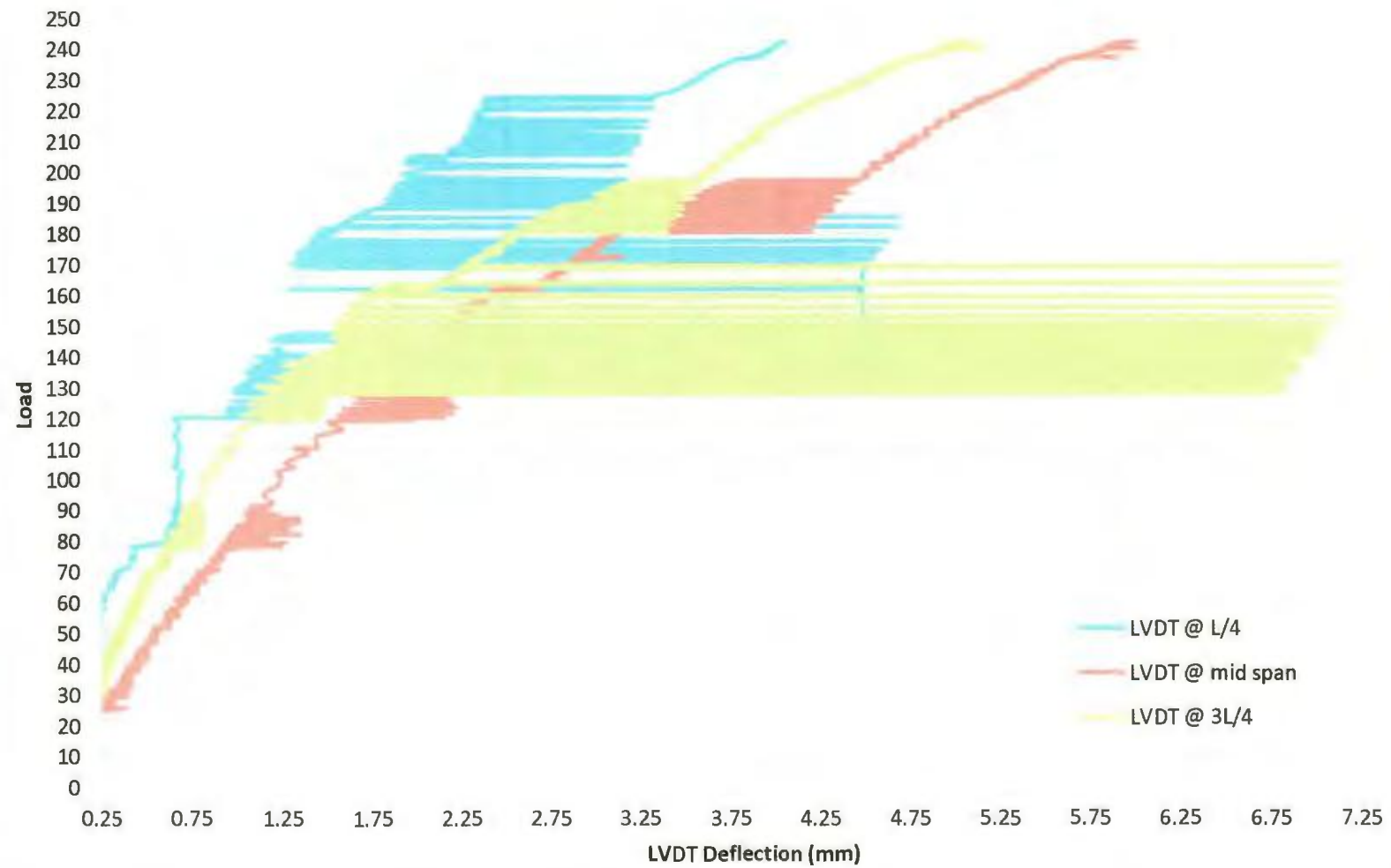


Figure B8 – LVDT Deflection vs. Loading for Beam 8

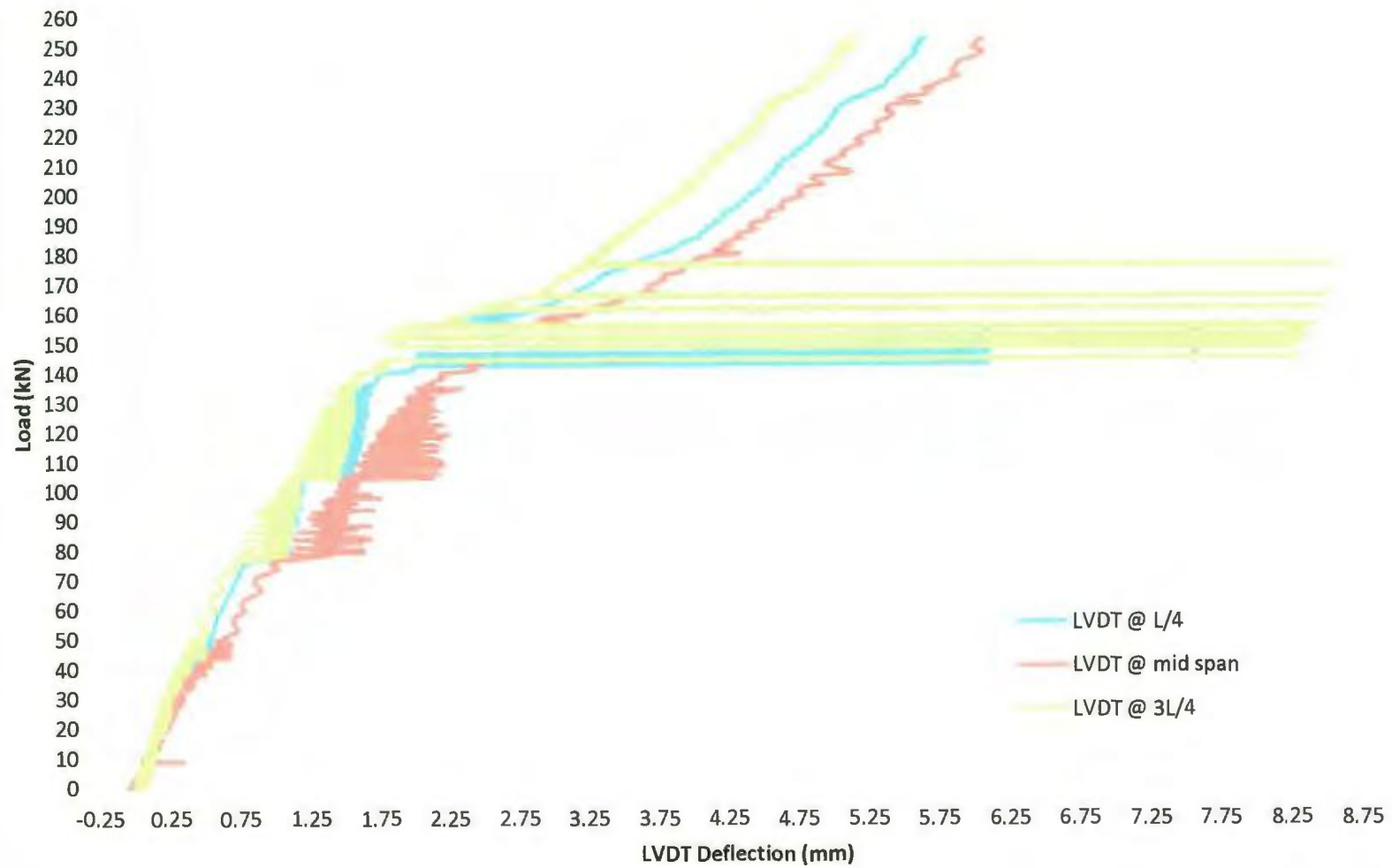


Figure B9 – LVDT Deflection vs. Loading for Beam 9

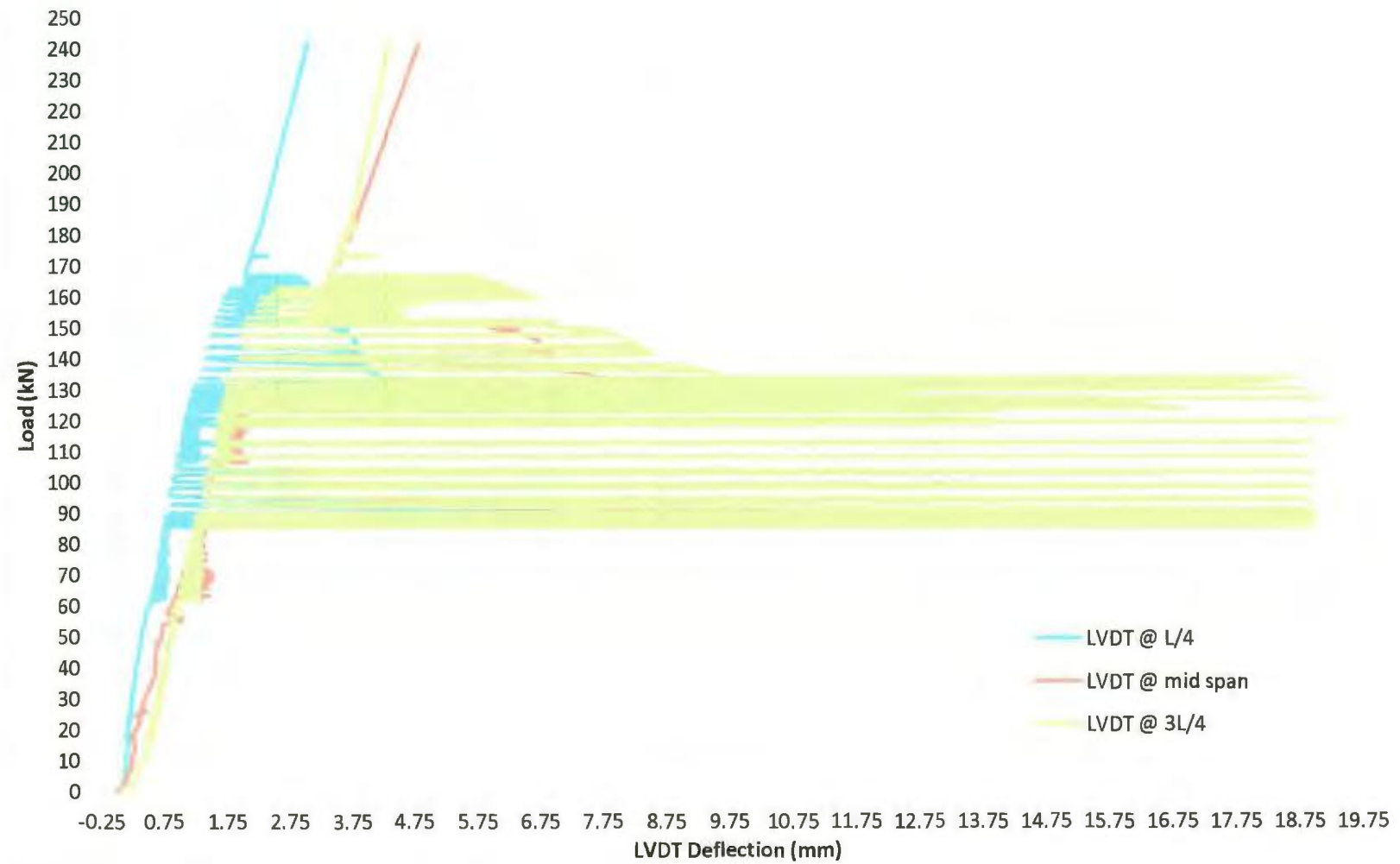


Figure B10 – LVDT Deflection vs. Loading for Beam 10

8.3 Appendix C -- Strain vs. Loading Graphs for 10 SCC Beams

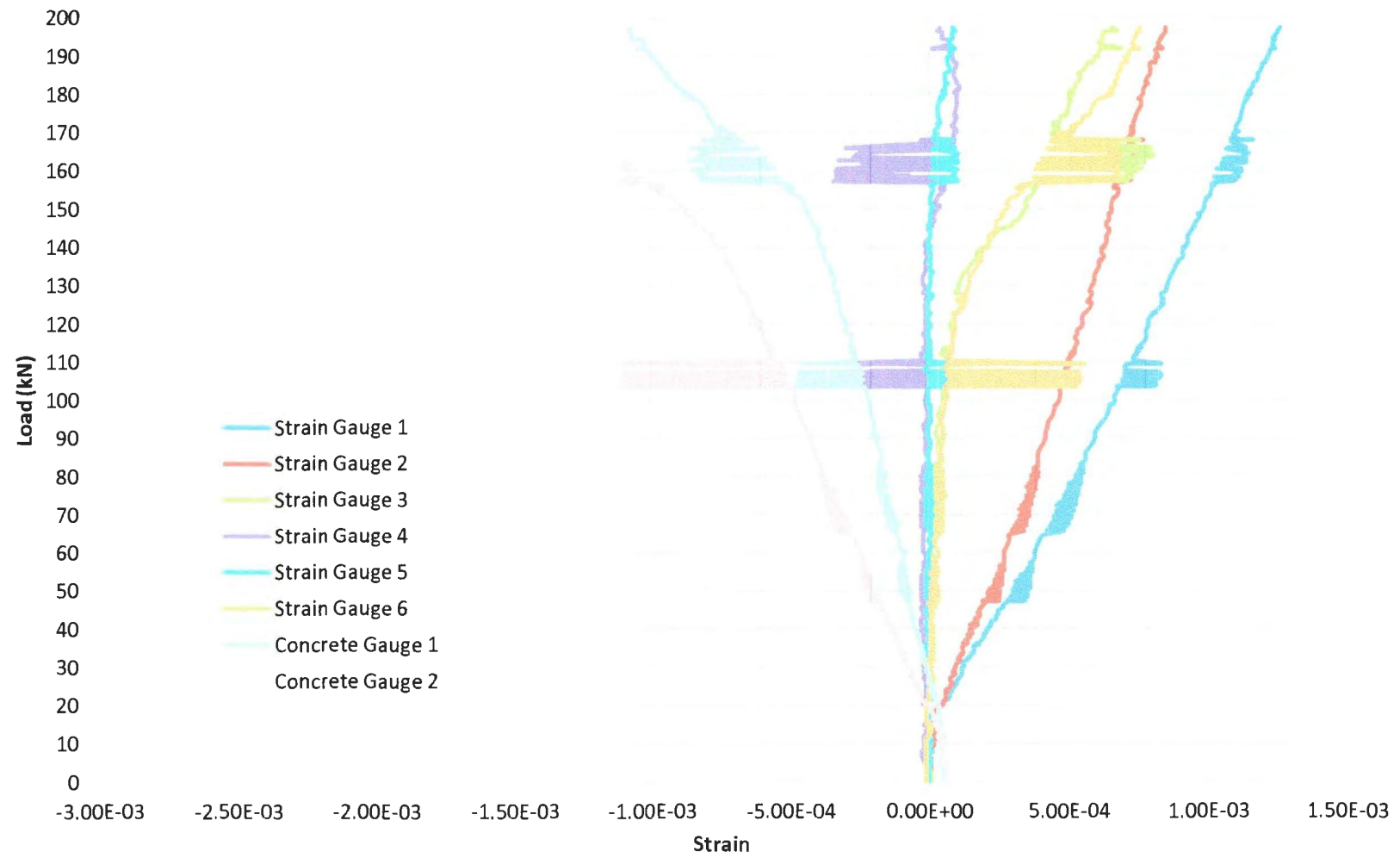


Figure C1 – Strain vs. Loading for Beam 1

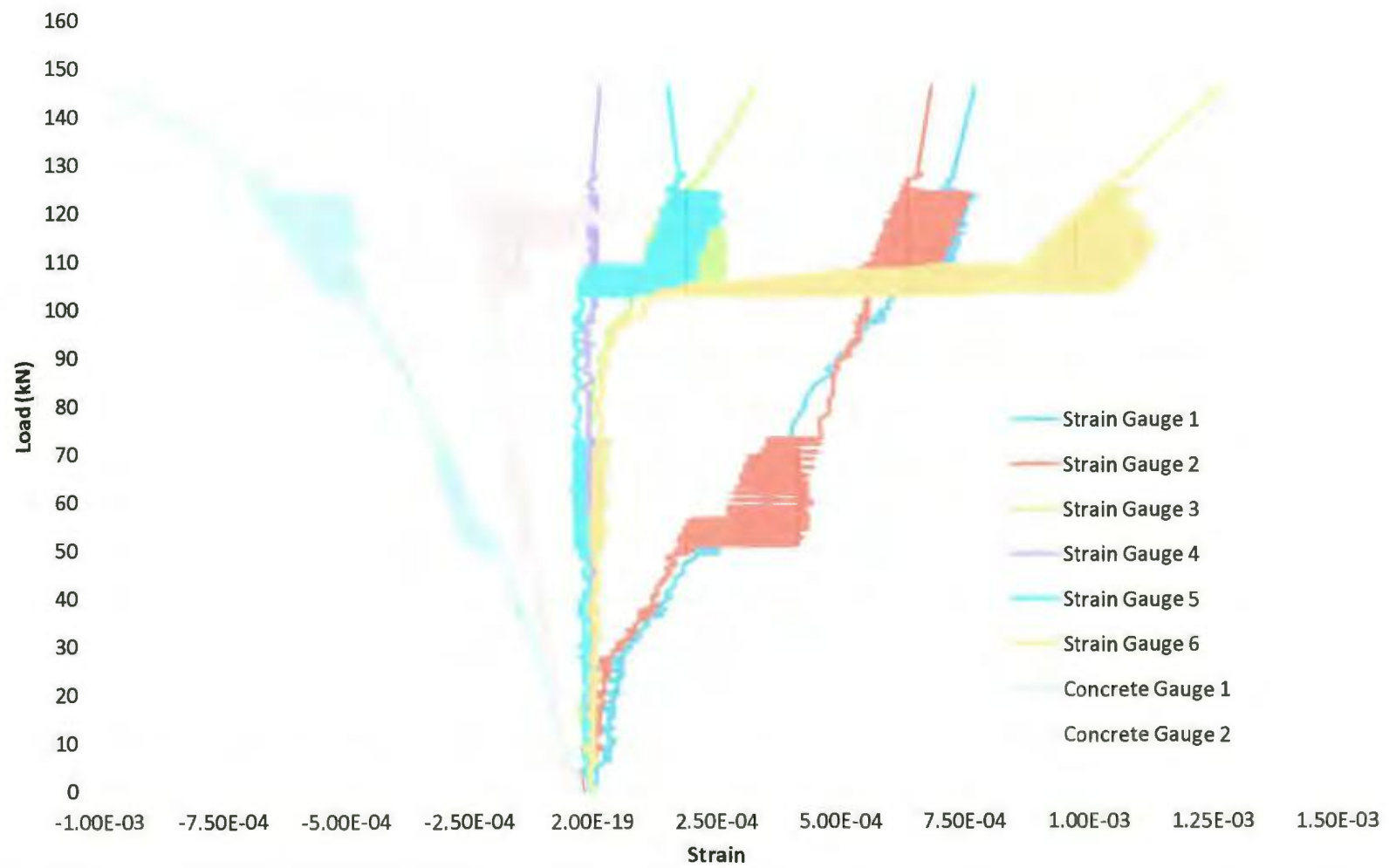


Figure C2 – Strain vs. Loading for Beam 2

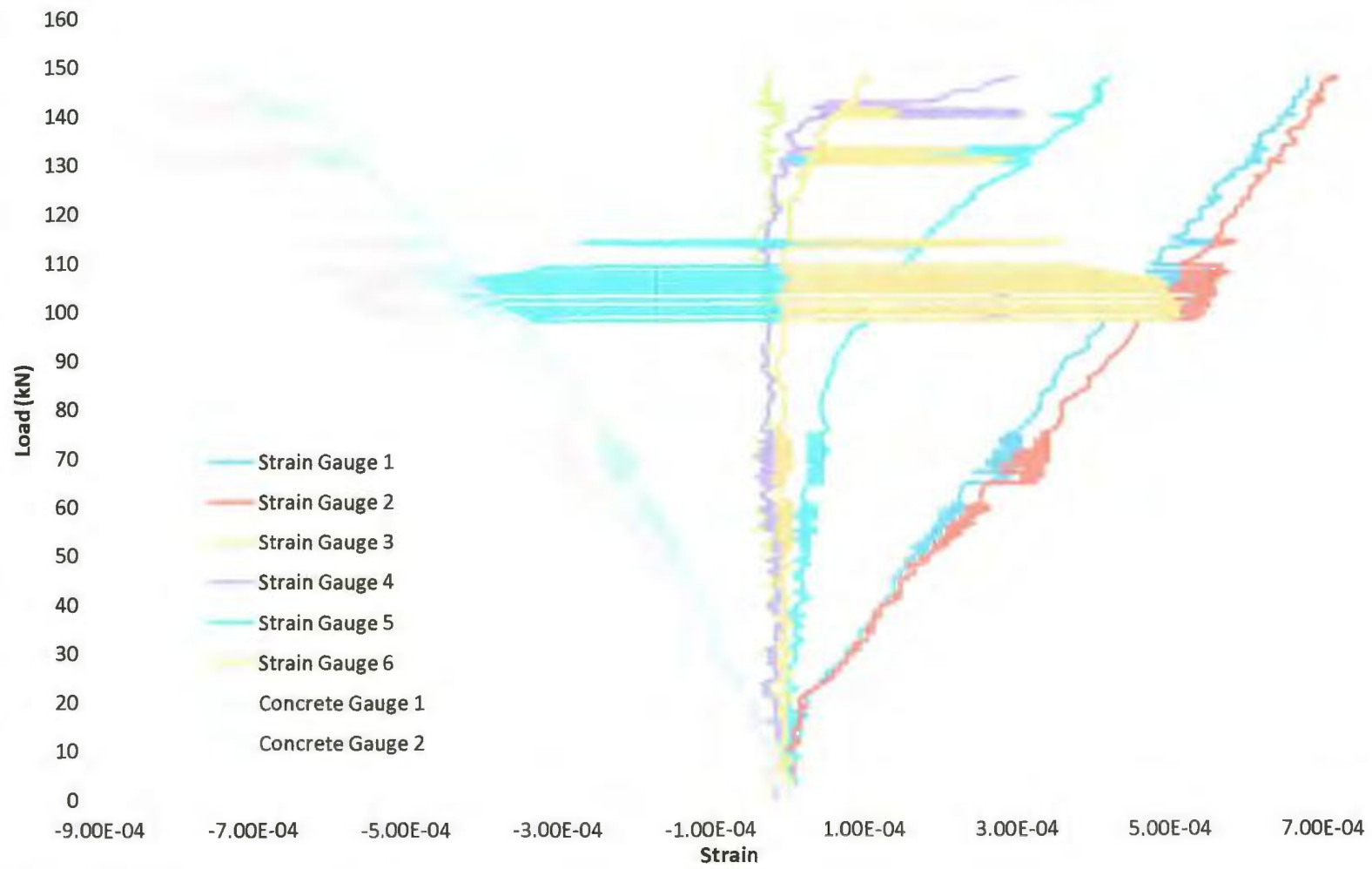


Figure C3 – Strain vs. Loading for Beam 3

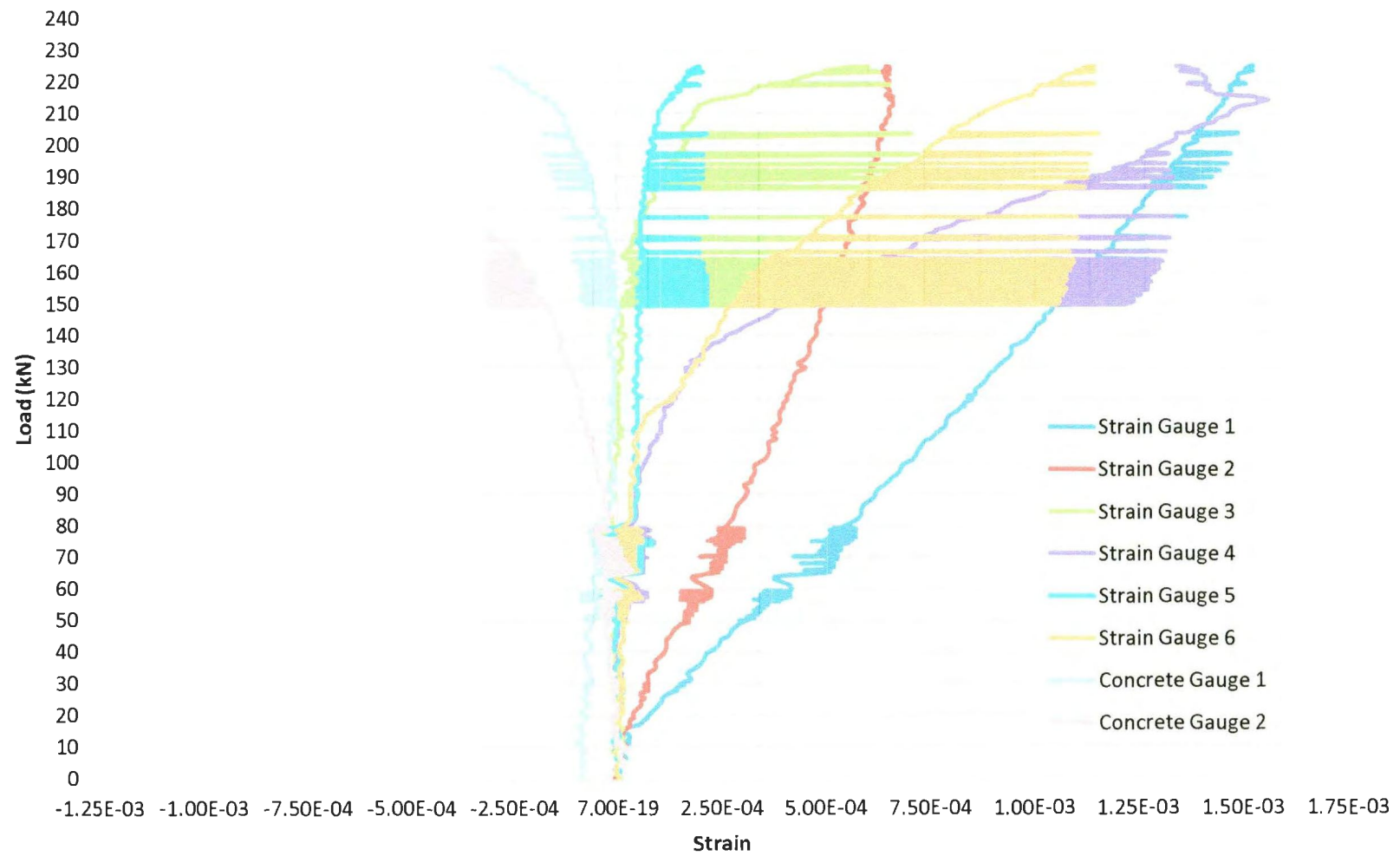


Figure C4 – Strain vs. Loading for Beam 4

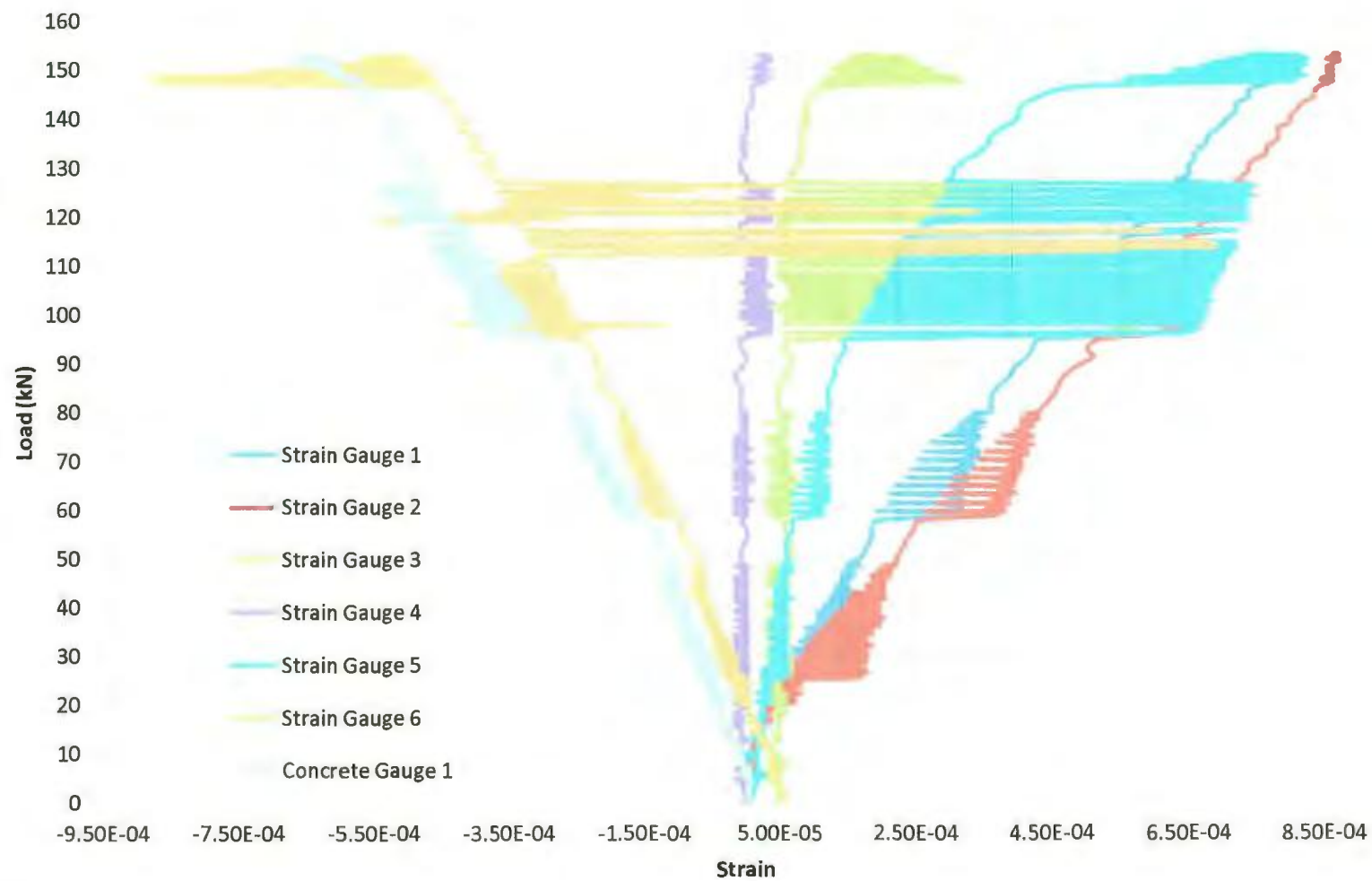


Figure C5 – Strain vs. Loading for Beam 5

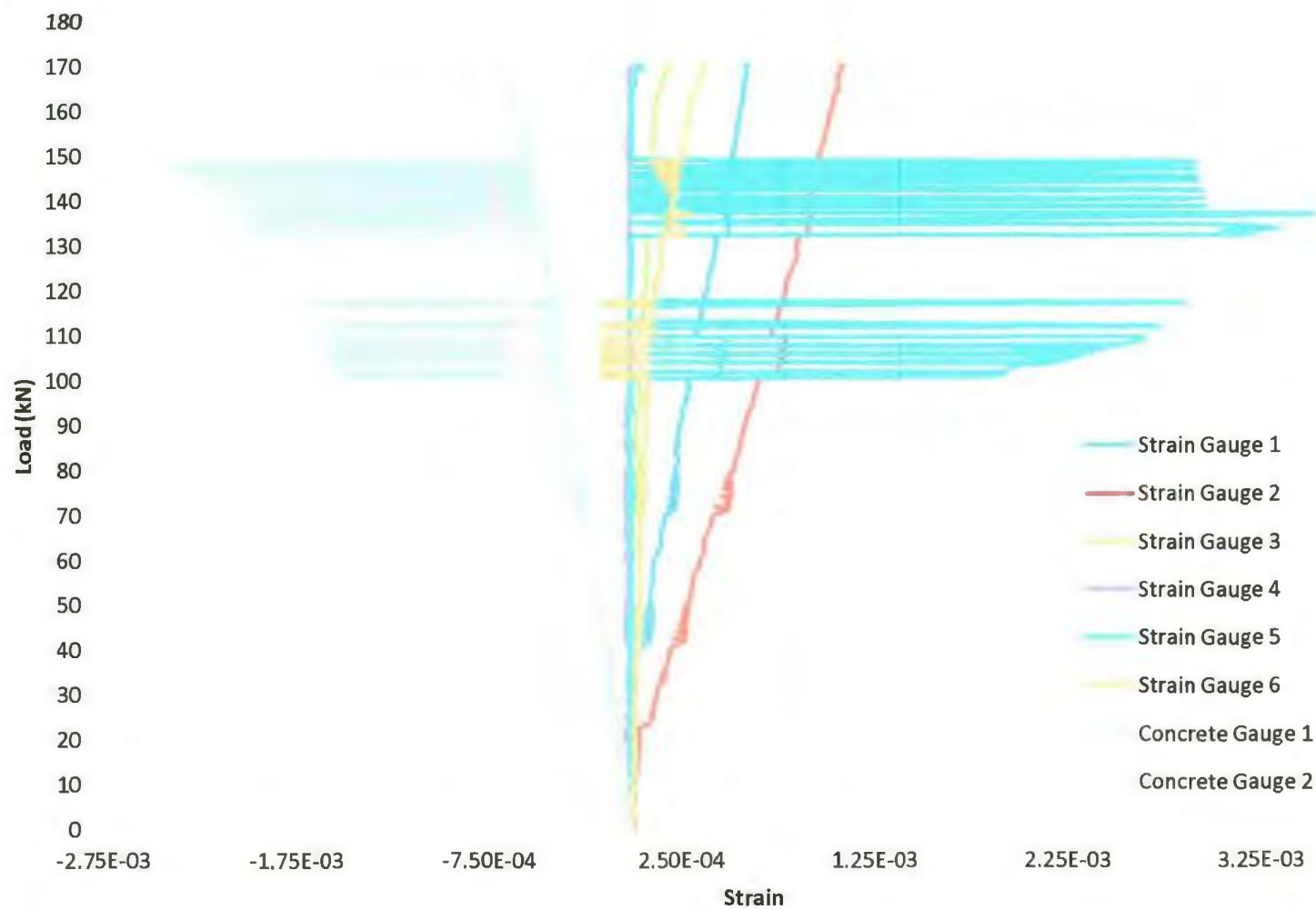


Figure C6 – Strain vs. Loading for Beam 6

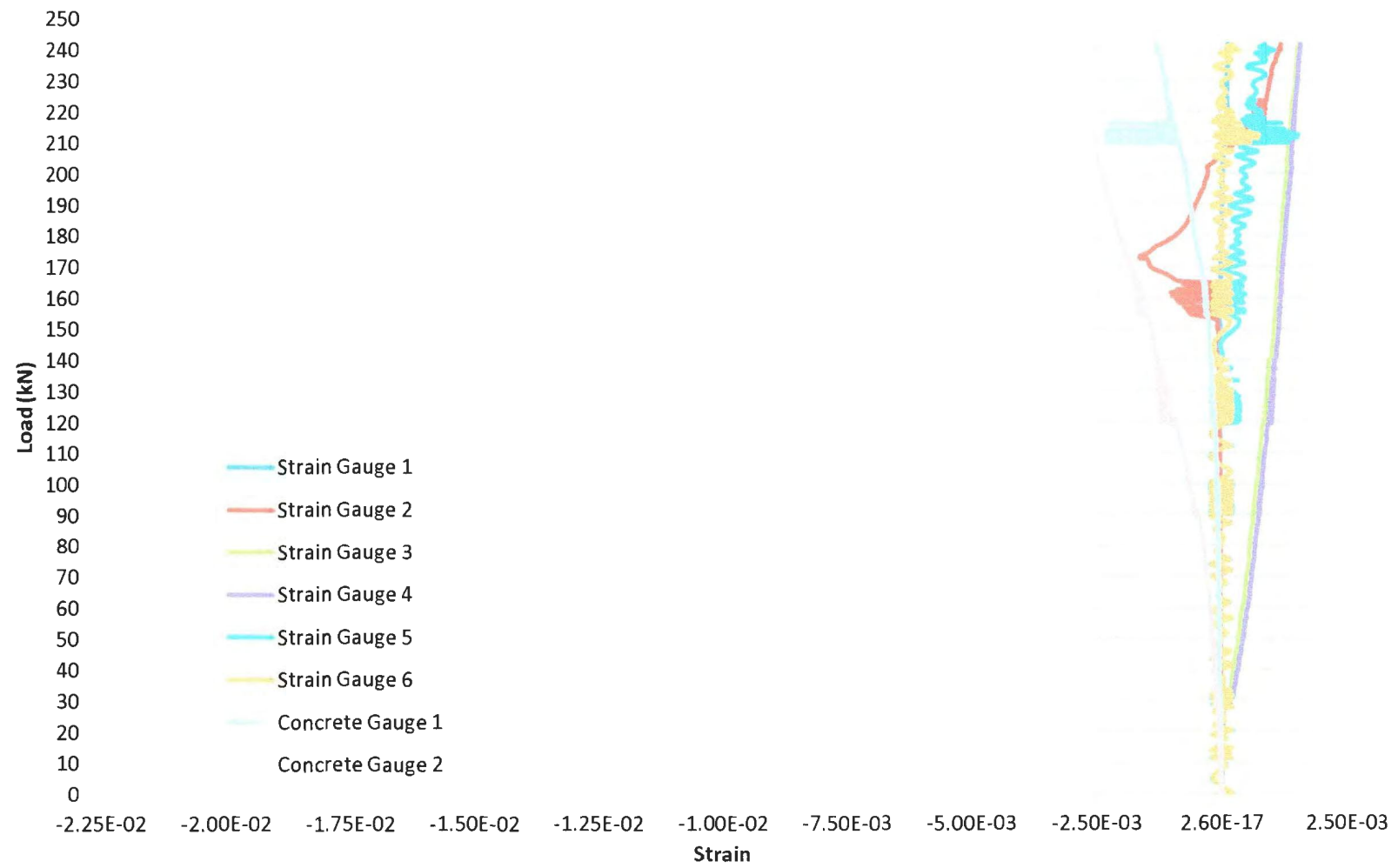


Figure C7 – Strain vs. Load for Beam 7

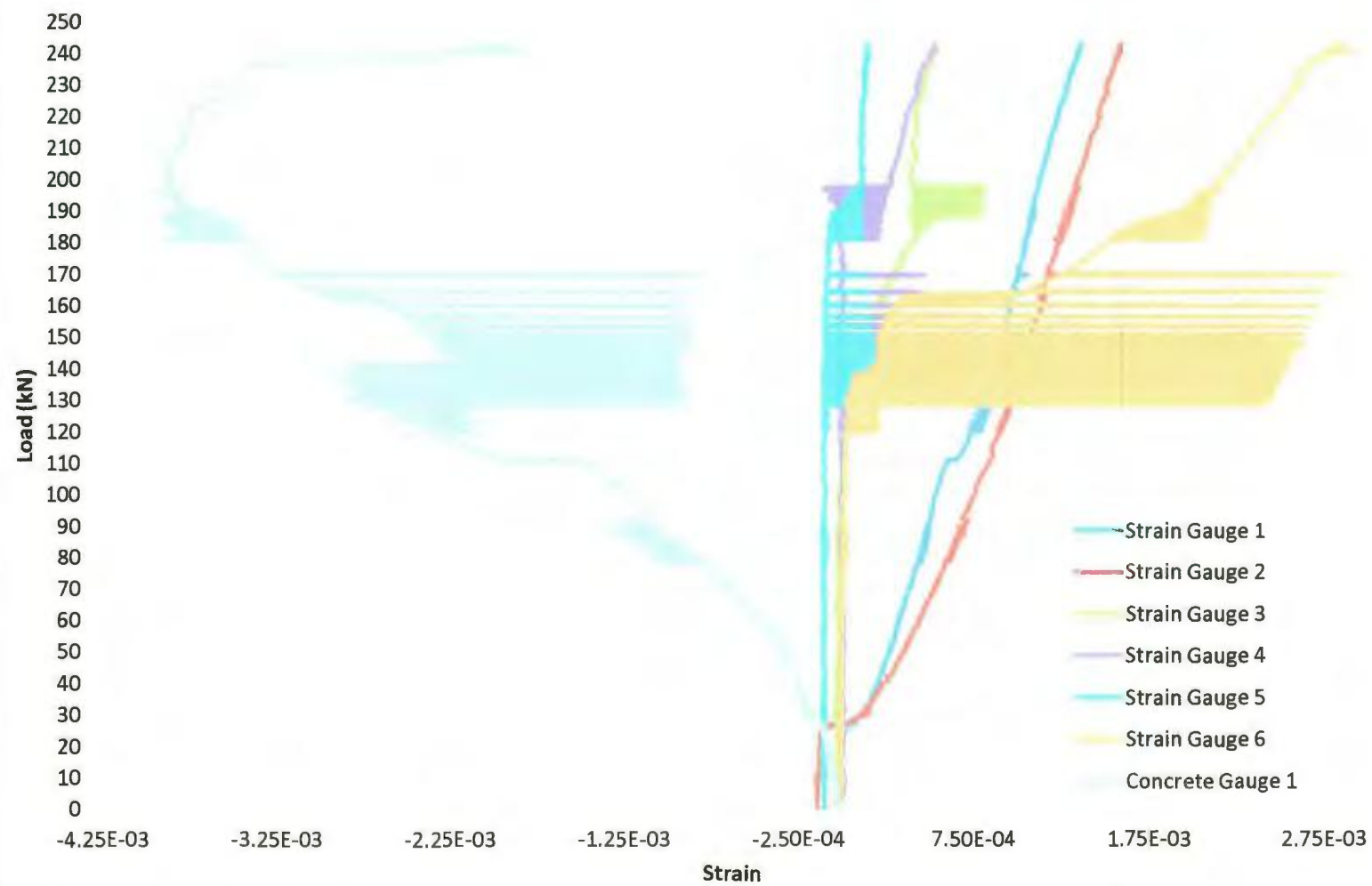


Figure C8 – Strain vs. Loading for Beam 8

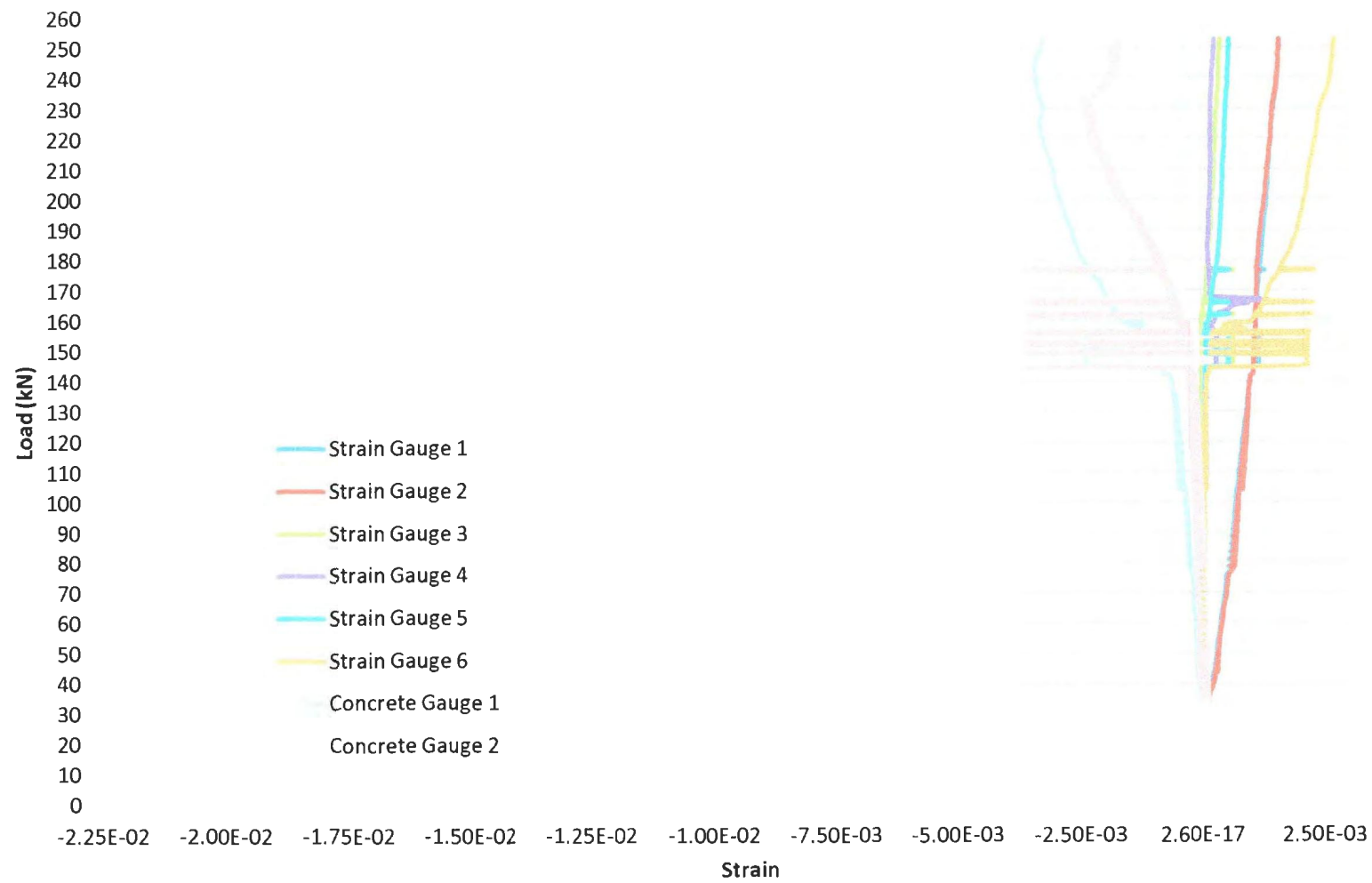


Figure C9 – Strain vs. Loading for Beam 9

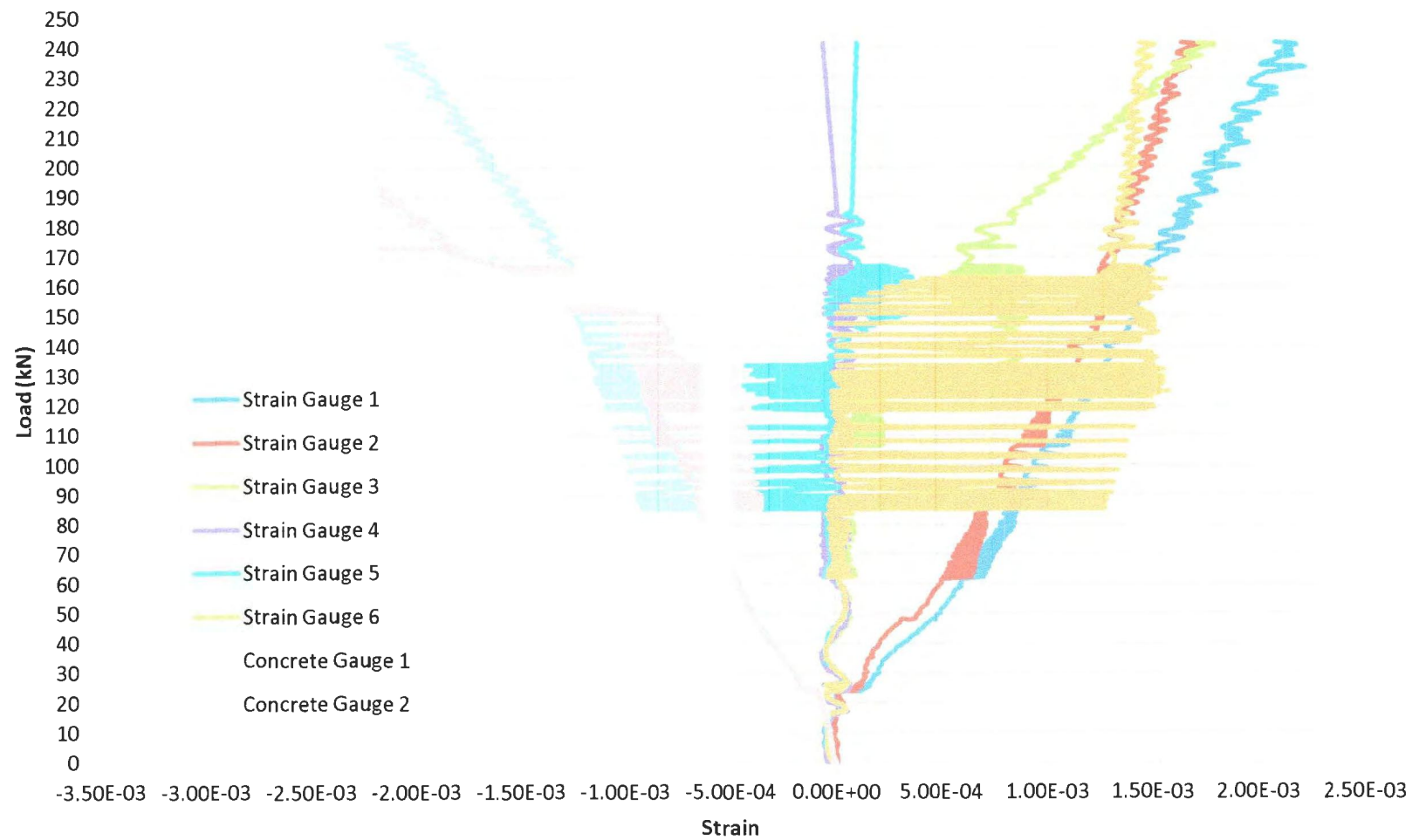


Figure C10 – Strain vs. Loading for Beam 10



